

**MODELING AND SIMULATION OF UNIFIED  
POWER QUALITY CONDITIONER IN POWER  
SYSTEMS TO IMPROVE POWER QUALITY**

**THESIS**

*Submitted*

*in partial fulfilment for the award of the degree of*

**DOCTOR OF PHILOSOPHY**

**IN THE DEPARTMENT OF**

**ELECTRICAL AND ELECTRONICS ENGINEERING**

*By*

**KANNAN P**

**(Regn. No.: SP11EEDA142)**



**DEPARTMENT OF ELECTRICAL AND ELECTRONICS**

**ENGINEERING**

**St. PETER'S INSTITUTE OF HIGHER EDUCATION AND**

**RESEARCH**

**St. PETER'S UNIVERSITY**

**CHENNAI - 600 054**

**JUNE 2016**

## DECLARATION

Certified that the thesis, entitled “**MODELING AND SIMULATION OF UNIFIED POWER QUALITY CONDITIONER IN POWER SYSTEMS TO IMPROVE POWER QUALITY**”, is the bonafide record of independent work done by me under the supervision of Dr. V. RAJAMANI. Certified further that the work reported herein does not form part of any other thesis or dissertation on the basis of which a degree or award was conferred earlier.

Dr. V. RAJAMANI  
SUPERVISOR

KANNAN P

Place :

Date :

## CERTIFICATE

I hereby certify that the thesis entitled “**MODELING AND SIMULATION OF UNIFIED POWER QUALITY CONDITIONER IN POWER SYSTEMS TO IMPROVE POWER QUALITY**”, to the St. Peter’s University, for the award of Degree of Doctor of Philosophy is the record of research work done by the candidate **Mr. KANNAN P** under my guidance and that the thesis has not formed previously the basis for the award of any degree, diploma, associateship, fellowship or other similar titles.

Place :

Dr. V. RAJAMANI,  
SUPERVISOR.

Date :

## **ACKNOWLEDGEMENTS**

I thank the vice chancellor, Registrar, Dean and HOD of EEE Dept., St.Peters University for providing the facilities.

I am very thankful to Dr. G.P.Ramesh, Professor & HOD of ECE Dept., St.Peters University Chennai for his useful discussions and review.

I sincerely express my deep gratitude to my supervisor Dr. V.Rajamani, Professor, Dept. of Electronics & Comm. Engg., Vel Tech Multi Tech and Dr. Rangarajan and Dr. Sakunthala Engg. College, Avadi, Chennai, India, for guiding me.

I extend my sincere thanks to the Doctoral Committee members Dr.V.Rajasekar, Professor and Head, PSNA College of Engineering and Technology, Dindigul and Dr. V.Saravanan, Assistant Professor, EEE Dept. Thayagaraja College of Engineering, Madurai, for offering their valuable suggestions.

I am indebted to my organization "TANGEDCO" for facilitating me to pursue research. I thank my superiors and colleagues in TANGEDCO.

I am indebted to my parents, wife and son for their keen interest shown throughout my research.

**KANNAN P**

## ABSTRACT

Unified Power Quality Conditioner (UPQC) can improve the power quality by injecting a voltage in series with the line and also can supply harmonics to the non-linear load. This work deals with the design and the simulation of the UPQC system to improve the power quality in multiBus system. The two Bus system is modeled using the elements of Simulink and it is simulated using MATLAB. A sag is created by applying a heavy load at the receiving end. The sag is compensated by using the UPQC. The harmonics required at the receiving end are supplied by the inverter part of UPQC. The DC required by the UPQC is supplied by Solar cell and Boost converter system. The simulation results are compared with the experimental results. The experimental voltage is 2% less than that of simulation value.

This work also deals with design, modeling and simulation of UPQC in eight Bus system to improve the power quality in multiBus system. A dip in voltage is produced by applying a heavy load at the receiving end. The sag is compensated by using the UPQC. The simulation results of eight Bus system are presented. The real power increases by 18% and the reactive power increases by 15%.

The present work deals with digital simulation of the UPQC in fourteen Bus system which mitigates the sag and reduces the losses. The simulation results of fourteen Bus system are depicted. The real power increases by 36% and reactive power by 6%. The present work also deals with simulink modeling of thirty Bus system. Multiple UPQCs are proposed to improve the power quality. Modelling and simulation of fifty Bus system are also done and the results are presented. Power quality improvement in fifty Bus system is investigated to improve the voltage in multi Bus system. The requirement of multiply UPQCs is also presented. The real and reactive power near UPQC increases by 155% and 125% respectively.

## CONTENTS

	<b>Page</b>
<b>Declaration</b>	ii
<b>Certificate</b>	iii
<b>Acknowledgement</b>	iv
<b>Abstract</b>	v
<b>List of Tables</b>	x
<b>List of Figures</b>	xi
<b>List of Symbols and Abbreviations</b>	xvi
<b>CHAPTER 1 INTRODUCTION</b>	<b>1</b>
1.1. General	1
1.2. Power Quality	2
1.2.1. Steady – State Voltage Frequency and Magnitude	3
1.2.2. Voltage Sags	5
1.2.3. Grounding	7
1.2.4. Harmonics	9
1.2.5. Voltage Fluctuations and Flicker	11
1.2.6. Transients	12
1.2.7. Monitoring and Measurement	13
1.3. Organization of Thesis	14
1.4. Summary	15
<b>CHAPTER 2 LITERATURE REVIEW</b>	<b>16</b>
2.1. General	16
2.2. Literature Survey	17
2.3. Scope of present investigation	34
2.4. Research problem	35
2.5. Solution methodology	35
2.6. Summary	36

<b>CHAPTER 3 POWER SYSTEM CONTROL USING FACTS CONTROLLERS</b>	<b>37</b>
3.1. General	37
3.2. Power Transfer Limit	38
3.3. Power System Constraints	39
3.4. Controllability of power systems	39
3.5. Benefits of Control of Power Systems	40
3.6. Conventional Devices for Enhancing Power System Control	41
3.7. Facts Technology	42
3.8. Relative importance of controllable parameters	43
3.9. Types of facts controllers	44
3.9.1. Series Controller	44
3.9.2. Shunt Controller	44
3.9.3. Combined Series – Series Controller	44
3.9.4. Combined Series – Shunt Controller	45
3.10. Controllers for enhancing power system control	45
3.11. Advantages of facts technology	45
3.11.1. Future direction of facts technology	46
3.11.2. Unified Power Quality Conditioner (UPQC)	46
3.11.3. Controller designing	49
3.11.3.1. Shunt inverter control	50
3.11.3.2. Series inverter control	50
3.12. Conclusion	50
<b>CHAPTER 4 MODELING AND SIMULATION OF UPQC SYSTEM</b>	<b>51</b>
4.1. Introduction	51
4.2. Circuit model of Single phase Two Bus System With UPQC	52
4.3. Circuit model of Three phase Two Bus System With UPQC	60

4.4.	Experimental verification	66
4.4.1.	Experimental setup and procedure	66
4.4.2.	Parameters Considered	66
4.4.3.	Conditions and Constraints During the Study	66
4.4.4.	Waveforms and Explanation	67
4.5.	Results & Discussions	70
4.5.1.	Results of Single Phase Two Bus System with UPQC	70
4.5.2.	Results of Three Phase Two Bus System with UPQC	71
4.5.3.	Results of Experimental verification	71
4.6.	Validation of simulation Results with the Experiment Results	71
4.7.	Result comparison with desirables and analysis	71
4.8.	Conclusion	71

## **CHAPTER 5 EIGHT, FOURTEEN, THIRTY AND**

	<b>FIFTY BUS SYSTEMS</b>	<b>72</b>
5.1.	Introduction	72
5.2.	Model of Eight Bus System using UPQC in Power Systems to improve power quality	72
5.3.	Results & Discussions on Eight Bus System	78
5.4.	Results comparison with desirables and analysis	78
5.5.	Model of Fourteen Bus System using UPQC in Power Systems to improve power quality	78
5.6.	Results & Discussions	86
5.7.	Results comparison with desirables and analysis	86
5.8.	Model of Thirty Bus System with Single UPQC in Power Systems to improve power quality	86
5.9.	Model of IEEE Thirty Bus System with Multiple UPQC	98
5.10.	Results comparison with desirables and analysis	<b>107</b>



5.11.	Fifty Bus System	107
5.12.	Model of IEEE Fifty Bus System with Multiple UPQC	108
5.13.	Results & Discussions	128
5.14.	Results comparison with desirables and analysis	129
5.15.	Conclusion	129
<b>CHAPTER 6</b>	<b>CONCLUSION AND FUTURE SCOPE</b>	<b>130</b>
6.1.	Conclusion	130
6.2.	Scope for further work	131
	<b>Appendix</b>	<b>132</b>
	<b>References</b>	<b>147</b>
	<b>Publications</b>	<b>157</b>

## LIST OF TABLES

<b>Table</b>		<b>Page</b>
1.1.	Ansi C84.1 Voltage Ranges	04
5.1.	Summary of Real and Reactive Power of 8 Bus System	77
5.2.	Summary of Real and Reactive Power of 14 Bus System	85
5.3.	Summary of Real and Reactive Powers of IEEE 30 Bus System	97
5.4.	Summary of Real and Reactive Powers of 50 Bus System	126

## LIST OF FIGURES

<b>Figure</b>		<b>Page</b>
3.1	Controllability of Power System	40
3.2	General Structure of Grid Connected PV System	47
3.3	Configuration of UPQC with PV Array	48
4.1	Circuit model of the UPQC System	52
4.2	Inverters used in the UPQC System	53
4.3	Boost Converter Circuit	54
4.4	Voltages across Load-2 and Load-1	55
4.5	Real Power	56
4.6	Reactive Power	56
4.7	Circuit Diagram of Two Bus System Without the Active Filter	57
4.8	Frequency Spectrum for Current	58
4.9a	Circuit Diagram with the Active Filter	59
4.9b	Frequency Spectrum for the Current	60
4.10	Circuit Model of Three-phase System with the Additional Load	61
4.11	Voltage Across Load-1	61
4.12	Voltage Across Load-2	62
4.13	Frequency Spectrum	62
4.14	Circuit Model of the Three-phase System with UPQC	63
4.15	Circuit of UPQC	64
4.16	Three phase Voltage with Compensation	64

4.17	Voltage of each phase with Compensation	65
4.18	Frequency Spectrum	65
4.19a.	Hardware Implementation	67
4.19b.	Output of the Solar Cell	67
4.19c.	Switching Pulses for M1	68
4.19d.	Switching Pulses for M2	69
4.19e.	Output Voltage of the Inverter 1	69
4.19f.	Output Voltage of the Inverter 2	70
5.1	Eight Bus System without UPQC	73
5.2	Real and Reactive Power at Bus-7	74
5.3	Real and Reactive Power at Bus-3	74
5.3a	Voltage Across Load-1 and Load-2	75
5.4	Eight Bus System with UPQC	75
5.5	Real and Reactive Power Across Bus – 1	76
5.6	Real and Reactive Power Across Bus – 3	76
5.7	Voltage Across Load-1 and Load-2	77
5.6.1	Fourteen Bus System without UPQC	79
5.6.2	Real and Reactive Power Across Bus-7	80
5.6.3	Real and Reactive Power Across Bus-3	80
5.6.4	Voltage Across Load-1 and Load-2	81
5.6.5	Block Diagram of the Fourteen Bus System with UPQC	82
5.6.6	Circuit model of the 14 Bus System	83
5.6.7	Voltage Across Load-1 and Load-2	83
5.6.8	Real and Reactive Power Across Bus-7	84
5.6.9	Real and Reactive Power Across Bus-1	84
5.6.10	Real and Reactive Power Across Bus-3	84

5.7.1a.	Thirty Bus System	87
5.7.1b.	Real and Reactive Power Across Bus-7	88
5.7.1c.	Real and Reactive Power Across Bus-3	88
5.7.1d.	Real and Reactive Power Across Bus-21	89
5.7.1e.	Voltage Across Load-1 and Load-2	89
5.7.2a.	Thirty Bus System with the UPQC	90
5.7.2b.	Thirty Bus Network	91
5.7.2c.	Real and Reactive Power Across Bus-1	92
5.7.2d.	Real and Reactive Power Across Bus-7	92
5.7.2e.	Real Power at Bus-15	93
5.7.2f.	Voltage Across Load-1 and Load-2	94
5.7.2g.	Real and Reactive Power Across Bus-7	94
5.7.2h.	Reactive Power at Bus-15	95
5.7.2i.	Real and Reactive Power Across Bus-21	95
5.7.2j.	Real Power at Bus-29	96
5.7.2k.	Reactive Power at Bus-29	96
5.7.3.1	30 Bus system without UPQC	99
5.7.3.2	Voltage at Bus-4	100
5.7.3.3	Real Power at Bus-4	100
5.7.3.4	Reactive Power at Bus-4	101
5.7.3.5	Voltage at Bus-12	101
5.7.3.6	Real Power at Bus-12	102
5.7.3.7	Reactive Power at Bus-12	102
5.7.3.8	Voltage at Bus-26	102
5.7.3.9	Real Power at Bus-26	103
5.7.3.10	Reactive Power at Bus-26	103

5.7.3.11	30 Bus systems with multiple UPQCs	104
5.7.3.12	Circuit of UPQC	105
5.7.3.13	Voltage at Bus-4	105
5.7.3.14	Real Power at Bus-4	106
5.7.3.15	Reactive Power at Bus-4	106
5.8.2.1	50 Bus system without the UPQC	109
5.8.2.2	Voltage at Bus-4	110
5.8.2.3	Real Power at Bus-4	110
5.8.2.4	Reactive Power at Bus-4	111
5.8.2.5	Voltage at Bus-12	111
5.8.2.6	Real Power at Bus-12	112
5.8.2.7	Reactive Power at Bus-12	112
5.8.2.8	Voltage at Bus-26	113
5.8.2.9	Real Power at Bus-26	113
5.8.2.10	Reactive Power at Bus-26	114
5.8.2.11	THD	114
5.8.2.12	50 Bus Systems with UPQC	115
5.8.2.13	Circuit of UPQC	116
5.8.2.14	Voltage at Bus-4	117
5.8.2.15	Real Power at Bus-4	118
5.8.2.16	Reactive Power at Bus-4	118
5.8.2.17	Voltage at Bus-12	119
5.8.2.18	Real Power at Bus-12	119
5.8.2.19	Reactive Power at Bus-12	120
5.8.2.20	Voltage at Bus-18	120
5.8.2.21	Real Power at Bus-18	121
5.8.2.22	Reactive Power at Bus-18	121

5.8.2.23	Voltage at Bus-26	122
5.8.2.24	Real Power at Bus-26	122
5.8.2.25	Reactive Power at Bus-26	123
5.8.2.26	Voltage at Bus-45	123
5.8.2.27	Real Power at Bus-45	124
5.8.2.28	Reactive Power at Bus-45	124
5.8.2.29	Voltage at Bus-48	124
5.8.2.30	Real Power at Bus-48	125
5.8.2.31	Reactive Power at Bus-48	125
5.8.2.32	Frequency spectrum for current	126

## LIST OF SYMBOLS AND ABBREVIATIONS

### Symbols

$\rho$	–	Angle of Series Converter Voltage of UPQC in Degrees
$V_c$	–	Controllable Voltage Source
$I_c$	–	Controllable Current Source
$\alpha$	–	Converter Firing Angle of UPQC in Degrees.
$I_p$	–	Direct Axis Component of Current in amps
$E_L$	–	Load Voltage in volts
$V_{pq}$	–	Magnitude of Series Converter Voltage of UPQC in Volts
$Q$	–	Reactive Power in KVAR
$P$	–	Real Power in KW
$E_2$	–	Receiving End Voltage of Transmission line in volts
$\theta$	–	Reference Angle in Degrees
$V_{ref}$	–	Reference Voltage in volts
$E_1$	–	Sending End Voltage of Transmission line in volts
$\delta$	–	Transmission Line Angle in degrees
$Z$	–	Transmission Line Impedance in Ohms
$V$	–	Transmission Line Voltage in Volts
$I_q$	–	Quadrature Axis Component of Current in amps



**Abbreviations**

AC	–	Alternating Current
APF	–	Active Power Filter
ANSI	–	American National Standards Institute
ACR	–	Automatic Circuit Recloser
BESS	–	Battery Energy Storage System
CT	–	Current Transformer
DC	–	Direct Current
d-q axis	–	Direct – Quadrature Axis
DVR	–	Dynamic Voltage Restorer
FACTS	–	Flexible AC Transmission System
GIPFC	–	Generalized Interline Power Flow Controller
GA	–	Genetic Algorithm
Hz	–	Hertz
IEEE	–	Institute of Electrical and Electronics Engineers
IDVR	–	Interline Dynamic Voltage Restorer
IPFC	–	Interline Power Flow Controller
IEC	–	International Electro technical Commission
KVAR	–	Kilovolt Ampere Reactive
KW	–	Kilo Watts
MW	–	Mega Watts
MLI	–	Multi Level Inverter
NEC	–	National Electric Code
PI	–	Proportional Integral

PIV	–	Peak Inverse Voltage
Pu	–	Per Unit
PT	–	Potential Transformer
PWM	–	Pulse Width Modulation
RMS	–	Root Mean Square
STATCOM	–	Static Compensator
SSSC	–	Static Synchronous Series Compensator
SVC	–	Static Var Compensator
SVM	–	Space Vector Modulation
SVPWM	–	Space Vector Pulse Width Modulation
TCSC	–	Thyristor Controlled Series Capacitor
THD	–	Total Harmonic Distortion
UPFC	–	Unified Power Flow Controller
UPQC	–	Unified Power Quality Conditioner
VSC	–	Voltage Source Converter
VSI	–	Voltage Source Inverter

# CHAPTER 1

## INTRODUCTION

### 1.1. General

Power electronics and power quality in power systems are irrevocably linked together as it strives to advance both broad areas. With the dramatic increases over the last 20 years in energy conversion systems utilizing power electronic devices, it is seen that the emergence of 'power quality' and simple control algorithm modification to this same technology can often play an equally dominant role in enhancing overall quality of electrical energy available to end-users.

Power electronics has given, in an industrial society, a plethora of new ways to manufacture products, provide services, and utilize energy. From a power quality impact viewpoint, applications such as

1. Switched-mode power supplies,
2. DC arc furnaces,
3. Electronic fluorescent lamp ballasts,
4. Adjustable speed drives, and
5. Flexible AC transmission components

are often cause for concern. From a utility supply system viewpoint, these converter-based systems can lead to operational and life expectancy problems for other equipment, possibly not owned or operated by the same party. It was from this initial perspective that the field of power quality emerged.

In most cases, the same devices and systems that create power quality problems can be used to solve power quality problems. 'Problem solving' applications such as

1. Active harmonic filters,
2. Static and adaptive var compensators, and
3. Uninterruptable power supplies

all utilize the same switching device technology as the 'problem causing' applications.

As the number of potentially problematic power electronic based loads have increased over time, the attention is given to enhanced converter control to maximize power quality. Typical examples of these improvements include:

1. Unity power factor converters,
2. Dip-proof inverters, and
3. Limited-distortion electronic lamp ballasts.

While many studies suggest increases in power electronics-based energy utilization as high as 70-80% (of all energy consumed), it is evident that we are beginning to realize the total benefit of such end-use technologies. Power quality problems associated with grounding, sags, harmonics, and transients will continue to increase because of the sheer number of sensitive electronic loads expected to be placed.

## **1.2. Power Quality**

The term 'Power Quality' means different things to different people. To utilities, power quality initially referred to the quality of the service delivered as 'measured' by the consumer's ability to use the energy delivered in the desired manner. This conceptual definition included such conventional utility planning topics as voltage and frequency regulation and reliability. The end-user's definition

of power quality also centers around their ability to use the delivered energy in the desired manner, but the topics considered can be much more specific and include magnitude and duration of different events as well as wave shape concerns. Fortunately, a good working definition of power quality has not been a point of contention, and most parties involved consider 'quality power' to be that which allows the user to meet their end use goals. The working definition is not complicated by particular issues; engineers are well aware that topics from many aspects of power engineering may be important. Power quality can be roughly broken into a few categories as follows:

1. Steady-state voltage magnitude and frequency,
2. Voltage sags,
3. Grounding,
4. Harmonics,
5. Voltage fluctuations and flicker,
6. Transients, and
7. Monitoring and measurement.

The remainder of this section discusses each of the major categories in turn.

### **1.2.1. Steady – State Voltage Frequency and Magnitude**

In most areas of North America, steady-state frequency regulation is not a significant issue due to the sufficient levels of generating capacity and the strong interconnections among generating companies and control areas. In other parts of the world, and North America under extreme conditions, frequency can drive  $\frac{1}{4}$  to  $\frac{1}{2}$ Hz during periods of insufficient generating capacity. Under transient conditions, frequency can deviate up to 1 to 2Hz.

Frequency deviations can affect power electronic equipment that use controlled switching devices unless the control signals are derived from a signal

that is phase-locked with the applied voltage. In most cases, phase locks are used, or the converters consist of uncontrolled rectifiers. In either case, frequency deviations are not a major cause of problems. In most cases, frequency deviations have more impacts on conventional equipment that do not use electronics or very inexpensive electronic devices. Clocks can run fast (or slow), motor speeds can drop (or rise) by a few revolutions per minute impact and are not considered a real power quality problem.

Steady-state voltage regulation is a much more pronounced issue that can impact a wide range of end-use equipment. In most cases, utility supply companies do a very effective job of providing carefully regulated voltage within permissible ranges. In North America, ANSI Standard C84.1 suggests steady-state voltage ranges both at the utility service entrance and at the point of connection of end-use equipment. Further-more, equipment manufacturers typically offer equipment that is tolerant of steady-state voltage deviations in the range of  $\pm 10\%$ . Table 1.1 shows the voltage ranges suggested by ANSI C84.1, with specific mention of normal (Range A) and contingency (Range B) allowable voltages, expressed in percent.

ANSI C84.1 voltage ranges. Range A is for normal conditions, Range B is for emergency or short-time conditions.

**Table 1.1. Ansi C84.1 Voltage Ranges**

	Service Voltage (%)	Utilization Voltage (%)
Range A	114-125V	108-125V
Range B	110-127V	104-127V

Virtually all equipment, especially sensitive electronic equipment, can be affected by voltage deviating outside the  $\pm 10\%$  range. In most cases, over

voltages above +10% lead to loss of life, usually over times excessive over voltages can immediately fail the equipment. Under voltages, below -10% usually lead to excessive current demands, especially for equipment that has a controlled output like an adjustable speed drive controlling a motor to a constant speed / torque point. The impacts of these prolonged excessive currents can be greater voltage drop, temperature rise in conductors. In the extreme, under voltages of more than 15-20% can cause the equipment to trip immediately. In most cases, such extreme under voltages are associated with system faults and the associated protection system. These extreme under voltages are so important that they are classified in a power quality category of their own, called voltage sags.

### **1.2.2. Voltage Sags**

Other than improper grounding, voltage sags are probably the most problematic of all power quality problems. A number of standards-making bodies, including IEEE, ANSI, and IEC, are working on standards related to sags. In most cases, sags are generally agreed to be more severe and outside of the scope and they are temporary in nature due to the operation of system protection elements. Because the electrical system is a continuous electrical circuit, faults in any location will have some impact on voltages throughout the network. Of course, areas closer to the faulted area will see a greater voltage sag due to the fault than other, more (electrically) remote areas. Sags can originate anywhere in a system, but are more pronounced in utility distribution systems because of the greater exposure of low-voltage systems to the causes of short circuits.

Most utility companies implement distribution system protection in what is known as a 'fuse saving' methodology. In overhead distribution / system, two feeders (named 1 and 2) are supplied from the same substation transformer. Each primary circuit has its own automatic circuit recloser (ACR).

With the protection system set up based on fuse-saving methodology, any fault downstream of a fault will be cleared first by the substation recloser

followed by a reclosing operation (re-energization of the circuit) in  $\frac{1}{2}$  to 2 seconds later. If the fault is still present, the closer fuse should blow to permanently isolate the fault.

For a fault on the load side of fused Tap 2, customers on Feeder 1 will see a voltage sag determined by the system 1 and transformer impedance at the substation. Because this impedance is typically in the same order (or larger) as the feeder circuit impedance, a sag in substation bus voltage of 50% is common. This sag will persist until Feeder 2 is cleared by the recloser opening. When the recloser re-energizes the circuit, a permanent fault will still be present and the substation bus will again experience voltage sag. Of course, any sag in substation bus voltage will be delivered directly to all customers on Feeder 1, even though there is no electrical problem on that feeder.

Voltage sags are probably the most common power quality problem that is 'given' to the end-user by the supplying utility. However, improper equipment grounding is responsible for the vast majority of power quality problems on the customer's side.

Voltage sags cause interruption to the production with raw material loss in the production lines and damage in electronic boards. This has been a major complaint by big customers like large industrial firms, it may be ranked as the second complaint of power quality after the harmonics. However, the extent of damage and business interruption due to the voltage sag is higher than the harmonics. Most of the electronic equipment cannot be repaired locally and have to be imported from the manufacturer, which takes more time and involves cost high. The harmonics, damaging capacitors and cables, with higher occurrence than voltage sags, are more easy to repair by substitution from the local market. The problem is more severe in large industrial areas where cables and substations are highly loaded. In some cases where the voltage sag lasted to many cycles,



damage to motors has been recorded. The use of reactive compensation is more feasible from the economic point of easy installation and maintenance. (Fabio Tosato and Stefano Quaia 2001).

Voltage sag may be defined as momentary decrease from 0.1-0.9 p.u, in the RMS voltage magnitude at the power frequency for duration from 0.5 cycle to one minute. Its main reasons are, large motor starting and electrical faults associated with heavily loading of cables and transmission systems. Due to their small duration, voltage sags do not cause damage to motor or large equipments, although they cause some stresses on the insulation and disturbance to the operation. However, they can disrupt electronic equipments such as variable speed drives, Personal Computers etc., thus disrupting the operation (McGranaghan et. al. 1993)

### **1.2.3. Grounding**

Grounding of equipment was originally conceived as a personnel safety issue. However, the presence of an electrical conductor that is at zero potential has been widely used in many power electronic and microprocessor-controlled loads. The electrical systems in residential, commercial, and industrial facilities fall under the purview of the National Electric Code which establishes specific criteria for grounding of equipment. While it was once thought that proper grounding according to the NEC was detrimental to power quality concerns, these opinions have gradually faded over time.

From a power quality perspective, improper grounding can be considered of three broad categories:

1. Groups loops,
2. Improper neutral-to-ground connections, and
3. Excessive natural-to-ground voltage.

The group loop problem is a significant issue when power, communications and control signals all originate in different locations, but come together at a common electrical point. Transients induced in one location can travel through the created ground loop, damaging equipment along the way. Improper neutral-to-ground connections will create a 'noisy' ground reference that may interfere with low-voltage communications and control devices. Excessive neutral-to-ground voltage may damage equipment that is not properly insulated or that has an inexpensive power supply.

For any shift in ground potential for the power circuit, often caused by lightening, potentially large currents can flow through the grounding circuits and through the sensitive electronic equipment. Such currents can easily lead to equipment damage. Situations like these are common in

1. Residential areas, if power and telephone grounds are not the same.
2. Commercial and industrial complexes consisting of multiple buildings with linking communications, computer, or control circuits when each building has its own power service (and therefore ground).

Load current returning in the neutral conductor will, at the point of improper connection to ground, divide between neutral and ground. This current flow in the ground conductor will produce a voltage at the load equipment, which can easily disrupt equipment operation.

For load equipment that produces significant voltage drop in the neutral, such as laser printers and copying machines when the thermal heating elements are on, the voltage from the neutral to the ground reference inside the equipment can exceed several volts. This voltage is sufficient to damage printed circuit boards, disrupt control logic, and fail components.

#### 1.2.4. Harmonics

In most cases, power electronic equipment is considered to be the 'cause' of harmonics. While switching converters of all types produce harmonics because of the non linear relationship between the voltage and current across the switching device, harmonics are also produced by a large variety of "conventional" equipment including:

1. Power generation equipment (slot harmonics),
2. Induction motors (saturated magnetics),
3. Transformers (over excitation leading to saturation),
4. Magnetic-ballast fluorescent lamps (arcing), and
5. AC electric arc furnaces (arcing).

All these devices will cause harmonic currents to flow, and some devices actually directly produce voltage harmonics.

Any alternating current flow through any circuit at any frequency will produce a voltage drop at that same frequency. Harmonic currents, which are produced by power electronic loads, will produce voltage drops in the power supply impedance at those same harmonic frequencies. Because of this inter relationship between current flow and voltage drop, harmonic currents created at any location will distort the voltage in the entire supply circuit.

In most cases, equipment is not overly sensitive to the direct impacts of harmonic current flow. However, equipment heating is a function of the RMS value of the current, which can significantly exceed the fundamental frequency value when large harmonic components are present. It is because harmonic currents produce harmonic voltages that are is a real power quality concern.

Most equipment can operate satisfactorily as long as the voltage distortion at the equipment terminals do not exceed around 5%. Exceptions to this general rule include ripple-control systems for converters (which are impacted by

small even-order harmonics) and small harmonics at sufficiently high frequency to produce multiple zero crossing in a wave-form. (Note that voltage notching due to simultaneous commutation of switching devices can also create multiple zero crossings).

Converters that have a time-limited firing signal can directly suffer from excessive voltage distortion. For a six-pulse converter, a maximum time of  $1/(6 \times 50)$  seconds is available to turn on a switching device. Similarly, for a twelve-pulse converter, a maximum of  $1/(12 \times 50)$  is available to turn on a switching device. Considering that all switching devices have a short (but nonzero) turn-on time, manufacturers tend to design drive circuits that bring up the firing pulse for a limited amount of time.

For example, a firing pulse is maintained for 100 ps and the device must begin conduction at that time. In situations where voltage distortion is excessive, the device to be switched could be reverse biased during the first several milliseconds of the time available for device firing during which time conduction cannot begin. If the firing signal is removed before the certain classes of switching devices which are correctly biased, conduction will not begin at all. This situation, commonly balled a 'misfire', can lead to equipment misoperation and failure.

Because some switching devices can conduct in both directions when the firing signal is applied (but only one direction is intended to carry appreciate current), applying the firing pulse at a time when the voltage is of the wrong polarity can destroy the device. Excessive voltage distortion can certainly lead to such a situation, and manufacturers typically design products to function only under limited-distortion conditions.

Because of the numerous potential problems with harmonic currents, standards exist for their control. The IEEE takes a more 'system-level' point of view and prescribes limits for harmonic currents for a facility as a whole, including one or more harmonic producing loads.

### **1.2.5. Voltage Fluctuations and Flicker**

Voltage flicker is not directly caused by electronic loads except in the largest of applications. Voltage fluctuations, and the corresponding light flicker due to them, where are usually created by large power fluctuations at frequencies less than about 30 Hz. In most applications, only

1. Large DC arc furnaces and welders,
2. Reactive power compensators, and
3. Cyclo converters

are potentially problematic. Each of these types of end-use devices can create large, low-frequency (about 30 Hz or less) variations in the system voltage, and can therefore lead to voltage flicker complaints. At this time, the IEEE prescribes a 'flicker curve' based originally on research conducted by General Electric. The IEC, however, has adopted a different methodology that can consider voltage fluctuations and flicker that are more complex than those considered by the IEEE flicker curve.

Most equipment are not sensitive to the voltage fluctuations that cause flicker complaints. The change in output of incandescent lamps as viewed by human observers becomes objectionable at levels of change around 0.3%, but electronic equipment will not be affected at all. Because most utility supply companies limit voltage fluctuations, regardless of the frequency of repetition, to less than a few percent, equipment malfunction or damage due to flicker is very rare.

Because of the advances in power electronics that have offered devices with higher power ratings, reactive compensation systems have been developed to compensate for voltage fluctuations by adding or removing reactive power from the supply circuit. These devices have allowed large flicker-producing loads like arc furnaces to be served from utility circuits. However, because the compensators can directly impact system voltage, they can create flicker problems if they are not properly applied and controlled.

### **1.2.6. Transients**

Transients, especially in the voltage supply, can create numerous power quality problems. The major sources of transients are

1. Lightning,
2. Utility circuit switching and fault clearing,
3. Capacitor switching and
4. Load switching.

Lighting events can create the most severe overvoltages, but these transients decay rapidly. A typical lightning transient has decayed to zero in a few hundred microseconds, but it can reach a peak magnitude of several hundred percent if not controlled with surge suppression devices. Other categories of transients associated with power system switching are much smaller in magnitude, but at least in the order of several hundred milliseconds. Considering the energy available in a transient, therefore, there is considerable overlap in the range of severity of lighting and switching transients. It is the available energy that typically determines whether or not equipment will be affected or damaged. The device's protection system sees these over currents as a fault, and trip the drive. Similarly, the over voltage at the terminals can be passed through to the DC bus and accumulate, where the drive may trip due to over voltage on the DC bus.

### **1.2.7. Monitoring and Measurement**

To consider or to diagnose power quality related problems, it is imperative to measure various power quality parameters. Several different categories of monitoring and measurement equipment exist for these purposes, with various costs for fully equipped disturbance analyzers.

The most basic category of power quality measurement tool is the hand-held voltmeter. It is important that the voltmeter be a true-rms meter, or erroneous readings will be obtained, that incorrectly suggest low or high voltage when harmonics are present in the signal. It is especially important to have true rms capability when measuring currents; voltage distortion is not typically severe enough to create large errors in the reading of non-true-rms meters. Virtually all major measurement equipments are true-rms meters.

The next step up from the basic voltmeter is a class of instruments that have come to be called 'power quality analyzers'. These instruments are hand held and battery powered. These instruments can measure and display various power quality indices, especially those that relate to harmonics like THD, etc., and can also display the input waveform. New models feature 20MHz (and higher) bandwidth oscilloscopes, inrush measurements, time trending, and other useful features. Manufacturers such as Fluke, Dranetz, BMI, and Tektronix offer these types of instruments.

In most power quality investigations, it is not possible to use handheld equipment to collect sufficient data to solve the problem. Most power quality problems are intermittent in nature, so some type of long-term monitoring is usually required. More advanced long-term monitors can record numerous power quality events and indices, including transients, harmonics, sags, flicker, etc. These devices are often called 'line disturbance analyzers'.

It is important to use the right instrument to measure the phenomenon that is suspected to cause the problem. Some meters record specific parameters, while others are more flexible. With this flexibility comes an increased learning curve for the user, so it is important to spend time on them before going out to monitor, to make sure all aspects and features of the equipment are understood.

It is equally important to measure in the correct locations. The best place to measure power quality events is at the equipment terminals that are experiencing problems. With experience, an engineer can evaluate the waveforms recorded at the equipment terminals and correlate them to events and causes elsewhere, in the power system. In general, the farther away from the equipment location the monitoring takes place, the more difficult it can be to diagnose a problem.

### **1.3. Organization of the Thesis**

The work reported in the thesis is organized into six chapters.

Chapter 1: This chapter provides introduction and the power quality problems and power quality improvements.

Chapter 2: This chapter provides the complete and detailed review of the literature surveyed. This chapter also explains the motivation for taking up the research problem and objectives of the research carried out.

Chapter 3: This chapter describes the basic concepts and theory of Flexible AC Transmission System Controllers, Power quality improvement and the concept of UPQC.

Chapter 4: This chapter deals with modeling and simulation of two bus system. Variation of reactive and real powers with the variation in the magnitude and angle of injected voltage is presented.



Chapter 5: This chapter deals with the modeling and simulation of eight bus system and the power quality improvement in eight bus system using UPQC.

Chapter 6: This chapter discusses the modeling and simulation of fourteen bus system and the power quality improvement with UPQC. This chapter also presents voltage sag compensation in 14 bus system using UPQC.

Chapter 7: This chapter deals with use of multiple UPQCs in thirty bus system. The effect of UPQC on real & reactive powers are studied.

Chapter 8: This chapter deals with modelling and simulation of fifty bus system.

Chapter 9: This chapter summarizes the major contributions of research presented in various chapters. The conclusion of the research work presented. This chapter also provides the direction for future work and possible extensions.

#### **1.4. Summary**

The fundamentals of power quality are presented in this chapter. The concepts about voltage sags, grounding, and transients are introduced.

## CHAPTER 2

### LITERATURE REVIEW

#### 2.1. General

Unified power quality conditioner (UPQC) is a combination of Dynamic Voltage Restorer (DVR) and Active Filter (AF). Unified power flow controller (UPFC) was used for power quality improvement. The UPFC is constructed from two power electronic inverters which are connected together by a common DC link. Two transformers are used to isolate the UPFC and to match the voltage levels between the power system and the power electronic inverters. One of the inverters is connected to the transmission line. The series connected inverter can generate a voltage which can have adjustable magnitude and phase angle. This inverter therefore can provide both real and reactive power to the transmission line. The second inverter primarily provides the real power required by the series inverter and it can also operate as an independent VAR compensator. Therefore the UPFC can control the flow of real and reactive power in the transmission line.

The two VSIs can work independently by separating the DC side. So in that case, the shunt inverter operates as a STATCOM that generates or absorbs reactive power to regulate the voltage magnitude at the connecting point. The series inverter operates as SSSC that generates or absorbs reactive power to regulate the current flow, and hence the power flow on the transmission line is regulated.

The UPFC can be used to improve the power quality due to the separate controlling capability of real and reactive power. In this proposed work two bus system is modeled and simulated with UPFC. A 14 bus system is also modeled and simulated with or without UPFC. The real and reactive power are investigated

and observed. The real power increases with the increase in the angle of injection. The reactive power increases with the shunt voltage injection.

## **2.2. Literature Survey**

From IEEE Transactions on power delivery, the UPFC, which was proposed by Gyugyi in 1991, is one of the most complex FACTS devices in a power system today. It is primarily used for independent control of real and reactive power in transmission lines for a flexible, reliable and economic operation and loading of power system. Until recently, all three parameters that affect real and reactive power flow on the line, i.e. the line impedance, voltage magnitudes at the terminals of the line and power angle, were controlled separately using either mechanical or other FACTS devices such as a Static Var Compensator (SVC), a Thyristor Controlled Series Capacitor (TCSC), a phase shifter, etc. However, the UPFC allows simultaneous or independent control of these parameters with transfer from one control scheme to another in real time. Also, the UPFC can be used for voltage support, transient stability improvement and damping of low frequency power oscillations.

UPFC, which consists of a series and shunt converter connected by a common DC link capacitor can simultaneously perform the function of transmission line's real and reactive power flow control in addition to bus voltage shunt reactive power control (Schauder et. al. 1998). The shunt converter of the UPFC controls the UPFC bus voltage/shunt reactive power and the DC link-capacitor voltage. The series converter of the UPFC controls the transmission line real/reactive power flows by injecting a series voltage of adjustable magnitude and phase angle (Renz et. al. 1999). The interaction between the series injected voltage and the transmission line current leads to real and reactive power exchange between the series converter and power / system. Under steady state conditions, the real power demand of the series converter is supplied by the shunt converter (Mihilac et. al. 1996). But during transient conditions, the series converter's real

power demand is supplied by the DC link capacitor. If the information regarding the series converter's real power demand is not conveyed to the shunt converter control system, it could lead to the collapse of the DC link capacitor voltage, and the subsequent removal of the UPFC from operation. Very little or no attention has been given to the important aspect of co-ordination control between the series and the shunt converter control systems (Padiyar et. al. 1998 and Round et. al. 1996).

From European Journal of scientific research, in contrast to real power coordination between the series and shunt converter control system, the control of transmission line reactive power flow leads to excessive voltage excursions of the UPFC bus voltage during reactive power transfers. This is due to the fact that any change in transmission line reactive power flow achieved by adjusting the magnitude/phase angle of the series injected voltage of the UPFC is actually supplied by the shunt converter. The excessive voltage excursion of the UPFC bus voltage is due to the absence of reactive power coordination between the series and the shunt converter control system. This aspect of UPFC control also has not been investigated (Nashiren.F; Mailah et. al. 2009).

From IEE proceedings – Generation, Transmission and Distribution, the feasibility of achieving a dynamic voltage restoration without the use of the injection transformer is investigated by Li et. al. (2002). The injection transformer used in the conventional DVR is expensive, bulky and contributes towards losses. From the design, operation and maintenance point of view, the transformer is an added complexity to the restorer. Investigation is made into the feasibility of the DVR without the injection transformer. It shows that by introducing a separate DC link/energy storage in each phase, and a cascaded switch/ inverter connection as well as online energy replenishing charging circuitry, the proposed transformer-less DVR can satisfactorily mitigate the voltage sag problems. The design is promising, as it indicates a less costly restorer of a more compact structure.

Hongfa Ding et. al. (2002) presented a novel DVR consisting of a conventional three phase voltage source inverter together with an emitter follower and it is applicable in unbalanced three phase four wire power distribution system. The three phase voltage source inverter is used to eliminate the adverse influences of the negative sequence components of the load voltage and to restore the load voltage to the given level, while the emitter follower is used to eliminate the zero sequence components.

The modeling aspects of the DVR working against voltage sags by simulation in the PSCAD/EMTDC have been presented by Nguyen et. al. (2004). First, a DVR using a six-pulse inverter, and a three phase Root Mean Square (RMS) voltage measurement and sine wave PWM control was described. The DVR provides excellent performance to protect critical loads against balanced voltage sags. Then, a DVR using single-phase RMS voltage measurement, which works very well against not only balanced voltage sags but also unbalanced ones, resulting from both single line and line - line faults was presented. Finally, the study of the DVR capability and performance was examined thoroughly.

Chairs Fitzer et. al. (2004) presents and verify a novel voltage sag detection technique for use in conjunction with the main control system of a DVR. It is necessary for the DVR control system not only to detect the start and end of the voltage sag but also to determine the sag depth and any associated phase shift. The DVR, which is placed in series with a sensitive load, must be able to respond quickly to voltage sag. A problem arises when fast evaluation of the sag depth and phase shift is required, and this informer is not readily available to either user monitoring the state of the grid or parallel controllers. Typical standard information tracking or detection methods such as the Fourier transform or phase-locked loop are too slow in returning this information. As a result of this the voltage sag detection method in this work proposes a new matrix method, which is

able to compute the phase shift and voltage reduction of the supply much quicker than the Fourier transform.

Kaifei Wang et. al. (2004) described an uninterrupted three phase DVR based on three phase four wire inverter. A rectifier is used to supply the inverter of DVR and it makes the DVR compensate sag continuously. The soft phase locked loop method is used to detect the source voltage. The inverter is controlled by voltage space vector PWM algorithm that is different from the traditional method. This SVPMM produces low harmonics in the output.

Hyosung Kim and seung-Ki Sul (2005) discussed the control of the compensation voltages in dynamic voltage restorers (DVR). The power circuit of a DVR system is analyzed in order to come up with control limitations and control targets for compensation voltage control. Based on this power stage analysis, a combined feed forward and state feedback control structure for the compensation voltages of DVRs is developed. Digital control systems normally have control delay from the sampling period, the switching frequency of the inverter, the sensor transmission time, etc. The control performance related with the control delay, closed loop damping factor, and the output filter parameters in DVR systems are analyzed and design guidelines are proposed for the control gains and the inverter switching frequency of DVRs.

Oscar and Prasad (2005) developed an algorithm that provides a reliable and fast detection method for voltage disturbances, such as voltage sags, swells, flicker, frequency change in the utility voltage and harmonic distortion. The algorithm is based on the theory that allows a set of three phase voltages which can be presented as DC voltages in a d-q synchronous rotating frame. In this work, the utility input voltages are sensed and then converted to DC quantities in the d-q reference frame. Thus any disturbance / at the utility input voltage will be promptly reflected as disturbances in the d-q values. The analysis, simulation and experimental results are presented for a three phase system.

The performance of a DVR in mitigating voltage sags/swells is demonstrated with the help of MATLAB. The DVR handles both balanced and unbalanced situations without any difficulty and injects the appropriate voltage component to correct any anomaly in the supply voltage to keep the load voltage balanced and constant at the nominal value. In the case of voltage sag, which is a condition of a temporary reduction in the supply voltage, the DVR injects an equal positive voltage to correct it. This is done by using a step up transformer. On the other hand, the voltage swell case, which is a condition of a temporary increase in the supply voltage, the DVR injects an equal negative voltage in all the three phases, which are anti-phase with the supply voltage. For unbalanced conditions, the DVR injects an appropriate unbalanced three phase voltage component, positive or negative, depending on whether the condition is an unbalanced voltage sag or unbalanced voltage swell (Paisan Boonchiam et. al. 2006).

Bingsen Wang et. al. (2006) described the detailed design of a closer loop regulator to maintain the load voltage within acceptable levels in a DVR using a transformer coupled H bridge converters. The multiloop regulator with complex state feedback decoupling is designed with an inner current loop and outer voltage loop. Detailed numerical simulation has been carried out using MATLAB to verify the power circuit operation and control scheme. A laboratory scale experimental prototype was developed that verifies the, power circuit operation and controller performance. The experimental results indicate an excellence with the digital simulations.

Poh Chiang Loh et. al. (2004) described a detailed analysis on Z source inverter modulation, showing how various conventional PWM strategies for controlling a conventional VSI can be modified to switch a voltage type Z source inverter either continuously or discontinuously. Through the proper placement of shoot-through states, Z source inverter modulation can be made to reproduce the desired performance features of various reported conventional PWM strategies.

The theoretical and modulation concepts presented have been verified both in simulation and also experimentally.

Mahinda Vilathgamuwa et. al. (2006) proposed a new topology based on the Z source inverter for the DVR, in order to enhance the voltage restoration property of the device. The Z source impedance network along with the shoot-through capability of the proposed inverter would ensure a constant DC voltage across the DC link, despite dwindling voltage in the storage devices connected in the DC link during the process of voltage compensation. A new topology derived from the Z source inverter enhances the capability of the DVR through better utilization of the stored energy. Moreover, it incorporates enhanced electromagnetic of the developed DVR system and its controller was tested with simulations and experiments. It was observed that the DVR compensates the disturbance caused by a sag effectively, while utilizing the stored energy fully by the use of the buck -boost capability of the proposed Z source inverter.

Liew Zhan Liu et. al. (2007) presented a dynamic Voltage Restorer (DVR) system using a three dimensional space vector pulse width modulation (3D-SVPWM). In the proposed 3D-SVPWM control scheme, the inclusion of zero-axis, in addition to conventional alpha-beta axes, enables the mitigation of zero sequence components. The two null switching vectors, which are located at the origin in alpha-beta two dimensional spaces, are now separated into two totally independent vectors in the opposite directions. It is a versatile voltage sag compensating solution that can be applied to restore fault-affected three-phase power system.

Rosli Omar and Nasrudin Abd Rahim (2008) discussed the control for DVR biased on d-q transformation. A control system is based on d-q technique in which a scaled error of the source side of the DVR and its reference for sags/swells/correction, has been presented. The DVR compensates the sags/swells



quickly and provides excellent voltage regulation. The DVR handles both balanced and unbalanced situations without any difficulties and injects the appropriate voltage component to keep the load voltage balanced and constant at the nominal value.

Chi- Seng Lam et. al. (2008) discussed Voltage swell and overvoltage compensation problems in a diode bridge rectifier supported transformer-less coupled DVR. When a swell or over voltage happens, applying a conventional in phase or phase invariant boosting method causes a rapid rise in the DC link voltage, which may damage the storage capacitors and switching devices, and increase the switching loss. This work proposed a novel unidirectional power flow control algorithm with DVR maximum compensation limit consideration, which can effectively suppress problems of a continuous rise in the DC link voltage. The simulation and experimental results for unbalanced voltage swell compensation are presented.

Chellai Benachaiba and Brahmin (2008) describe principles of DVR and voltage restoration methods at the point of common coupling. The problem of voltage sags and swells and its severe impact on sensitive loads are well known. One of those devices used to solve this problem is the DVR, which is the most efficient and effective modern custom power device used in power distribution networks. Its appeal includes lower costs, smaller size, and fast dynamic response to the disturbance.

Ahmed A. Helal and Mohamed H. Saied (2008) presented a DVR based on a new firing control strategy for the three six switch Voltage Source Inverter(VSI). In this firing control strategy, one of the three- inverter legs is to be intentionally opened, in a pre-planned sequence. This strategy combines the commonly used 180° and 120° conduction modes to generate a new operating mode, defined as the 150° conduction mode. Thus, the inverter primarily obtains a

seven level, 12 step output voltage waveforms, which resemble the sinusoidal wave shape.

Naidu and Fernandes (2009) described the closed loop control of a four leg Voltage Source Converter based DVR. The three phase input variables are resolved into positive, negative and zero sequence components using a weighted, recursive, least square estimator. A laboratory model of the restorer has been constructed and its performance has been tested by simulation using MATLAB and experiments.

Sasitharan and Mahesh K. Mishra (2009) proposed a filter structure for improving the performance of switching band controller based DVR. The control method of the VSI inherits merits, such as fast dynamic response, robustness, zero magnitude/phase errors and ease of implementation. The proposed filter structure and the adaptive band controller for the DVR are presented by carrying out PSCAD simulation studies.

Ahad. Kazemi and Ali Azyhadast (2009) described the design and operation of a three phase DVR, including control strategies which are evaluated through simulation studies. The simulation results show that the proposed voltage sag compensator is able to protect sensitive loads against short term voltage disturbances, and can be an attractive alternative to low short term voltage disturbances, and also can be an attractive alternative to low voltage Uninterruptible Power Supply. Compared with the conventional DVR topologies, the voltage sag compensator considered here, presents the advantages of reduced switch count, no energy storage systems and the smaller ratings of the power converters. The use of converters with a reduced number of switches, however, increases the overall rating of the DC link capacitor bank.

Jowder (2009) proposed a DVR which can compensate deep and long duration voltage sag and simultaneously compensate steady state harmonics. The DVR consists of shunt and series converters connected back-to-back through a DC to DC step-up converter. The presence of the DC to DC converter permits the DVR to compensate deep voltage sags for a long duration. The series converter is connected to the load side. With this configuration, there is no need for large DC capacitors. A design procedure for components of the DVR is presented under a voltage sag condition. The control system of the proposed DVR is based on hysteresis voltage control. Besides voltage sag compensation, the capability of compensating load voltage harmonics has been added to the DVR to increase the power quality benefits to the load, with an almost negligible effect on the sag compensation capability. The proposed DVR is modeled and simulated using the MATLAB/SIMULINK package.

The modeling and simulation of a DVR using PSCAD/EMTDC has been presented by Rosli Omar and Nasrudin Abd Rahim (2009). The conversion efficiency of the DVR depends on the efficiency of the control technique involved in switching the inverter. The DVR handled both balanced and unbalanced situations without any difficulty, and injected the appropriate voltage component to correct rapidly any anomaly in the supply voltage to keep the load voltage balanced and constant at the nominal value. The results of the PSCAD/ EMTDC simulation also verify the proposed control algorithm based on the space vector modulation technique to generate the pulses.

Pedro et. al. (2009) proposed a repetitive controller which has a fast transient response and ensures zero error in the steady state for any sinusoidal reference input and for any sinusoidal disturbance whose frequencies are an integer multiple of the fundamental frequency. To achieve this, the controller has been provided with a feed forward term and a feedback term. The design has been carried out by studying the stability of the closed loop system including possible

modeling errors, resulting in a controller which possesses very good transient and steady state performances for various kinds of disturbances. Only one controller is required to eliminate three pq disturbances, namely, voltage sags, harmonic voltages and voltage imbalances. The well-developed graphical facilities available in the PSCAD/EMTDC are used to carry out all modeling aspects of the repetitive controller and test system. The simulation results show that the control approach performs very effectively and yields excellent voltage regulation.

Wijekoon et. al. (2003) proposed a new concept of the Interline Dynamic Voltage Restorer where two or more DVRs in different feeders are connected to a common DC link, while one of the DVR compensates the voltage sag, the other DVR connected to a common DC link replenishes the DC link energy storage. The proposed multiloop feedback control system is identical for both voltage regulation and the real power control modes. The only difference is the way in which the reference signal is generated, and it depends on the mode of operation. In the real power flow control mode the reference is generated according to the real power requirement demanded by the faulty line. The analysis shows that the two line Interline Dynamic Voltage Restorer system can mitigate about 40% voltage sag for a long duration, which appears in one of the lines. The limiting factor of the amount of real power that can be transferred from one line to the DC link as the load power factor. The power transfer capacity from the healthy lines to the DC link can be further increased if the number of DVRs connected to the DC link are increased.

The concept of the IDVR in which several DVRs are connected to a common DC link energy storage is proposed (Mahinda Vilathgamuwa et. al. 2004). The capability of a particular DVR to compensate long duration voltage sag depends mainly on the amount of energy stored within the DVR. This work has proposed a new concept of the IDVR which can minimize the DC link energy storage connecting two or more DVRs to a common DC link. One of the DVRs

replenishes the DC link energy storage to maintain the DC link voltage. A current mode voltage regulator has been used for controlling the converters of the IDVR system in both the modes, voltage sag compensation and power flow control. The reference signal for the power flow control mode is generated using the instantaneous active current calculated from the DC link error signal, while software PLL incorporating the Kalman filter is used to derive the reference signal for the voltage sag compensation mode. The simulation results are presented to verify the efficacy of the proposed IDVR design. The limiting factor of the proposed IDVR system is that the amount of real power that can be transferred to the DC link energy storage depends on the load power factor.

The concept of the IDVR, which is an economical approach to improve multiline power quality is proposed (Mahinda Vilathgamuwa et. al. 2006). As the voltage restoration process involves real power injection into the distribution system, the capability of a particular DVR topology, especially for compensating long duration voltage sags, depends on the energy storage capacity of the DVR. The IDVR consists of several DVRs, which are electrically far apart, connected to a common DC link. When one of the DVRs compensates the voltage sag appearing in that feeder, the other DVRs in the IDVR system work in the power flow control mode. The control scheme for the IDVR includes a multiloop feedback control system, which is identical for both voltage compensation and real power control. The experimental results are shown to improve the quality.

The concept of Inter line Dynamic Voltage Restorer is discussed. This device consists of two conventional DVRs which are installed in two different distribution feeders and in the DC link capacitor. DVR which is installed in low voltage feeder operates in voltage sag compensation mode. A novel control technique minimizes the energy flow from DC link capacitor to this feeder. The DVR, which is installed in medium voltage feeder, controls the voltage of DC link capacitor. The proposed device and its new control strategy have been modeled

and simulated by PSCAD/EMTDC. The results verify the effectiveness of IDVR and the suggested control method (Banaei et. al. 2006)

The design strategy for optimizing the total rating of an IDVR is presented (Karshenas and Moradiou 2008). An IDVR, which is two DVRs installed in two feeders with a common DC bus, has the ability of active power exchange between two DVRs, and thus the energy storage device is not an issue. Therefore, the design criteria for the selection of the rating of an individual DVR is not applicable to the IDVR obtained. A new step-by-step design procedure is proposed with the objective of the optimum selection of the rating for an IDVR structure.

A mathematical model of the Interline Power Flow Controller in the steady state has been developed (Diez-Valenica et. al. 2002). The model was used to investigate the operating limits based on the controllability of the power flow in the transmission line due to the initial loading levels in the network. It is shown that the range of power flow control could be maximized using special control strategies.

To improve the energy quality in distribution systems, many different solutions have been implemented like active filters, the UPFC, the UPQC and the IPFC. The IPFC concept using a probabilistic approach to the distribution system decreases the power rating of the parallel active filters when it is a component of the IPFC (Ryszard Strzelecki et. al. 2002).

An integrated approach of the radial basis function neural network and fuzzy scheme with a genetic optimization of their parameters has been developed to design intelligent adaptive controllers for improving the transient stability performance of power system (Mishra et. al. 2002). This concept is applied to a simple device, such as the Thyristor Controlled Series Capacitor (TCSC)

connected to the IPFC, connected in a multi machine power system. By combining both the intelligent techniques, the control strategy becomes less mathematical, and hence, it is faster in computation. The new neuro-fuzzy based control scheme adapts itself to generate a suitable variation of the control signals, depending on the operating condition of the power system, and hence, a superior performance in comparison to the linear PI controllers is used for the IPFC and TCSC.

The use of fuzzy logic in order to achieve a better co-ordination between the inverters that constitute the IPFC to improve their capability to track reference signals, has been presented (Menniti et. al. 2002). The proposed IPFC controller consists of a conventional controller based on the linear quadratic regulator technique, and a non-conventional controller based on fuzzy logic. Some simulation cases are considered to compare the performance of the proposed controller with respect to that of other conventional controllers. For this investigation an Electromagnetic Transients Program is used as a study tool.

Mathematical models of the IPFC and Generalized UPFC and their implementation in the Newton power flow have been presented (Zhang 2003). Numerical results based on the IEEE 30-bus, 118-bus and 300-bus systems are presented to demonstrate the performance of the Newton power flow algorithm with the incorporation of the IPFC and UPFC. In the test, some extreme power flow control cases for blocking the reactive power flow by the FACTS controllers have also been investigated. The blocking capability of the reactive power flow will be helpful in operating the networks efficiently, while reducing the active power losses.

A new dispatch strategy for an IPFC operating at rated capacity is proposed (Xuan Wei et. al. 2004). When an IPFC operates at its rated capacity, it can no longer regulate the line active power flow set points or the reactive power flow set points or both. In such cases, the dispatch strategy switches to a power

circulation set point control to co-optimize both series VSCs, without exceeding one or both the rated capacities. The concept is used to generate PV curves associated with the voltage stability analysis for maximizing power transfer. The modeling and computation are performed using a Newton-Raphson load flow algorithm. The voltage stability curves for two test systems are shown to illustrate the effectiveness of this proposed strategy.

An optimal power flow control in electric power systems incorporating the IPFC is presented (Jun Zhang and Akihiko Yokoyama 2006). The injection models of both the IPFC and the transmission lines embedded in the IPFC, which can be easily incorporated in load flow programs and optimal power flow programs are developed.

A new, simple approach based on a quadratic equation and its solution to model and analyze the series connected multiline VSC based FACTS controllers, namely, the Generalized Interline Power Flow Controller (GIPFC) and the IPFC have been presented (Leon Vasquez-Arnez et. al. 2007). The model and the analysis developed are based on the converter's power balanced method which makes use of the d-q orthogonal coordinates.

The regulation modes of an IPFC and its control strategies at rated capacity are discussed (Xia Jiang et. al. 2007). Based on this, the voltage stability limited IPFC dispatch on a 20 bus system is investigated. The dispatch results show that the IPFC can improve the power transfer in the system. A model decomposition approach is proposed to select the best damping control input signals. Damping control signals are selected based on two indices derived from effective control actions. Dynamic simulations show the damping effect of the controller designs, using selected signals.



A novel power injection model of the IPFC, suitable for power flow analysis, is described (Yankui Zhang et. al. 2006). In this model, the impedance of the series converter coupling transformer and the line charging susceptance are all included, while the original structure and symmetry of the admittance matrix can still be retained. Furthermore, the model can take into account the practical constraints of the IPFC. The power flow control capability and the constraints enforcement of the IPFC are also detailed.

In IEEE Transactions on power delivery, Padiyar and Nagesh Prabhu (2007) present the modeling of the IPFC of the IPFC with 12-pulse, three-level converters, and investigate the sub synchronous resonance characteristics of the IPFC at different operating modes. The application of the D-Q model is validated by the transient simulation of the three-phase model of the IPFC. It is observed that the D-Q model is quite accurate in predicting the system performance. The effectiveness of the various operating modes of the two VSCs comprising the IPFC in damping sub-synchronous resonance has been investigated.

A modified control strategy for UPFC (Jason Yuryevich and Kit Po Wong 1999) has been described. This indicates that broad study of UPFC is progressing accordingly to further explore its application, modeling and control strategy. Determination of UPFC parameters can also alter the solution in power flow. This is termed as optimal power flow, required optimization technique considering a particular objective function. Evolutionary programming was used to solve optimal power flow.

The voltage profile improvement using UPFC approach based on Artificial Immune System (AIS) optimization engine is developed (Ismail Musirin et. al. 2008). The voltage profile improvement which utilized UPFCs as control variables embedded into the system's data. Implementation on the IEEE reliability test system considering several variations in the AIS properties indicated AIS potential in solving voltage control problems.

Injection of the wind power into an electric grid affects the power quality. The performance of the wind turbine and thereby power quality are determined on the basis of measurements and the norms. The influence of the wind turbine in the grid system concerning the power quality measurements are the active power, reactive power, variation of voltage, flicker, harmonics, and electrical behavior of switching operation are measured to demonstrate the power quality problem due to installation of wind turbine with the grid. In this proposed scheme STATic COMpensator (STATCOM) is connected at a point of common coupling with a battery energy storage system (BESS) to mitigate the power quality issues. The battery energy storage is integrated to sustain the real power source under fluctuating wind power. The STATCOM control scheme for the grid connected wind energy generation system for power quality improvement is simulated using MATLAB/SIMULINK in power system block set. The effectiveness of the proposed scheme relieves the main supply source from the reactive power demand of the load and the induction generator.(Sharad et. al. 2010)

Yan Zhang and Jovica V. Milanovic (2010) presents an approach to optimally select and allocate flexible AC transmission (FACTS) devices in a distribution network in order to minimize the number of voltage sags at network buses. The method proposed is based on the optimization of a preselected objective function using simple and niching genetic algorithms (GA). The objective of the optimization is to achieve the improvement in overall system sag performance of the network. Using proposed GA-based optimization, the location, the type and the rating of six (in total) FACTS devices are optimized simultaneously. Three types of FACTS devices are implemented in this study, namely, static var compensator, static compensator, and dynamic voltage restorer.

Khadkikar et. al. (2006) presents a new, simple and effective approach to estimate the required quadrature injected voltage during utility voltage sag condition. This approach helps in voltage sag compensation through reactive power control using series part of unified power quality conditioner, generally termed as UPQC-Q. Thus utility sag compensation can effectively be done without utilizing any active power from source or from the inverter side. Moreover, this quadrature voltage injection during voltage sag compensation also helps to improve the source side power factor, which results in reduced shunt active power filter (APF) loading. The voltage harmonic compensation based on d-q transformation simultaneously with voltage sag compensation is also presented.

One of the comparative structures of the electric power is back to back converter. In respect to controlling structure, these converters may have various operations in compensation. For example, they can operate as series or shunt active filters for compensating the load current harmonics and voltage oscillation (Akagi et al., 2007). This is called UPQC (Areades and Watanabe, 1995).

UPQC is greatly studied by Akagi and Fujita, (1995), (Fujita and Akagi, (1998), as a basic device to control the power quality. The duty of UPQC is to reduce perturbations which affect the operation of sensitive loads. UPQC is able to compensate voltage using shunt and series inverters. In spite of this issue, UPQC is not able to compensate voltage interruption and active power injection to grid, because in its DC link, there is no energy source.

M.Hoseinpot and A.Yazdian(2008) presents an approach to generation of electricities from renewable and UPQC to improve the power quality.

M.Davati(2011) presents an approach to modeling the combination of UPQC and photovoltaic arrays with Multi - Input Single - Output DC-DC converter.

A.Jeraldine Viji and M.Suahakaran (2012) presents a new, simple and effective approach to compensate a technique of achieving both active current distortion compensation, power factor correction and also mitigating the supply voltage variation of the load side is compensated by UPQC.

The attention to Distributed Generating (DG) sources is increasing day by day. The reason is the important roll they play in the future of power system (Blaabjerg et al., 2004; Barker and De Mello, 2000). Recently, several studies were accomplished in the field of connecting DGs to grid using power electronic converters. Here, grid's interface shunt inverters are considered more where the reason is low sensitive of DGs to grids parameters and DG power transferring facility using this approach. Although DG needs more controls to reduce the problems like grid power quality and reliability, Photovoltaic array (PV) energy is one of the distributed generation sources which provides a part of human required energy nowadays and will also provide it in the future. The greatest shares of applying this kind of energy in the future will be its usage in interconnect systems. Nowadays, European countries have shown inter – connected systems development in their countries by choosing supporting policies. In this study, UPQC and PV combined system have been presented. UPQC introduced by (Chen et al., 2000), has the ability to compensate voltage sag and swell, harmonics and reactive power.

### **2.3. Scope of present investigation**

The above literature does not deal with modeling of UPQC - based eight, fourteen, thirty and fifty bus systems using MATLAB / SIMULINK. This

work proposes models for 14, 30 and 50 bus systems employing UPQC. The effects on real power, reactive power and voltage are not investigated.

This work deals with the control of real and reactive power in power system using UPQC. The above mentioned papers do not deal with the use of multiple UPQCs in fourteen/thirty/fifty bus systems. This work proposes multiple UPQCs for medium scale power systems to improve the power quality. The parameters considered are voltage, real power and reactive power.

#### 2.4. Research problem

Line data and load of multibus system are specified. It is required to model and simulate multibus system using the blocks of Simulink. The following equations are used for calculating the real and reactive powers.

$$P_{ik} = \frac{V_i V_k}{Z_{ik}} \sin(\delta_i - \delta_k) \quad (1.1)$$

$$Q_{ik} = \frac{V_k}{Z_{ik}} (V_i - V_k) \cos(\delta_i - \delta_k) \quad (1.2)$$

It is required to improve the voltage by using an inverter that can inject voltage with minimum harmonics.

It is also required to improve the voltage profile of the line. In order to improve the voltage profile, multiple UPQC systems are attempted.

#### 2.5. Solution Methodology

The proposed work deals with modeling and simulation of two, fourteen, thirty and fifty bus systems with and without UPQC. This work also

covers the variation of real power with variation in the angle of injected voltage. The effect of variation of reactive power with the variation in the magnitude of voltage is studied.

All the cases are modeled and simulated using MATLAB simulink version 7.9.(Sim Power Systems). The MATLAB uses state space modeling to solve the currents, voltages and powers in the network.

## **2.6. Summary**

This chapter deals with literature survey, scope and outline of the present investigation.

## CHAPTER 3

### POWER SYSTEM CONTROL USING FACTS CONTROLLERS

#### 3.1. General

The chapter deals with introduction to various types of FACTS controllers. The flexible AC transmission systems (FACTS) concept based on applying leading edge Power Electronics Technology to existing AC transmission systems, improves the stability to increase usable power transmission capacity to its thermal limit. A UPFC can simultaneously provide control of the transmission line impedance, phase angle and voltage.

With the ongoing expansion and growth of the electric utility industry, including deregulation in many countries, numerous changes are continuously being introduced to a once predictable business. Although electricity is a highly engineered product, it is increasingly being considered and handled as a commodity. Thus, transmission systems are being pushed closer to their stability and thermal limits while the focus on the quality of power delivered is greater than ever.

In the evolving utility environment, financial and market forces will continue to, demand a more optimal and profitable operation of the power system with respect to generation, transmission, and distribution. Now, more than ever, advanced technologies are paramount for the reliable and secure operation of power systems. To achieve both operational reliability and financial profitability, it has become clear that more efficient utilization and control of the existing transmission system infrastructure is required. Improved utilization of the existing power system is provided through the application of advanced control technologies. Power electronics based equipment, or FACTS, provide proven

technical solutions to address these new operating challenges being presented today. FACTS technologies allow for improved transmission system operation with minimal infrastructure investment, environmental impact, and implementation time compared to the construction of new transmission lines. Traditional solutions to upgrade the electrical transmission system infrastructure have been primarily in the form of new transmission lines, substations, and associated equipment. However, as experiences have proven over the past decade or more, the process to permit, site, and construct new transmission lines has become extremely difficult, expensive, time-consuming, and controversial.

FACTS technologies provide advanced solutions as cost-effective alternatives to new transmission line construction. The potential benefits of FACTS equipment are now widely recognized by the power systems engineering and T&D communities. With respect to FACTS equipment, voltage sourced converter (VSC) technology, which utilizes self-commutated thyristors/transistors, has been successfully applied in a number of installations world-wide.

### **3.2. Power Transfer Limit**

One or more of the following network characteristics limits power flow over a transmission system.

- Stability limit
- Thermal limit
- Voltage limit
- Loop flow

Technically limitations on power transfer can always be removed by adding new transmission and/or generator capacity. FACTS are designed to remove such limitations and meet the operator's goals without having to understand major system additions.



### 3.3. Power System Constraints

As noted in the introduction, transmission systems are being pushed closer to their stability and thermal limits while the focus on the quality of power delivered is greater than ever. The limitations of the transmission system can take many forms and may involve power transfer between areas (referred to here as transmission bottlenecks) or within a single area or region (referred to here as a regional constraint) and may include one or more of the following characteristics:

- Steady-State Power Transfer Limit
- Voltage Stability Limit
- Dynamic Voltage Limit
- Transient Stability Limit
- Power System Oscillation Damping Limit
- Inadvertent Loop Flow Limit
- Thermal Limit
- Short-Circuit Current Limit
- Others

Each transmission bottleneck or regional constraint may have one or more of these system-level problems. The key to solve these problems in the most cost-effective and coordinated manner is through systems engineering analysis.

### 3.4. Controllability of the Power Systems

To illustrate that the power system only has certain variables that can be impacted by control, consider the basic and well-known power-angle curve, shown in Fig.3.1. Although this is a steady-state curve and the implementation of FACTS is primarily for dynamic issues, this illustration demonstrates the point that there are primarily three main variables that can be directly controlled in the power system to impact its performance. These are

- Voltage (V)
- Angle between Bus Voltages ( $\delta$ )
- Impedance (Z)

One could also make the point that direct control of power is a fourth variable of controllability in power systems.

Fig.3.1 illustrates the controllability of power systems with the establishment of which variables can be controlled in power system and the solutions to control the variables are conventional equipment and FACTS controllers.

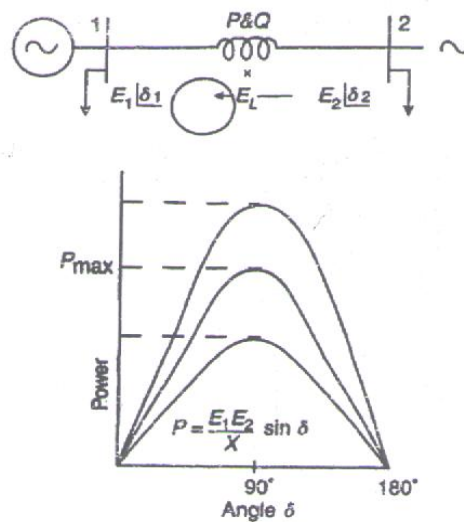


Fig.3.1 Controllability of Power System

### 3.5. Benefits of Control of the Power Systems

Once power system constraints are identified and through system studies viable solutions options are identified, the benefits of the added power system control must be determined. The following offers a list of such benefits:

- Increased Loading and More Effective Use of transmission Corridors
- Added Power flow Control
- Improved Power System Stability
- Increased System Security
- Increased System Reliability
- Elimination or Deferral of the Need for New Transmissions Lines

The advantages in this list are important to achieve in the overall planning and operation of power systems. However, for justifying the costs of implementing added power system control and for comparing conventional solutions to FACTS controllers, more specific metrics of the benefits to the power system are often required. Such benefits can usually be tied back to an area or region for a specific season and year at a defined dispatch (usually given by an ISO or equivalent) while meeting the following criteria, the examples are,

- Voltage Stability Criteria  
e.g., P-V voltage or power criteria with minimum margins e.g., Q-V reactive power criteria with minimum margins
- Dynamic Voltage Criteria  
e.g., Avoiding voltage collapse  
e.g., Minimum transient voltage dip/sag criteria (Magnitude and duration)
- Transient Stability Criteria
- Power System Oscillation Damping e.g., Minimum damping ratio

Each of the above listed items can usually be measured in terms of a physical quantity such as power transfer through a critical transmission interface, power plant output area or region load level. This allows for a direct quantification of the benefits of adding power system control and provides a means to compare such benefits by the various solution options considered, whether they be conventional or FACTS based.

### **3.6. Conventional devices For Enhancing Power System Control**

- Series Capacitor -Controls impedance
- Switched Shunt Capacitor and Reactor -Controls voltage
- Transformer LTC -Controls voltage
- Phase Shifting Transformer -Controls angle
- Synchronous Condenser -Control Voltage

- Special Stability Controls -Typically focuses on voltages control but can often include direct control of power
- Others (When Thermal Limits are Involved) - Can be included reconductoring, raising conductors, dynamic line monitoring, adding new lines, etc.

### **3.7. FACTS Technology**

The FACTS technology helps us to alleviate these difficulties by enabling utilities to get the maximum service from their transmission facilities and enhance grid reliability. FACTS technology is a collection of controllers which can control series impedance, shunt impedance, current, voltage and phase angle.

FACTS is nothing but the alternating current transmission systems incorporating power electronic-based and other static controllers to enhance controllability and increase power transfer capability. FACTS technology is a collection of controllers, which can be applied individually or in coordination with others to control one or more of the interrelated system parameters mentioned above.

FACTS Controller is power electronic-based system and other static equipment that provide control of one or more AC transmission system parameters.

When the power system is controlled through mechanical switches, there is no high-speed control. Also due to the increasing complexity of the power system, the grid operator is not able to meet the dynamic swings in the power system with the help of mechanical switches. As the mechanical switches tend to wear out quickly when compared to static electronic devices, the maintenance becomes tough and the life of the entire power system gets reduced.

As most of the transmission systems are AC transmission systems, FACTS technology is necessary to specify some but not all of these difficulties by enhancing the control over the transmission of power and to enhance the grid reliability with the same existing line itself, unlike HVDC where new transmission system has to be installed. FACTS pave way to control the current through the line at a reasonable cost. Hence, the capacity of the line can be increased with larger conductors. The FACTS controller enables the line to carry power closer to its thermal rating.

### **3.8. Relative Importance of Controllable Parameters**

- Control of the line impedance  $X$  can provide a powerful means of current control
- When the angle is not large, which is often the case, control of  $X$  or the angle substantially provides the control of active power
- Control of angle, which in turn controls the driving voltage, provides a powerful means of controlling the current flow and hence active power flow is controlled when the angle is not large
- Injecting a voltage in series with the line and with any phase angle with respect to the driving voltage can control the magnitude and the phase of the line current
- When the angle is not large, controlling the magnitude of one or the other line voltages can be a very cost-effective means for the control of reactive power -flow through the interconnection
- Combination of the line impedance control with a series controller and voltage regulation with a shunt controller can also provide a cost effective means to control both the active and reactive power flow between the two systems.

### **3.9. TYPES OF FACTS CONTROLLERS**

FACTS controllers can be divided into four categories.

#### **3.9.1. Series Controller**

Series Controller could be variable impedance or variable source. All series controllers inject voltage in series with the line. Variable impedance multiplied by the current flow through it, represents an injected series voltage in the line. As long as the voltage is in phase quadrature with the line current, the series controller only supplies or consumes variable reactive power.

#### **3.9.2. Shunt Controller**

Shunt Controller could be variable impedance, variable source or a combination of these. Shunt controllers inject current into the system at the point of connection. Variable shunt impedance connected to the line voltage causes a variable current flow and hence represents injection of current into the line. As long as the injected current is in phase quadrature with the line voltage, the shunt controller only supplies or consumes variable reactive power.

#### **3.9.3. Combined Series - Series Controller**

This could be a combination of separate series controllers, which are controlled in a coordinated manner, in multilane transmission system or it could be a unified controller in which series controllers provide independent series reactive compensation for each line and also transfer real power among the lines via the power link. The term unified means that the DC terminals of all controller converters are connected together for real power transfer.

### **3.9.4. Combined Series-Shunt Controller**

This could be a combination of separate shunt and series controllers, which are controlled in a coordinated manner, a Unified Power Flow Controller with series and shunt elements. Combined shunt and series controllers inject current into the system with the shunt part of the controller and voltage in series in the line with the series part of the controller.

### **3.10. CONTROLLERS FOR ENHANCING POWER SYSTEM CONTROL**

- Static synchronous Compensator (STATCOM) -Controls voltage
- Static VAR Compensator (SVC) -Controls voltage
- Unified Power Flow Controller (UPFC)
- Convertible Series Compensator (CSC)
- Inter-line Power Flow Controller (IPFC)
- Static Synchronous Series Controller (SSSC)

Each of the above mentioned (and similar) controllers impact voltage, impedance, and/or angle (and power)

- Thyristor Controlled Series Compensator (TCSC) -Controls impedance
- Thyristor Controlled Phase Shifting Transformer (TCPST) -Controls angle
- Super Conducting Magnetic Energy Storage (SMES) -Controls voltage and power

### **3.11. ADVANTAGES OF FACTS TECHNOLOGY**

- Rapid response
- Dynamic control of power flow in selected transmission lines within the network to enable optimal power flow conditions
- Damping of the power swings from local and inter-area oscillations
- Suppression of subsynchronous oscillations
- Decreases DC offset voltages
- Reduction of short circuit current
- Frequent variation in output
- Smoothly adjustable output

### **3.11.1. FUTURE DIRECTION OF FACTS TECHNOLOGY**

The technology behind phase – controlled thyristor – based FACTS controllers has been present for several decades and is therefore considered mature. More utilities are likely to adopt this technology in the future, even as the newer, more promising switch- mode GTO – based FACTS technology is fast emerging. Foreseen in the near future is the application of a hybrid technology involving both thyristors and GTOs; for instance, STATCOM – compensated HVDC converters that perform better than SVC-compensated HVDC links.

The second generation of FACTS controllers, such as the STATCOM, the SSSC, and the UPFC, use switch-mode GTO-based VSC configurations. Novel GTO-centered topologies are being researched and are expected to evolve into another mature family of FACTS controllers. Recent advances in silicon power switching devices that significantly increase their power ratings will contribute even further to the growth of FACTS technology.

### **3.11.2. UNIFIED POWER QUALITY CONDITIONER (UPQC)**

The modern power distribution system is becoming highly vulnerable to the different power quality problems. The extensive use of non-linear loads is further contributing to increased current and voltage harmonics issues. Furthermore, the penetration level of small / large-scale renewable energy systems based on wind energy, solar energy, fuel cell, etc., installed at distribution as well as transmission levels is increasing significantly.

Unified power quality control was widely studied by many researchers as an eventual method to improve power quality of electrical distribution system. The function of unified power quality conditioner is to compensate supply voltage flicker/imbalance, reactive power, negative sequence current and harmonics.



In other words, the UPQC has the capability of improving power quality at the point of installation on power distribution systems or industrial power systems. Therefore, the UPQC is expected to be one of the most powerful solutions to large capacity loads sensitive to supply voltage flicker / imbalance. The UPQC consisting of the combination of a series active power filter (APF) and shunt APF can also compensate the voltage interruption if it has some energy storage or battery in the DC link. The shunt APF is usually connected across the loads to compensate for all current-related problems such as the reactive power compensation, power factor improvement, current harmonic, compensation, and load unbalance compensation, whereas the series APF is connected in a series with the line through series transformers. It acts as controlled voltage source and can compensate all voltage sources and can compensate all voltage related problems, such as voltage harmonics, voltage sag, voltage swell, flicker, etc.

The proposed control technique has been evaluated and tested under non-ideal mains voltage and unbalanced load conditions using Matlab/simulink software. The proposed method is also validated through experimental study. The Fig.3.2 shows the generalized structure of grid connected PV system.

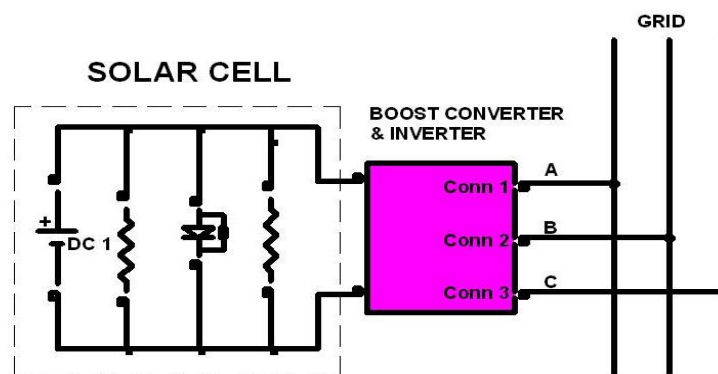


Fig.3.2. General Structure of grid connected PV system

UPQC has shunt and series voltage source inverters which are 3-phase, 3-wire shunt inverter connected to point of common coupling (PCC) by shunt

transformer. The series inverter stands between source and coupling as current source and it operates as voltage source.

The equations for real and reactive power through the line are as follows:

$$P = \frac{V_S V_R}{X} \sin(\delta_1 - \delta_2) \quad (3.1)$$

$$Q = \frac{V_R}{X} (V_S - V_R) \quad (3.2)$$

Where, P represents Real power and Q represents Reactive power.

These equations are given by neglecting the resistance of the line.

UPQC is able to compensate current harmonics, to compensate reactive power, voltage distortions and control load flow but cannot compensate voltage interruption because of non availability of sources.

Common interconnected PV systems structure is shown in Fig.3.3 is composed of PV array, DC/DC and DC/AC converters.

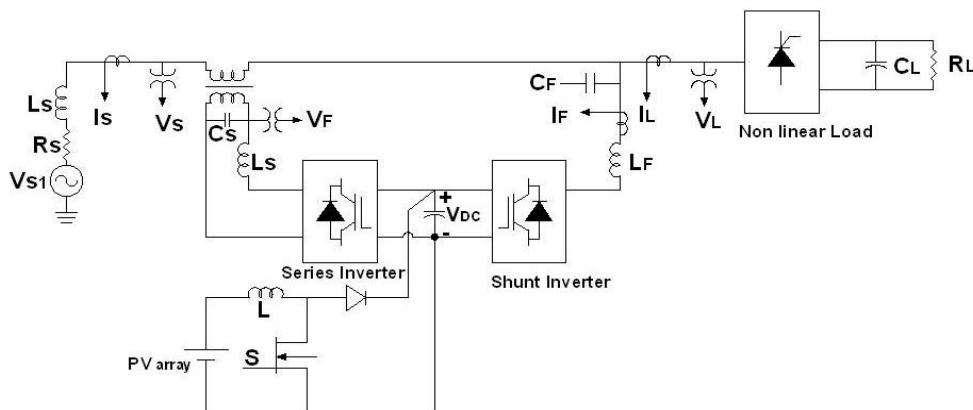


Fig.3.3. Configuration of UPQC with PV array

The design of the boost converter is done by using the following equations.

$$V_o = \frac{V_i}{(1 - \delta)} \quad (3.3)$$

Inductance and capacitance are calculated by using the following equations

$$L = \frac{V_i \delta}{f \Delta I} \quad (3.4)$$

$$C = \frac{\delta}{2 f R} \quad (3.5)$$

In this case, UPQC finds the ability of injecting power using PV to sensitive load during source voltage interruption. Two operational modes of UPQC are as follows:

#### **Interconnected mode**

In this mode, PV transfers power to load and source.

#### **Islanding mode**

In this mode, the source voltage is interrupted and PV provides a part of load power separately.

### **3.11.3. Controller designing**

Control strategy is designed and applied for two interconnected and islanding modes. In interconnected mode, source and PV provide the load power together while in islanding mode, PV transfers the power to the load alone. By removing voltage interruption, system returns to interconnected mode.

The controlling structure of the proposed system is composed of following parts:

### **3.11.3.1. Shunt inverter control**

In this study, shunt inverter undertakes two main duties. First is, Compensating both current harmonics generated by nonlinear load and reactive power, second is injecting active power generated by PV system.

The power loss caused by inverter operation should be considered in this calculation. Also, shunt inverter control undertakes the duty of (stabilizing) DC link voltage during series inverter operation to compensate voltage distortion.

### **3.11.3.2. Series inverter control**

The series converter of the UPQC provides simultaneous controls of real and reactive power flow in the transmission line. To do so, the series converter injected voltage is decomposed into two components. One component of the series injected voltage is in quadrature-injected component controls the transmission line real power flow. This strategy is similar to that of a phase shifter. The in-phase component controls the transmission line reactive power flow. This strategy is similar to that of a tap changer.

## **3.12. Conclusion**

The fundamentals of FACTS controllers and technology and concept of UPQC are presented in this chapter.

## CHAPTER 4

### MODELING AND SIMULATION OF UPQC SYSTEM

#### 4.1. Introduction

This chapter deals with modeling, simulation and implementation of UPQC system. The Two Bus System with UPQC is modeled and simulated using the blocks of Simulink. Sending end acts as one Bus and receiving end acts as another Bus. The function of UPQC is to compensate the sag and supply the harmonics using UPQC.

In a transmission system, the independent control of real power and reactive power is essential to maintain the desired voltage level in a transmission system. In this chapter, a two bus system is modeled and it is simulated modeled by using simulink. The UPQC is connected in this system to achieve the independent control of real and reactive power. The real power is independently controlled by varying the angle of voltage injection of the UPQC. The reactive power is controlled by varying the magnitude of shunt voltage injected by the UPQC.

Harmonic distortion originates in the nonlinear characteristics of devices and loads on the power system. The harmonic distortion is measured in single quantity as Total Harmonic Distortion (THD). THD is the ratio of harmonic voltage to the fundamental voltage. Voltages and currents having frequency components that are not integer multiples of the frequency at which the supply system is designed to operate are called interharmonics. It can be found in networks of all voltage levels. The main sources of interharmonics waveform



Design is done using the equations given in the previous section. The elements L and C are designed by assuming  $\Delta I = 0.4A$ ,  $f = 3kHz$  and  $R = 1K \Omega$ .

L and C for boost converter work out to be  $7.5mH$  and  $12\mu F$ ;  $T_{ON} : 0.25ms$ ;  $T_{OFF} : 0.08ms$ .

Power measurement block is connected in parallel with the load to measure real and reactive powers. Scopes are connected to measure receiving end voltage, receiving end current, real power and reactive power. The generator is represented as series combination of R, L, and E. Each line is represented by series impedance. The load at the receiving end is series combination of resistance  $200\Omega$  and inductance of  $100mH$ . The parameters of the additional load are  $50\Omega$  and  $50mH$ . DC required by UPQC is applied from a photo cell. The output of UPQC is injected using a series transformer. The circuit inside the UPQC block is shown in Fig.4.2.

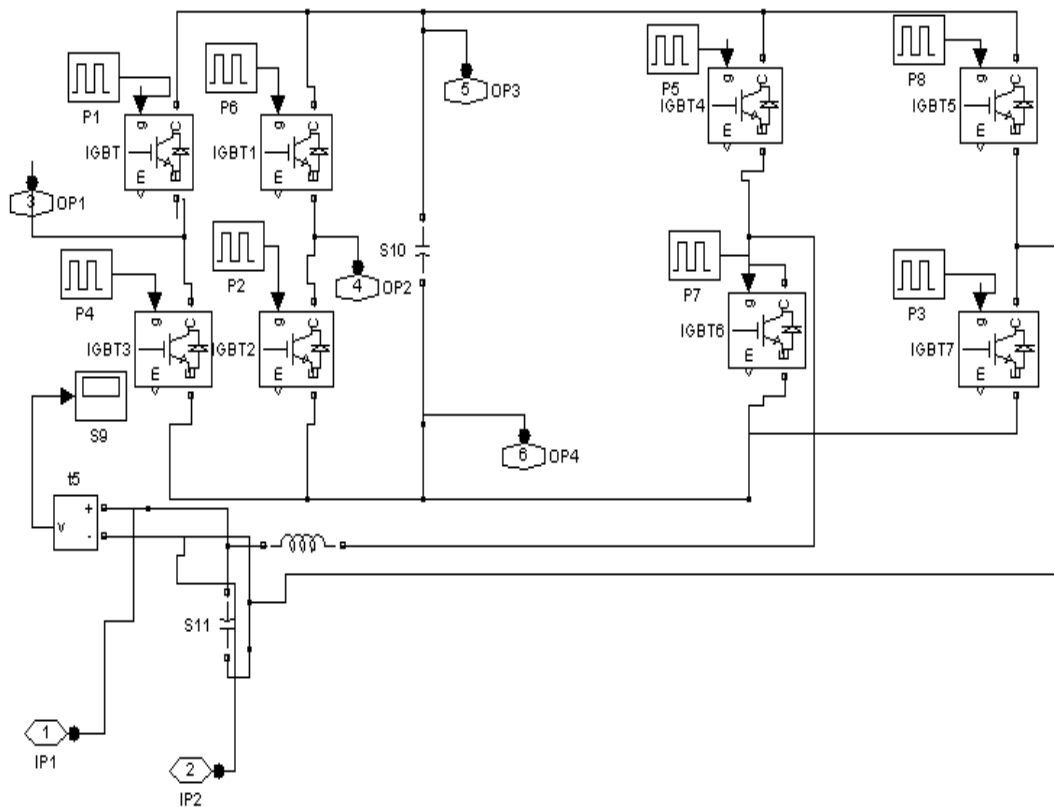


Fig.4.2. Inverters used in the UPQC System

The inverter of DVR used in the UPQC is triggered at 50Hz. All the switches are operated with pulse of width 10ms to obtain rated frequency. The pulse given to the other two switches are displaced by 10ms. The output of inverter is filtered by using LC filter. This will reduce heating since harmonics are reduced. The inverter switches of active filter are triggered at 250Hz. Fig.4.3 shows the boost converter circuit.

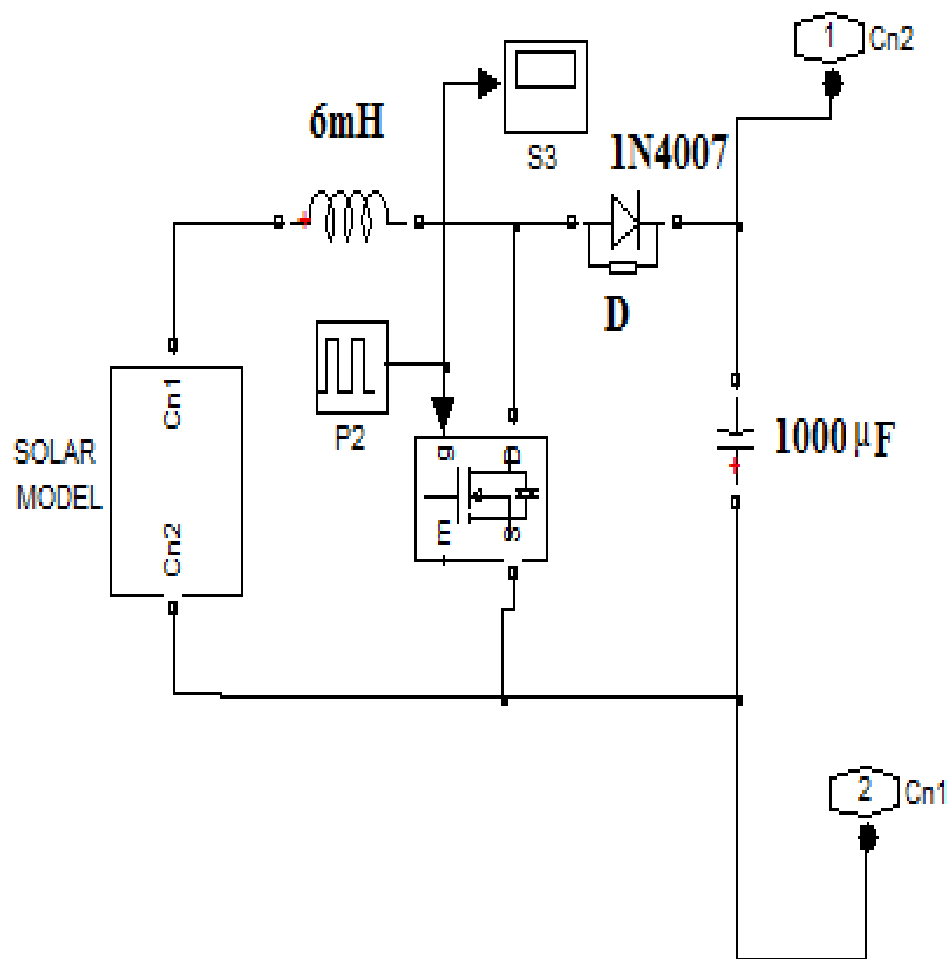


Fig.4.3. Boost Converter Circuit

The DC required by the DC link is supplied using solar cell and boost converter. The output of solar cell is not sufficient to drive the load at the output



of the inverter. Therefore the output of solar cell is boosted by using a boost converter. The boost converter uses boost inductor, capacitor and blocking diode.

The output voltage is controlled by using a MOSFET. The Fig.4.4 shows the variation of output voltage with time.

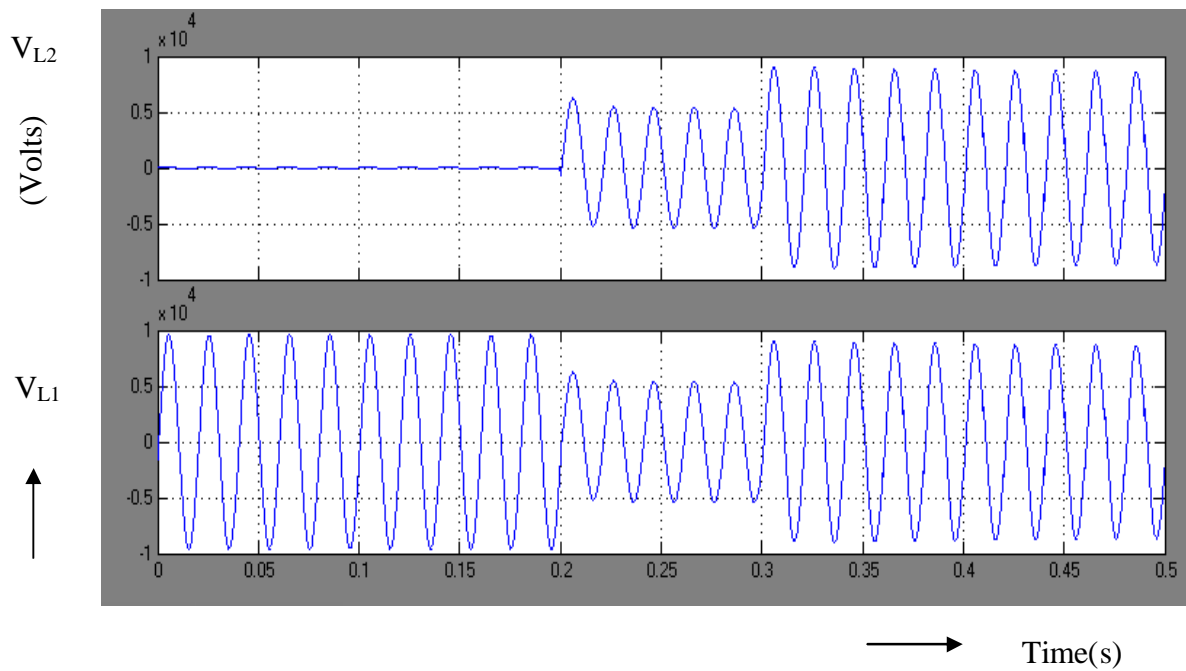


Fig.4.4 Voltages across Load-2 and Load-1

An additional load is applied at  $t=0.2$  s. The total load current increases and the drop in the line impedance increases. The receiving end voltage is reduced. At  $t=0.3$  s, the voltage is injected by the UPQC to bring the receiving end voltage to the normal value. From the waveform of  $V_{L1}$ , it can be seen that the sag is compensated by using the DVR part of UPQC.

The voltage  $V_{L2}$  is zero up to 0.2s, since the breaker is open. The waveforms of real and reactive powers are shown in Fig.4.5 and 4.6 respectively. The real and reactive powers increase at  $t=0.2$  s due to the increase in the load. This increases further at  $t=0.3$  s, due to the injection of the voltage by UPQC.

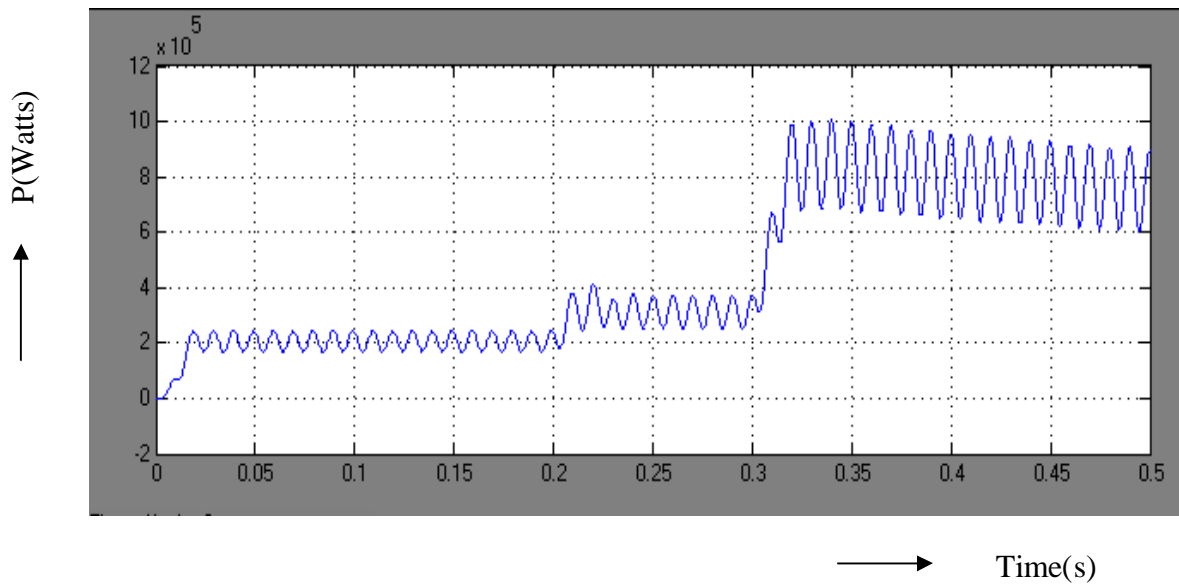


Fig.4.5 Real Power

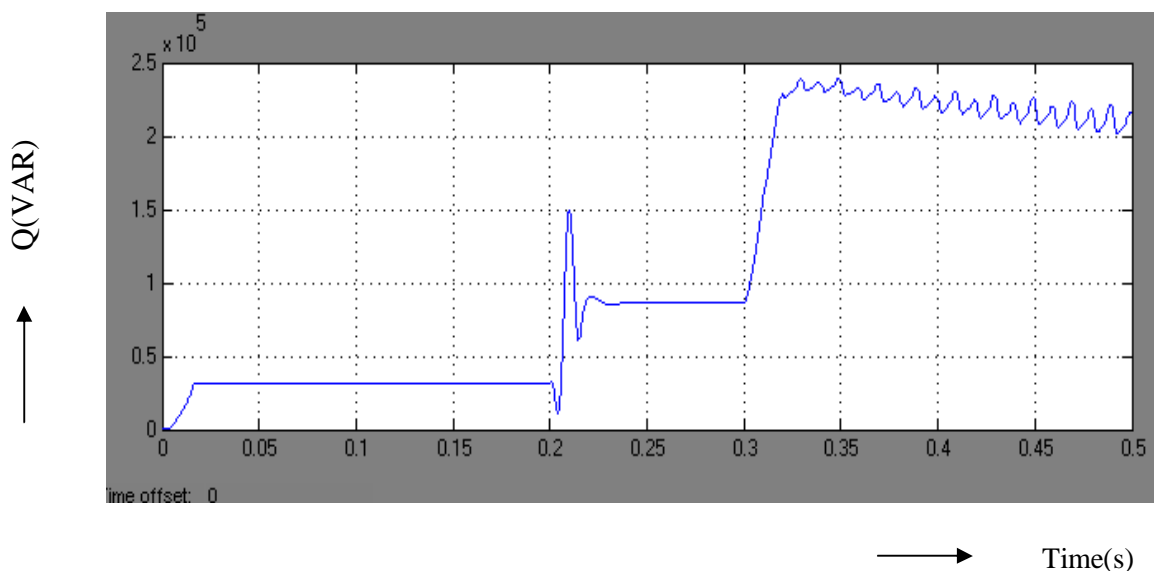


Fig.4.6 Reactive Power

Fig.4.5 shows the real power graph drawn between time on X axis and power on Y axis. From origin real power starts to increase and maintain a constant value up to  $t=0.2$ s. The real power increase at  $t=0.2$ Sec and it remains at the same value upto  $t=0.3$ s due to increase in load and again it increases due to the injection of the voltage by UPQC.

The Fig.4.6 represents the reactive power graph drawn between time on X axis and power on Y axis. The reactive power increases at  $t=0.2s$  and suddenly decreases and maintain the constant upto  $t=0.3s$  due to the increase in the load. At  $t=0.3s$  reactive power gets increased and maintains a constant value due to the injection of the voltage by UPQC.

The circuit diagram without enabling the active filter is shown in Fig.4.7.

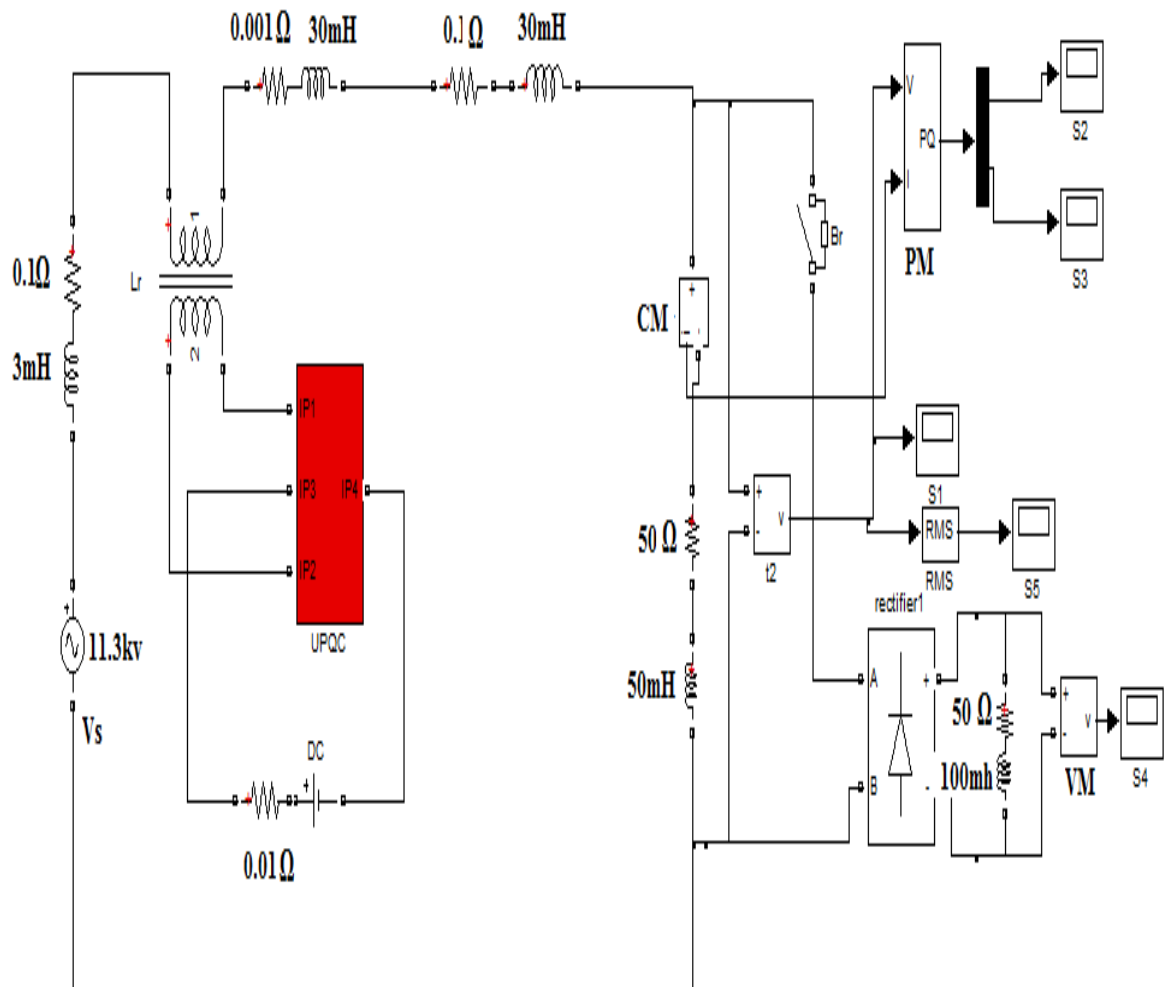


Fig.4.7. Circuit diagram of Two Bus System without the Active Filter.

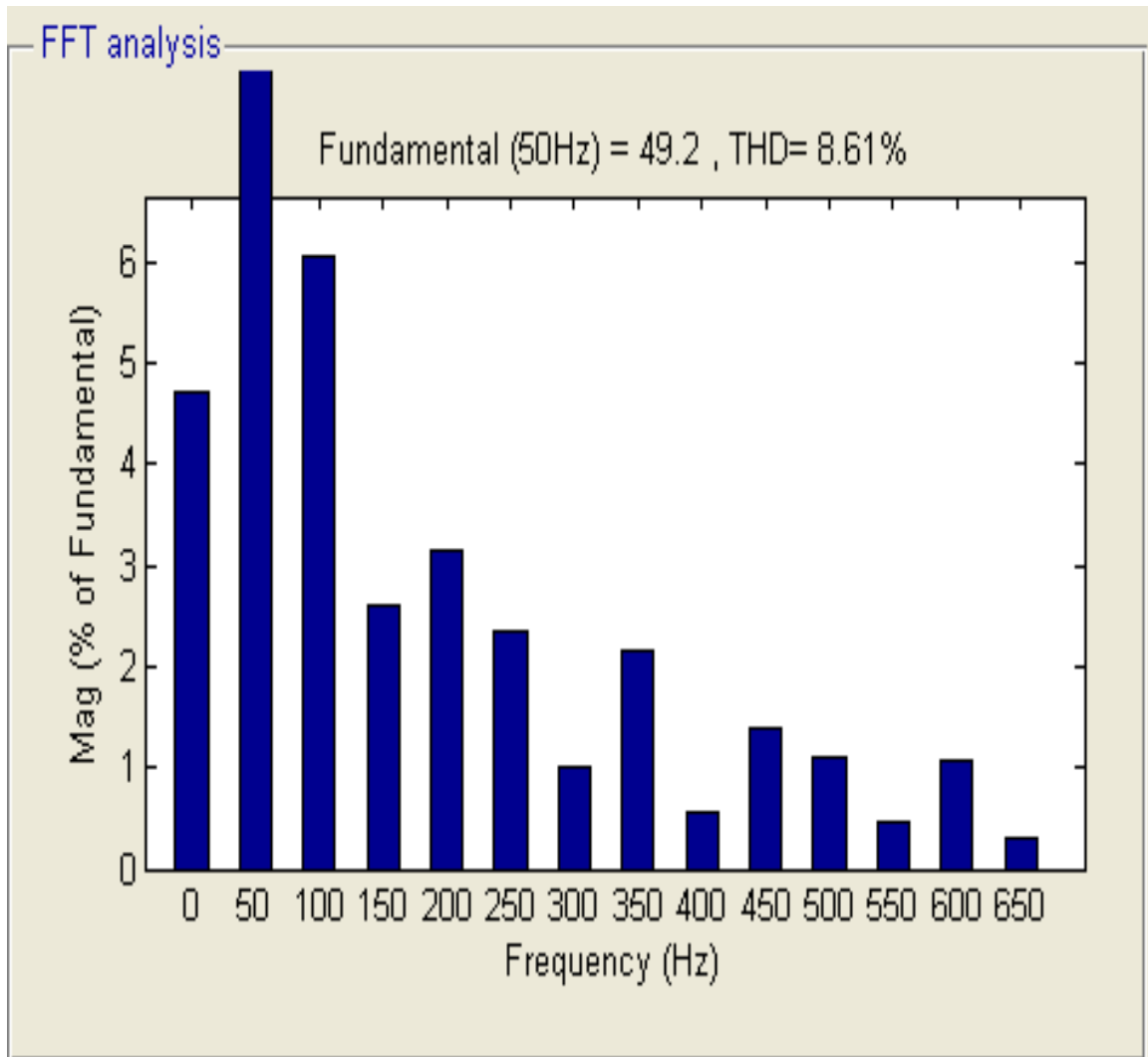


Fig.4.8. Frequency Spectrum for current

The frequency spectrum for current is shown in Fig.4.8. The frequency spectrum is drawn with frequency on x-axis and magnitude of voltage on y-axis. The magnitude of higher order harmonics are negligible. The height decreases with the increase in the order of harmonics. This is due to the increased impedance at high frequency. Fig.4.8. shows the THD is 8.6% and this can be reduced by adding a active filter. There is a small DC component in the current. This is due to the asymmetry in the transient part of the current.

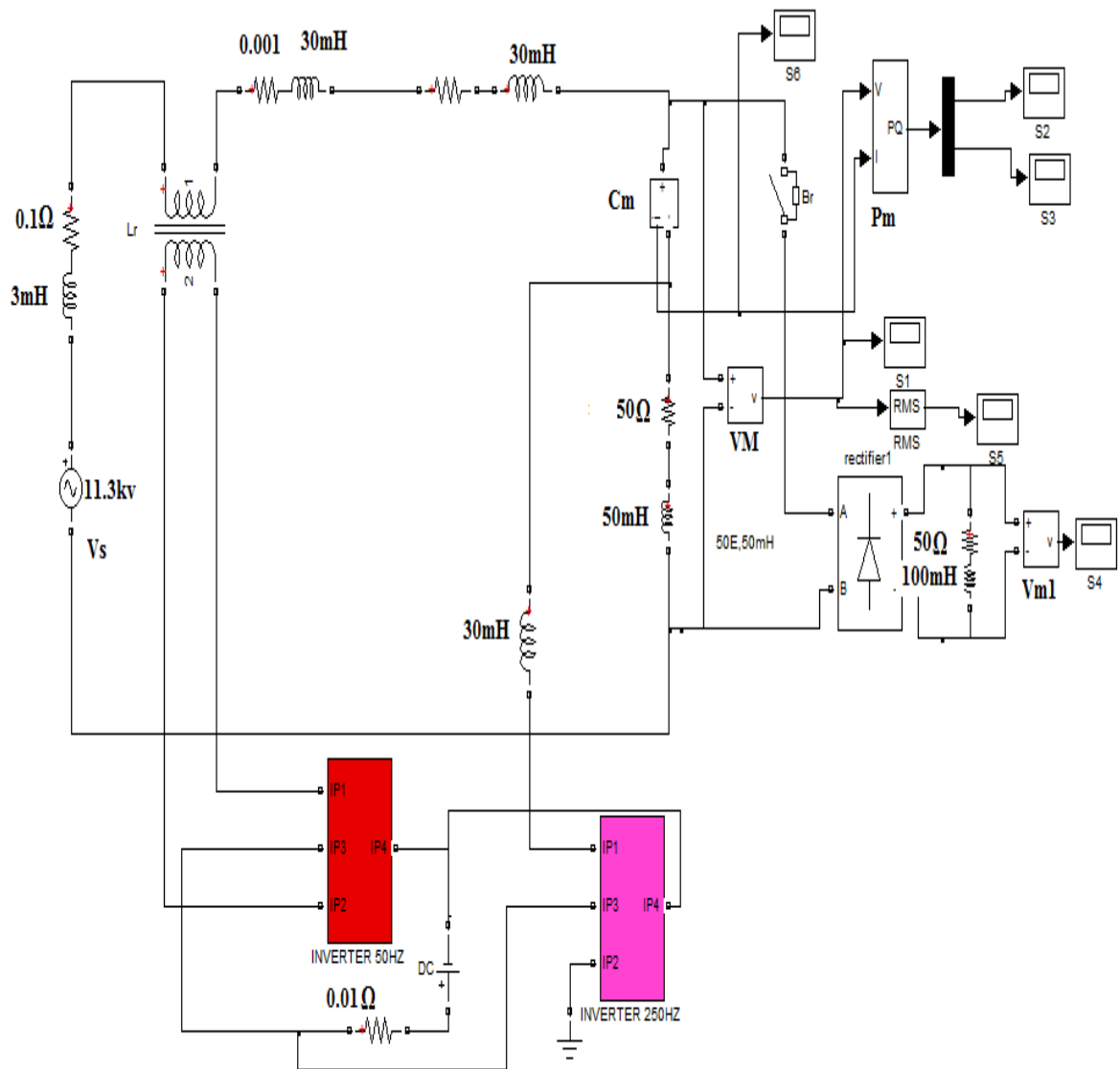


Fig.4.9a. Circuit diagram with the Active Filter

The circuit diagram with active filter is shown in Fig. 4.9a. The output of active filter is connected to the load. The inverter in the active filter is triggered at 250Hz. FFT analysis is done for the receiving end current and the frequency spectrum is obtained as shown in Fig.4.9b.

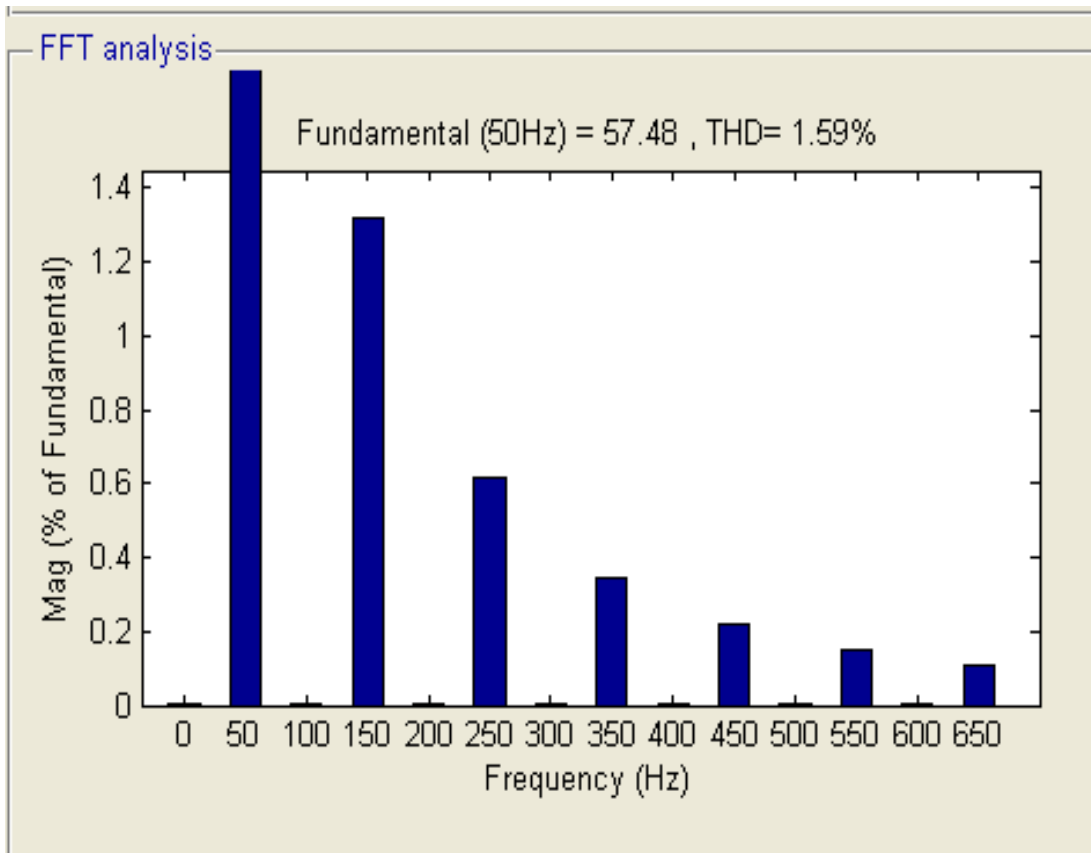


Fig. 4.9b. Frequency Spectrum for the current

The frequency spectrum is drawn with frequency on x-axis and magnitude of voltage on y-axis. The magnitude of higher order harmonics are negligible. The height decreases with the increase in the order of harmonics. This is due to the increased impedance at high frequency. The THD is 1.6%. Thus the THD is reduced to a minimum value by using active filter. Thus the quality of sending end current is improved by using UPQC.

### 4.3. Circuit model of Three phase Two Bus System with UPQC

The three phase circuit model of two bus system is shown in Fig.4.10. Generator is represented as a series combination of R, L and E. Line is represented as a series combination of R and L.

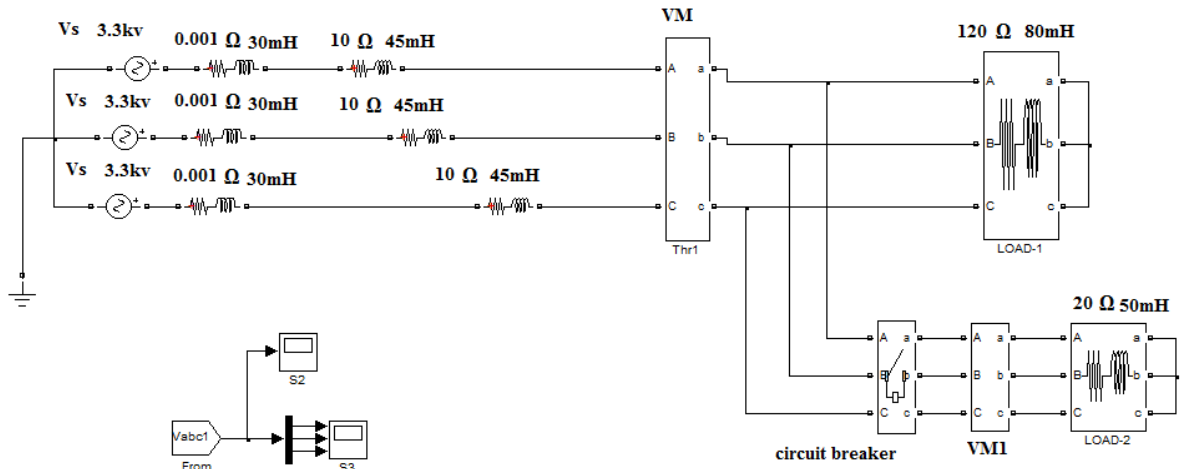


Fig.4.10. Circuit Model of Three Phase System with the additional load

The scope S2 shown in above figure gives three phase voltages in single figure. The scope S3 gives three voltages separately. An additional heavy load is connected in parallel with the existing load to create sag in the voltage. The line is represented by a series impedance. The voltages of all the three phases are shown in Fig.4.11.

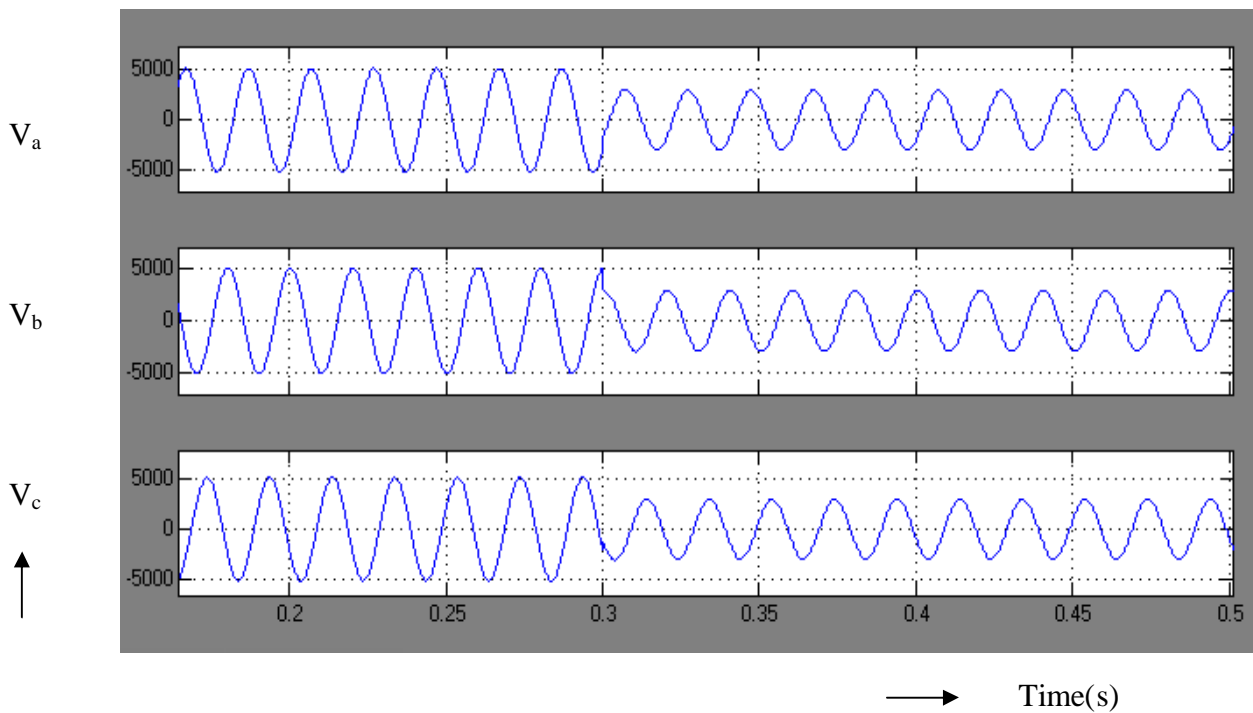


Fig.4.11. Voltage Across Load-1

The additional load is applied at  $t = 0.3\text{s}$ . Therefore the voltage decreases beyond  $0.3\text{s}$ . Voltage across load 2 is shown in Fig.4.12.

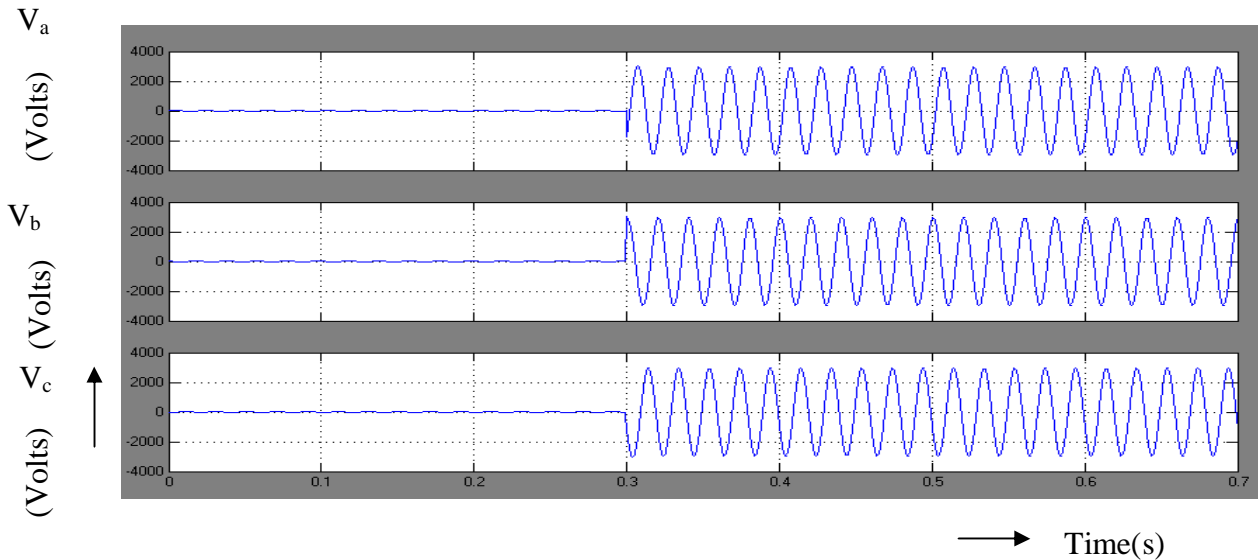


Fig.4.12 Voltage Across Load-2

The RMS value of voltage across load 2 reduced due to the voltage drop in the line impedance. The voltage exists beyond  $0.3\text{s}$  since the switch was closed at  $0.3\text{s}$ . The FFT analysis is done for load voltage and the spectrum is shown in Fig.4.13.

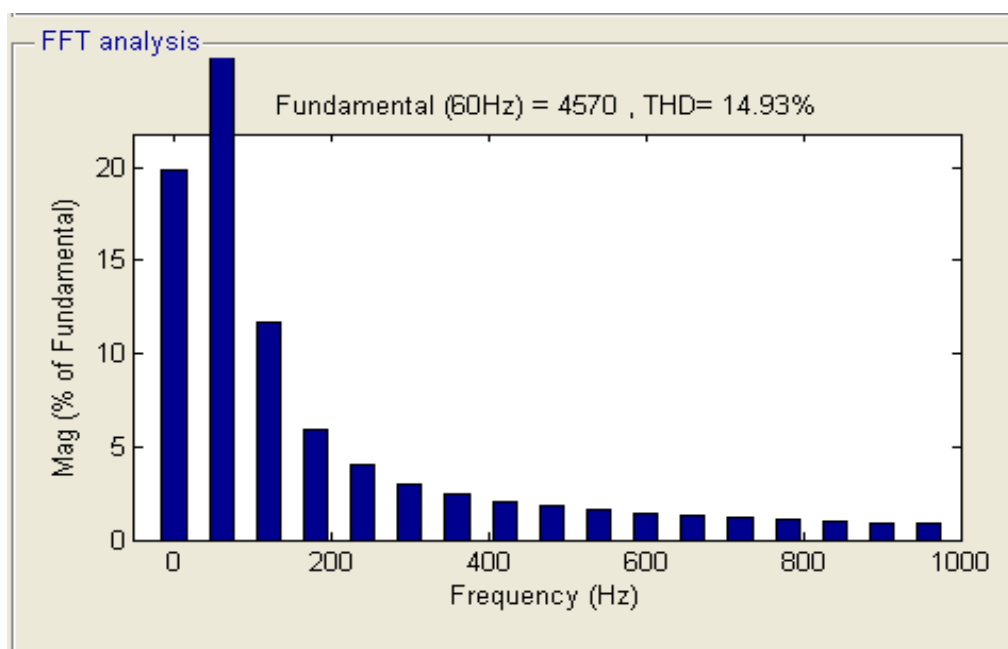


Fig.4.13 Frequency Spectrum



In Fig.4.13 the frequency spectrum is drawn with frequency on x-axis and magnitude of voltage on y-axis. The magnitude of higher order harmonics are negligible. The height decreases with the increase in the order of harmonics. This is due to the increased impedance at high frequency. The THD is 14.9%. The three phase circuit model with UPQC is shown in Fig.4.14. Three phase Two Bus System with UPQC is shown here. The voltage drop in the line is compensated by using the injected voltage of UPQC. The injected voltage is approximately equal to the line drop.

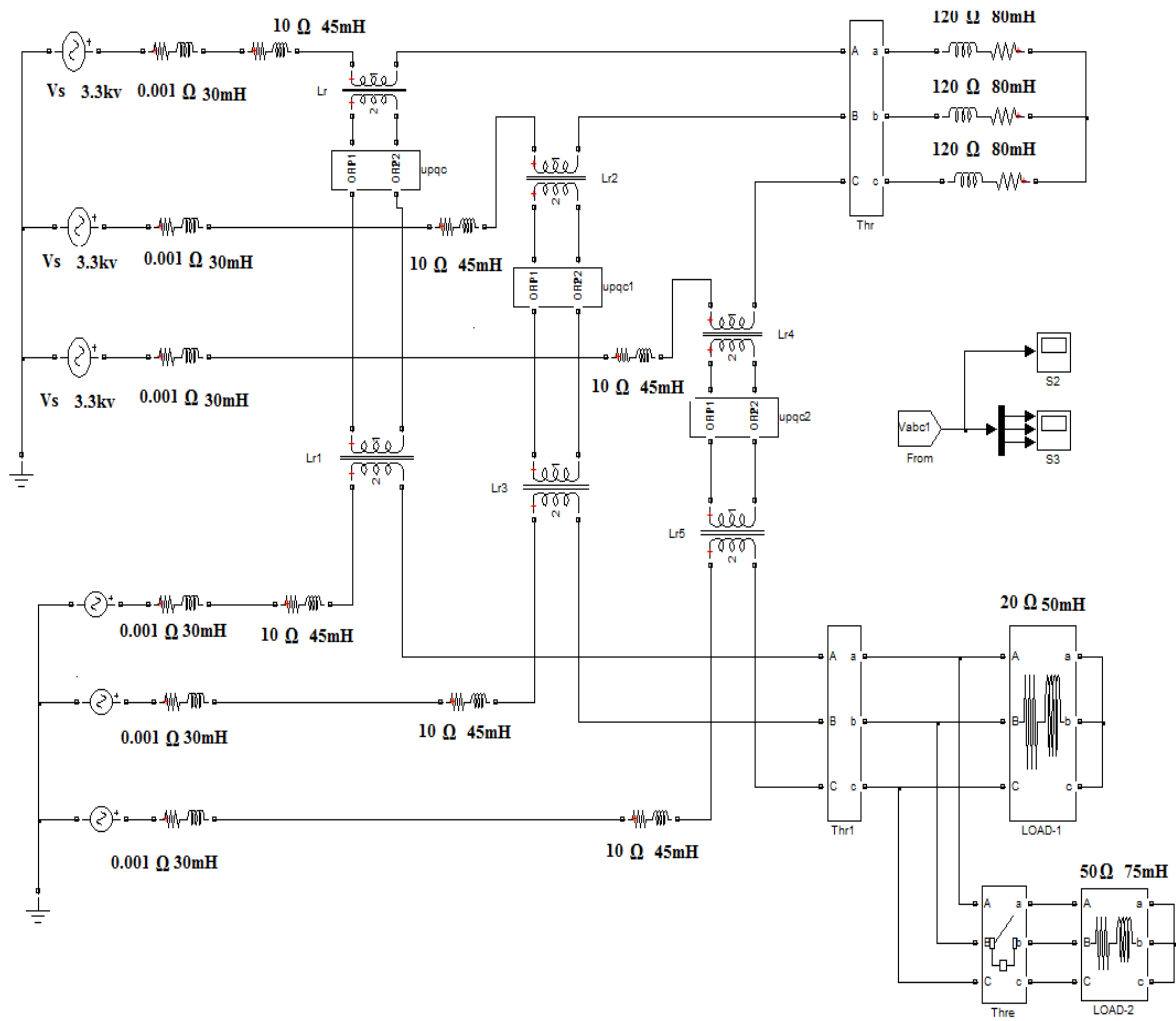


Fig.4.14. Circuit Model of the Three Phase System with UPQC

The sub system of UPQC in each phase is shown in Fig.4.15. Each UPQC consists of two inverters. The first inverter compensates the drop in line 1. The second inverter compensates the voltage in the second line using PV system.

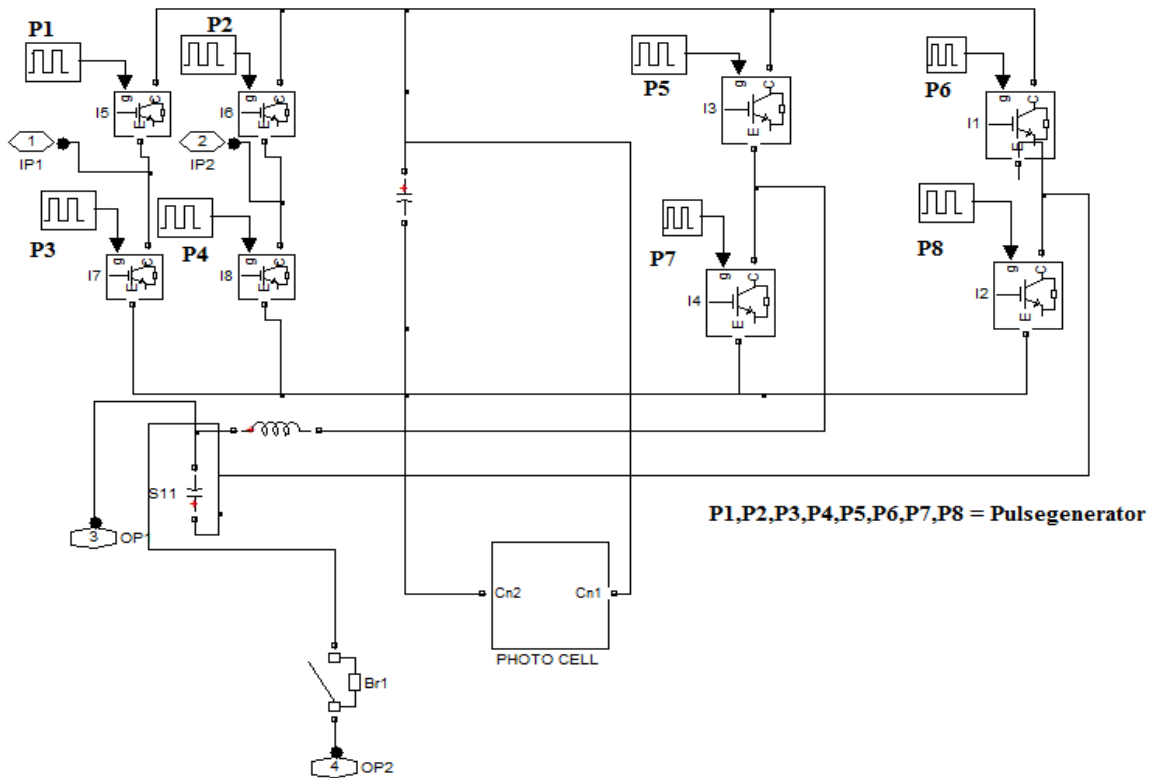


Fig.4.15. Circuit of UPQC

The output voltage with compensation is shown in Fig.4.16.

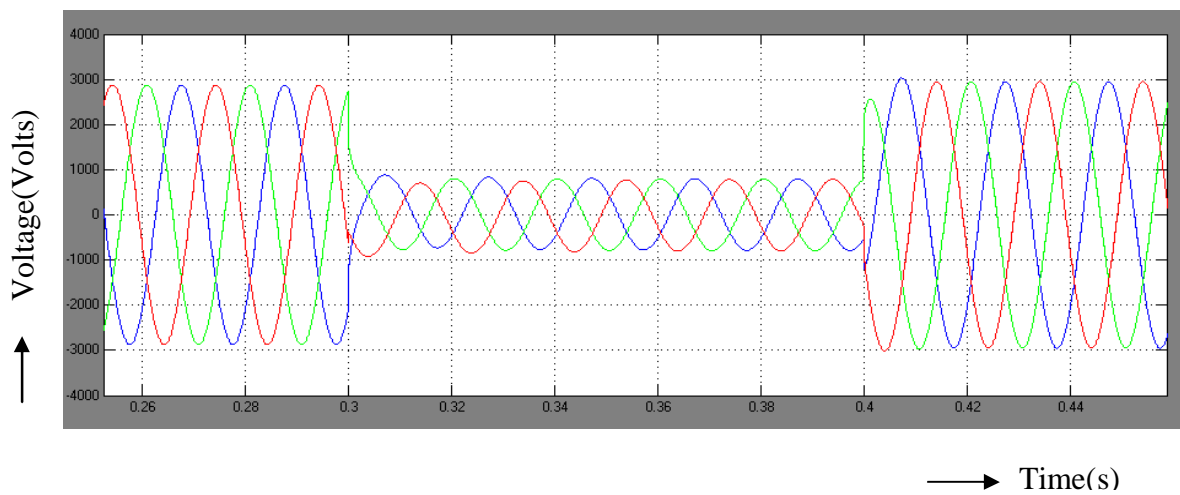


Fig.4.16 Three Phase Voltage with Compensation

In the above figure all the voltages are shown in single figure. The sag appears from 0.3 to 0.4s. At  $t = 0.4s$ , the UPQC injects voltage and the load voltage is brought to the rated value as shown in Fig.4.17.

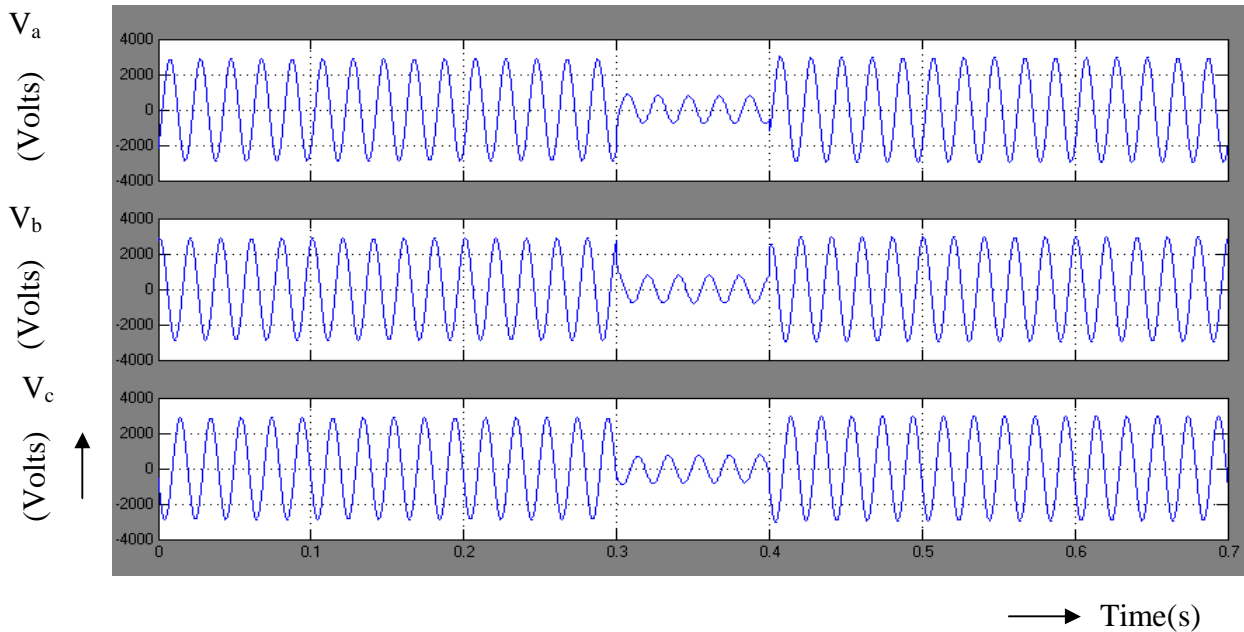


Fig.4.17. Voltage of each Phase with Compensation

In the above figure, individual phase voltages are shown. The voltage drop and recovery are also shown. The FFT analysis is done for the output voltage and the spectrum is shown in Fig.4.18.

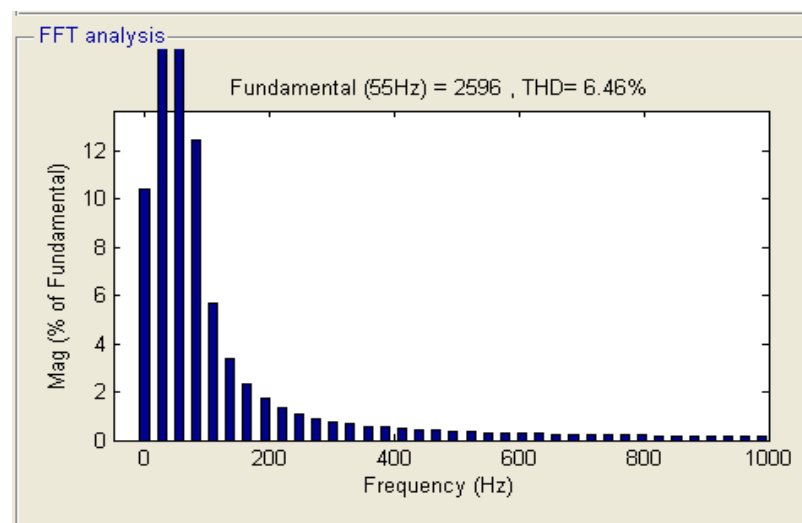


Fig.4.18. Frequency Spectrum

In Fig.4.18 shows, the frequency system is drawn with frequency on x-axis and magnitude of voltage on y-axis. The magnitude of higher order harmonics are negligible. The height decreases with the increase in the order of harmonics. This is due to the increased impedance at high frequency. The THD value is 6.4%.

#### **4.4. Experimental Verification**

##### **4.4.1. Experimental setup and procedure**

Hardware consists of power supply board, control board and two inverters boards, Pulse generator unit and pulse amplifiers unit are placed in the experiment. Two inverters act as a switches and one oscilloscope unit also involved.

DC input is applied from a solar cell. The micro controllers PIC 16F84 is used for generating the pulses. These pulses are amplified by using the driver circuit IR2110. The device IRF840 is used as the switch in the inverters. Pulses are triggered at 50HZ frequency. All the switches are operated with 10ms to obtain rated frequency. Pulse given to the switches are displaced by 10ms. A constant dc voltage obtained from solar cell is maintained as constant value throughout the system. Due to ON/OFF pulses given to inverter 1, Output voltage look like a square wave. The output voltage of Inverter 2 is nearly a sine wave due to presence of LC filter in the output side.

##### **4.4.2. Parameters Considered**

Power supply has diodes IN4007 and capacitor 1000 $\mu$ f/250V. Driver circuits consist of resistors value from 100ohm to 22Kohm. MOSFET IRF840 used as switching device. Optocoupler unit IR2110 consists of diode IN4007 and capacitor 1000mf/25V. Pulse generating circuit consists of PIC 16F84 micro controller and crystal oscillator 4mhz, Zener diodes of 5.1V.

##### **4.4.3. Conditions and Constraints During the Study**

Neglecting the resistance of the line throughout the system.

#### 4.4.4. Waveforms and Explanation

UPQC system is fabricated and tested in the laboratory. The Layout of the hardware implemented is shown in Fig.4.19a.



Fig.4.19a. Hardware Implementation

DC input is applied from a solar cell. The hardware consists of power supply board, control board and two inverters boards. The micro controller PIC 16F84 is used for generating the pulses. These pulses are amplified by using the driver IR2110. The device IRF840 is used as the switch in the inverters. The output of solar cell is shown in Fig.4.19b.

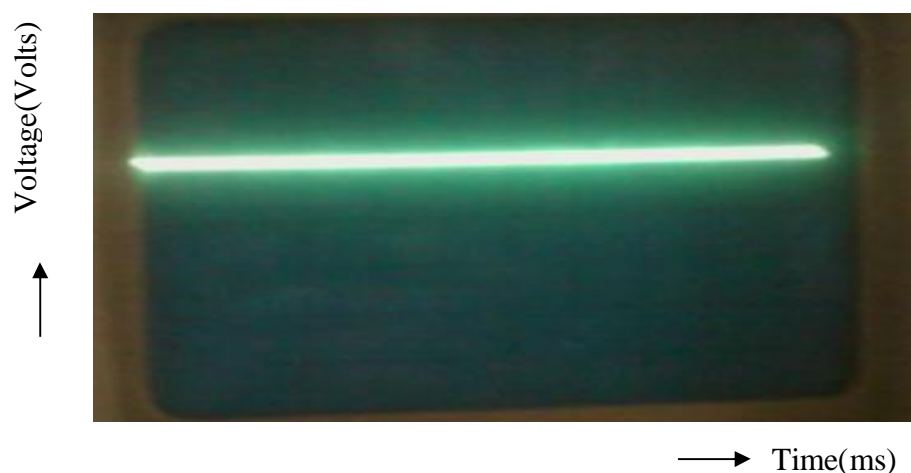


Fig.4.19b. Output of the Solar Cell

Scale:  
 X axis : 1 unit = 1 ms  
 Y axis : 1 unit = 10 V

In Fig 4.19b, the oxillograms are shown with time on x-axis and output voltage in y-axis. Scales are measured for time as 1unit as 1milliseconds and for voltage 1unit as 10 volts for output voltage. Output voltage is maintained at constant value throughout the system.

The switching pulses for  $M_1$  and  $M_2$  are shown in Fig.4.19c and 4.19d respectively. In Fig.4.19c the graph is drawn with time on x-axis and voltage on y-axis. Scale is measured with 1 unit as 20micro seconds per division for x-axis and 1 unit with 5volts per division for y-axis. The switching voltage is a square wave due to on and off process.

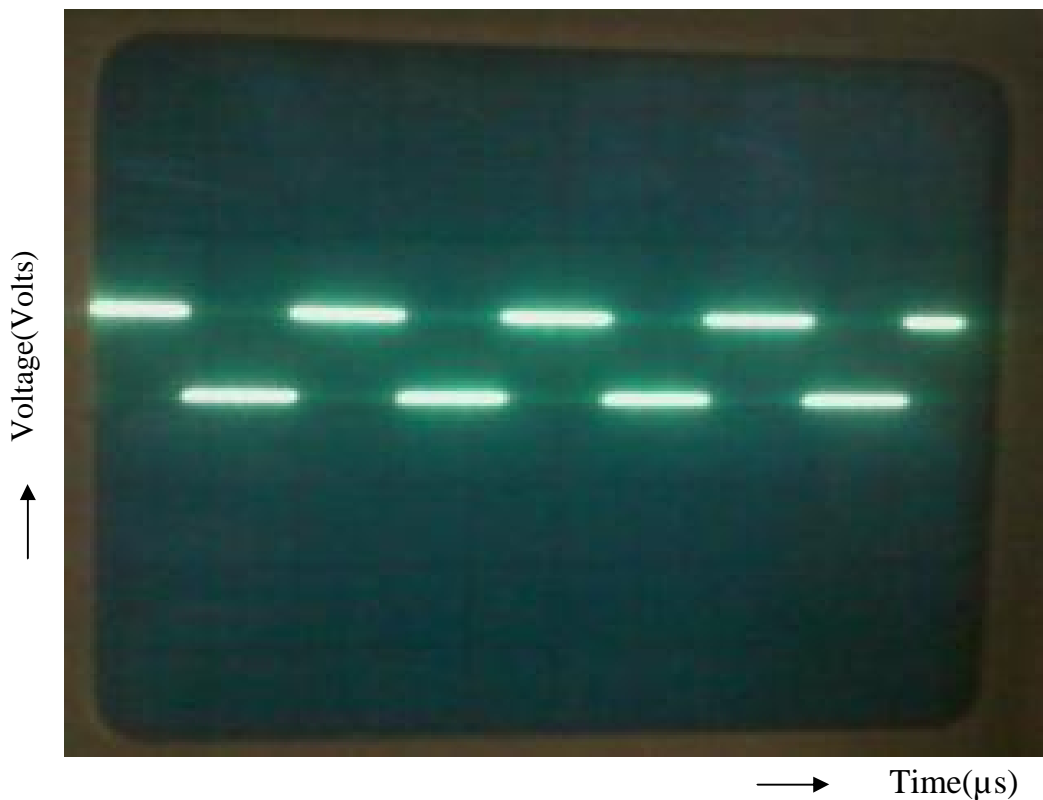


Fig.4.19c. Switching Pulses for  $M_1$

Scale:

X axis : 1 unit = 20  $\mu$ s / div

Y axis : 1 unit = 5 V / div

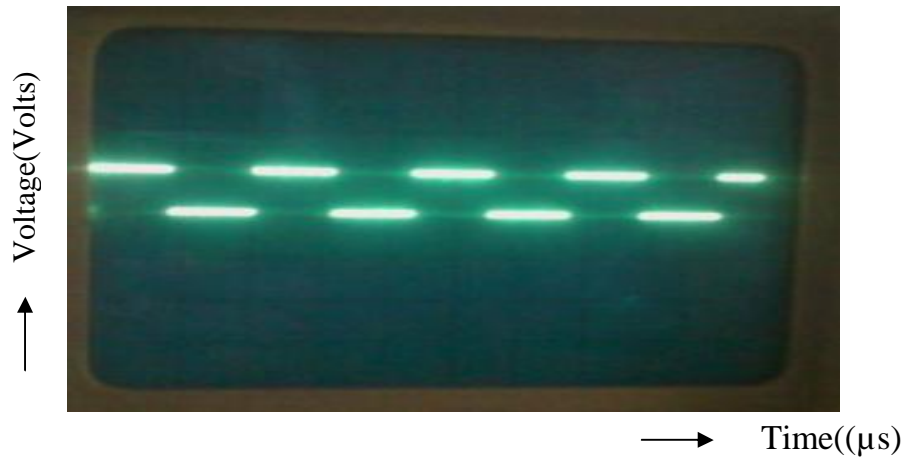


Fig.4.19d. Switching Pulses for  $M_2$

Scale:

X axis : 1 unit = 20  $\mu$ s / div

Y axis : 1 unit = 5 V / div

In Fig.4.19d, the graph is drawn between time on x-axis and voltage as y-axis. Scale is measured with 1 unit as 20micro seconds per division for x-axis and 1 unit as 5volts per division for y-axis. The switching voltage is a square wave due to on and off process.

The output of inverter 1 is shown in Fig.4.19e.

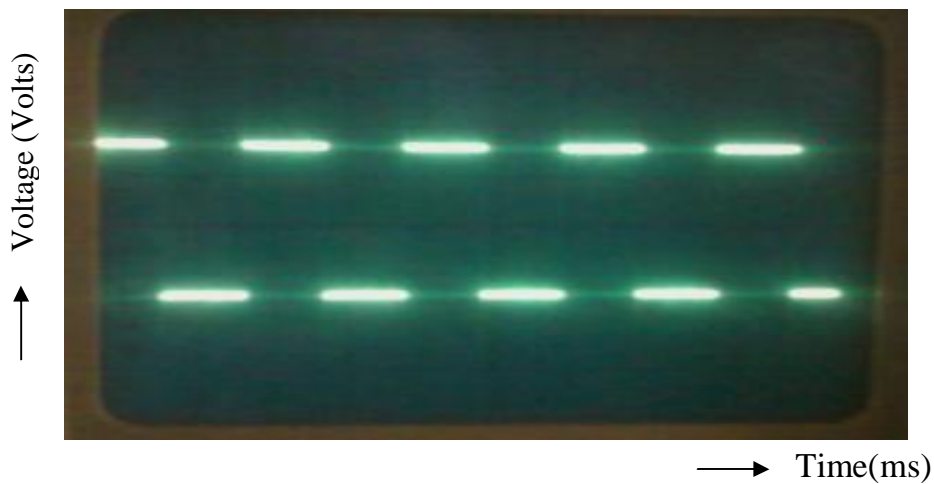


Fig.4.19e. Output Voltage of the Inverter 1

Scale:

X axis : 1 unit = 5 ms / div

Y axis : 1 unit = 20 V / div

In Fig.4.19e, the graph is drawn between time on x-axis and voltage as y-axis. Scale is measured with 1 unit as 5milli seconds per division for x-axis and 1 unit as 20volts per division for y-axis. Due to on and off process it look like a square wave.

The output of inverter 2 is shown in Fig.4.19f. The graph is drawn between time on x-axis and voltage on y-axis. Scale measured 1 unit as 5milli seconds per division for x-axis and 1 unit as 20volts per division for y-axis. This is nearly a sine wave due to the presence of LC filter in the output side.

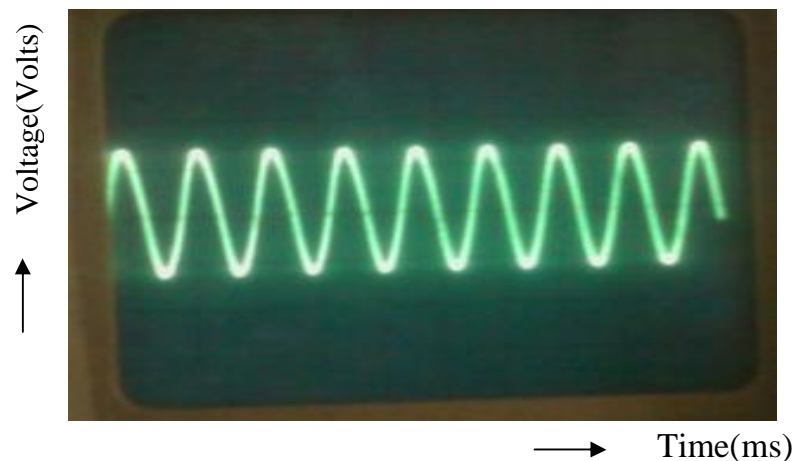


Fig.4.19f. Output Voltage of the Inverter 2

Scale:

X axis : 1 unit = 5 ms / div

Y axis : 1 unit = 20 V / div

## 4.5. Results and Discussions

### 4.5.1. Results of single phase Two Bus System with UPQC

From Fig.4.4, at  $t=0.3s$ , the voltage is injected by the UPQC to bring the receiving end voltage to the normal value. From the wave form of voltage across load 1, it is shown that the sag is compensated by using the DVR part of UPQC. From Fig4.5 and 4.6, the real and reactive power increase at  $t=0.2s$  due to



the increase in the load. This increase further at  $t=0.3\text{Sec}$ , due to the injection of voltage by UPQC. Total harmonic distortion is improved from 8.6% to 1.6%. Thus the THD is reduced to a minimum value by using UPQC.

#### **4.5.2. Results of Three phase Two Bus System with UPQC**

From Fig.4.16, at  $t=0.4\text{Sec}$  the UPQC injects voltage and the load voltage is brought to the rated value as shown in Fig.4.17. Total harmonic distortion is improved from 14.9% to 6.4%.

#### **4.5.3. Results of experimental verification**

From Fig.4.19e and 4.19f, output of inverter is nearly a sine wave due to presence of LC filter in the output side. The experimental results are similar to the simulation results.

#### **4.6. Validation of simulation Results with the Experiment Results**

From Experimental verification results, output voltage of inverters nearly a sine wave and in the case Two Bus system with UPQC voltage across load also nearly a sine wave. THD analysis is not possible practically since sensitive grid operation needs certain rules and regulations.

#### **4.7. Result comparison with desirables and analysis**

The experimental results are similar to the simulation results. THD is improved to a minimum value in the case of three phase Two Bus System with UPQC.

#### **4.8. Conclusion**

Single phase and three phase UPQC systems are modeled and simulated successfully. Basic UPQC system is fabricated, tested and the experimental results are presented. The experimental results are similar to the simulation results. The THD is reduced from 8.6% to 1.6% by adding the UPQC.

## **CHAPTER 5**

### **EIGHT, FOURTEEN, THIRTY AND FIFTY BUS SYSTEMS**

#### **5.1. Introduction**

Standard Eight, Fourteen, Thirty and Fifty bus systems are considered for simulation studies. Eight bus system with and without UPQC are studied and the corresponding results are discussed. They are modeled and simulated using the blocks of Simulink. There are three generator buses and five load buses.

The UPQC system is connected in a Eight bus system to control the real power, reactive power and voltage. The real power, reactive power and voltage is observed without connecting the UPQC in a Eight bus system and connecting the UPQC system. The readings are tabulated.

#### **5.2. Model of Eight Bus System using UPQC in power systems to improve power quality**

Simulink model of 8 bus system is shown in Fig.4.1. The specifications are as follows.

L and C are designed by assuming  $\Delta I = 0.4A$ ,  $f = 3kHz$  and  $R = 1K\Omega$ .

L and C for boost converter works out to be

7.5mH and 12 $\mu$ F;  $T_{ON} = 0.25ms$ ;  $T_{OFF} = 0.08ms$ .

Scopes are connected to measure receiving end voltage, receiving end current, real power and reactive power. The generator is represented as series combination of R, L, and E. Line is represented by series impedance. The load at the receiving end is series combination of resistance 200 $\Omega$  and inductance of 100mH. The parameters of the additional load are 50 $\Omega$  and 50mH. DC required by

UPQC is applied from a photo cell. The output of UPQC is injected using a series transformer.

The inverter of DVR used in the UPQC is triggered at 50Hz. All the switches are operated with puls of 10ms width. The puls given to the other two switches are delayed by 10ms. The output of inverter is filtered by using LC filter. This will reduce heating since harmonics are reduced. The inverter switches of active filter are triggered at 250Hz.

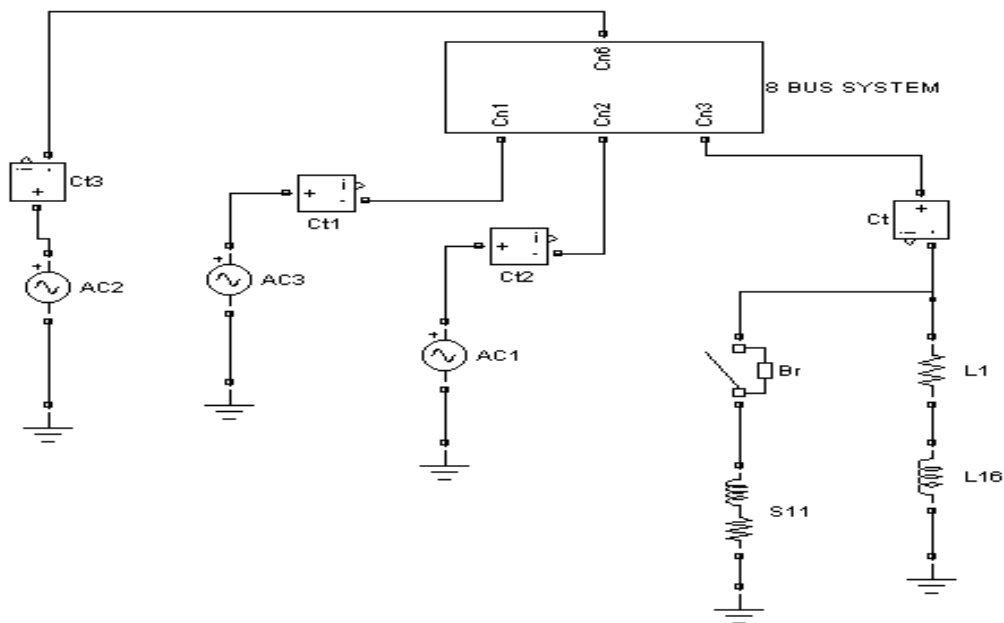


Fig.5.1. Eight Bus System without UPQC

The circuit of eight bus system without UPQC is shown in Fig.5.1. Additional load is applied by closing the breaker at  $t = 0.2s$ .

In Fig.5.2, shows the real and reactive powers at bus 7 is drawn. It is drawn between time on x-axis and power on y-axis. From origin the real and reactive power starts to increases and maintain a constant value upto  $t=0.2s$ . The real and reactive power increased at  $t = 0.2s$ , since the current drawn is increased.

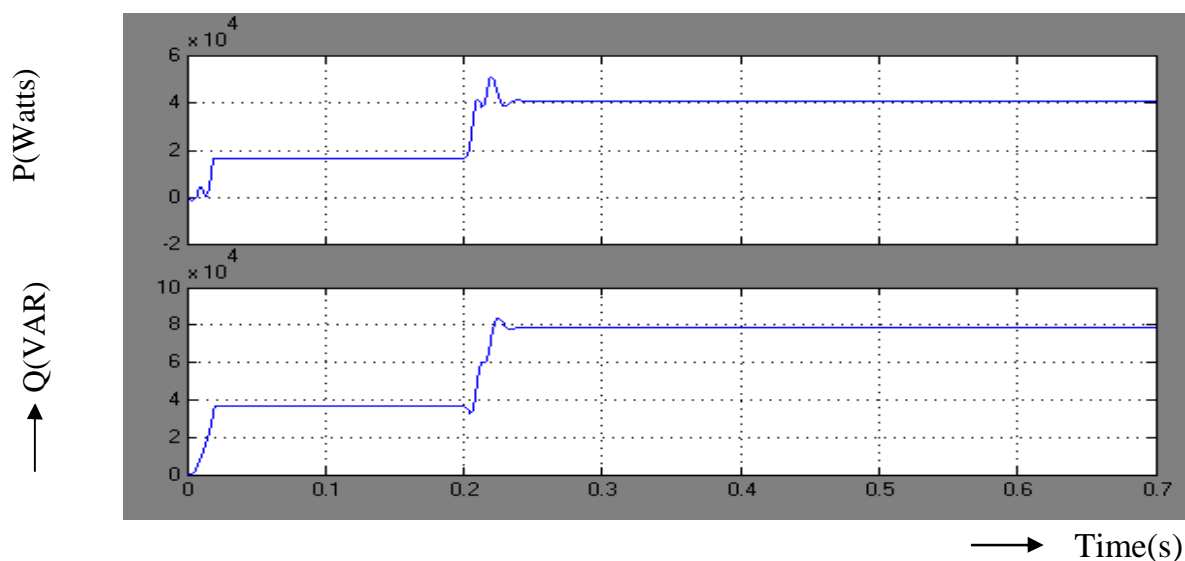


Fig. 5.2. Real and Reactive Power at Bus-7

In Fig.5.3, shows the real and reactive powers at bus 3 is drawn. It is drawn between time on x-axis and power on y-axis. From origin the real and reactive power starts to increase and maintain a constant value upto  $t=0.2s$ . The real and reactive power increased at  $t = 0.2s$ , since the current drawn is increased.

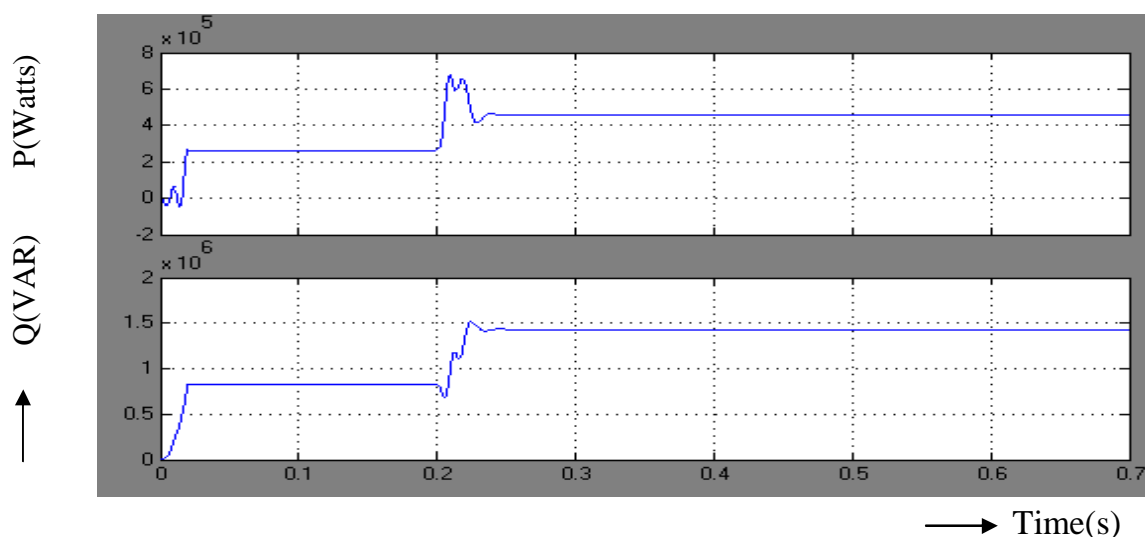


Fig. 5.3. Real and Reactive Power at Bus-3

In Figure 5.3 a, voltage across load 1 and 2 is drawn with time on x-axis and voltage on y-axis. At  $t = 0.2s$  the voltages across loads 1 and 2 decrease due to the addition of heavy load.

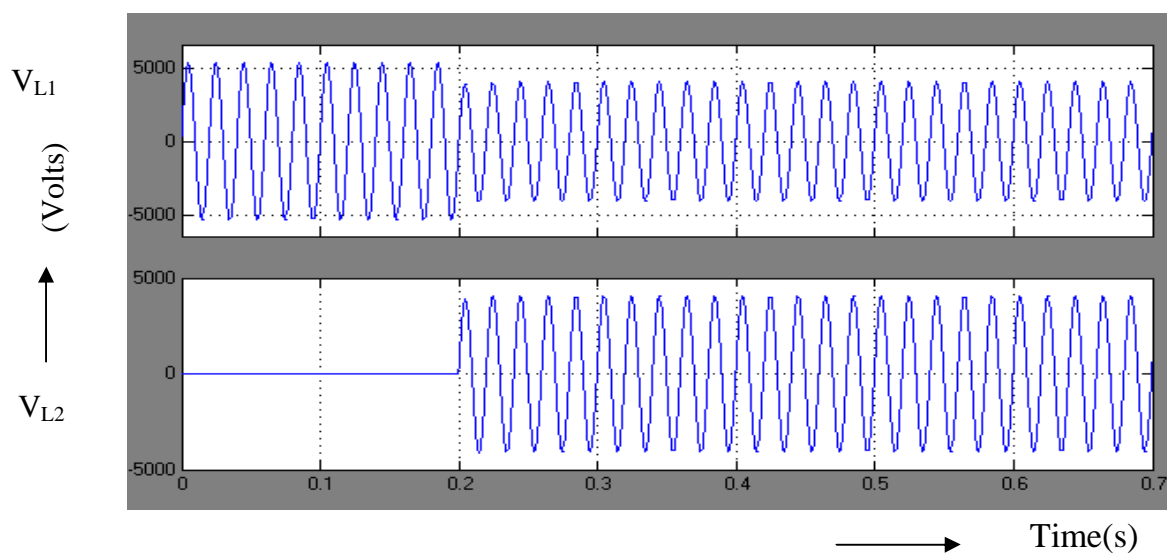


Fig. 5.3 a. Voltage across Load-1 and Load-2

The circuit of eight bus system with UPQC is shown in Fig.5.4. The network of 8 bus system is represented as the sub-system here. The circuit model of UPQC Eight Bus is shown in figure. The UPQC is connected near bus three.

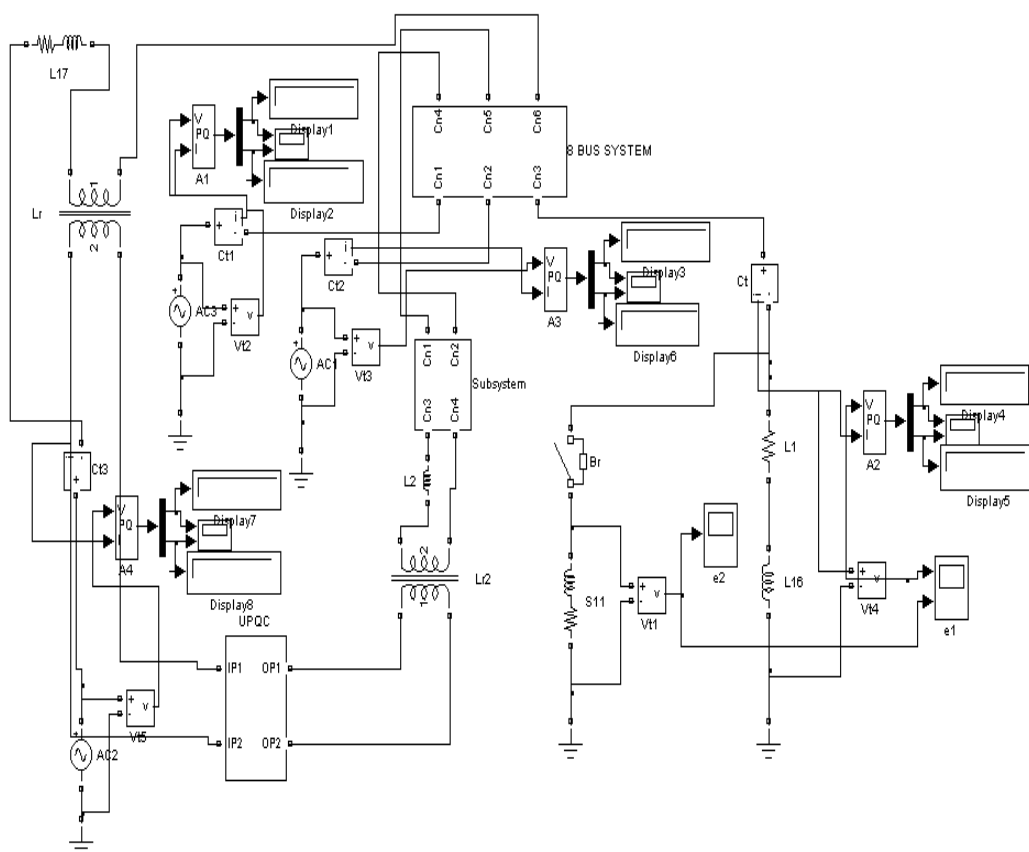


Fig.5.4. Eight Bus System with UPQC

Fig.5.5, shows the real and reactive power at bus 1. It is drawn with time on x-axis and power on y-axis. The load is applied at  $t = 0.2s$ . The DVR part of UPQC injects voltage at  $t = 0.3s$ . The real and reactive power at bus 1 decreases.

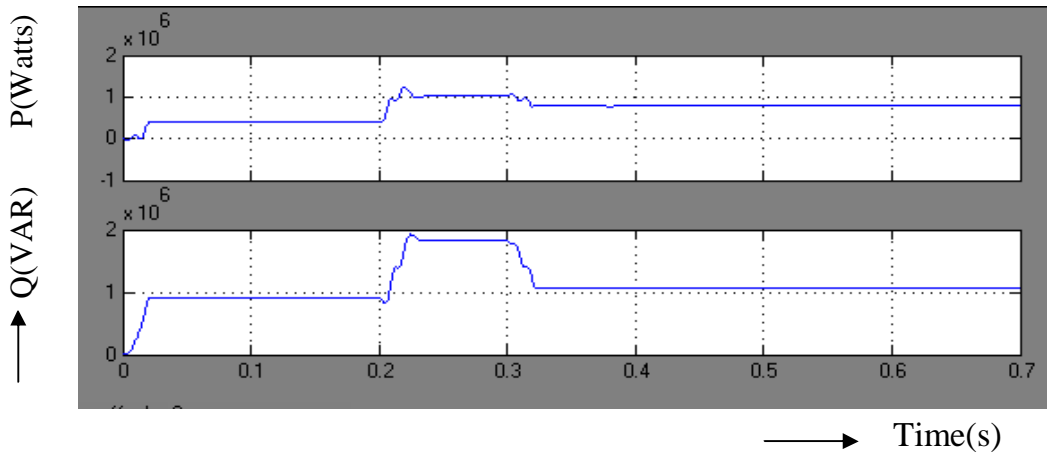


Fig.5.5. Real and Reactive Power Across Bus-1

Fig.5.6, shows the real and reactive power at bus 3. It is drawn with time on x-axis and power on y-axis. The load is applied at  $t = 0.2s$ . The DVR part of UPQC injects voltage at  $t = 0.3s$ . The real and reactive power at bus 1 decreases, and that of bus 3 increases due to the transfer of power from bus 1 to 3.

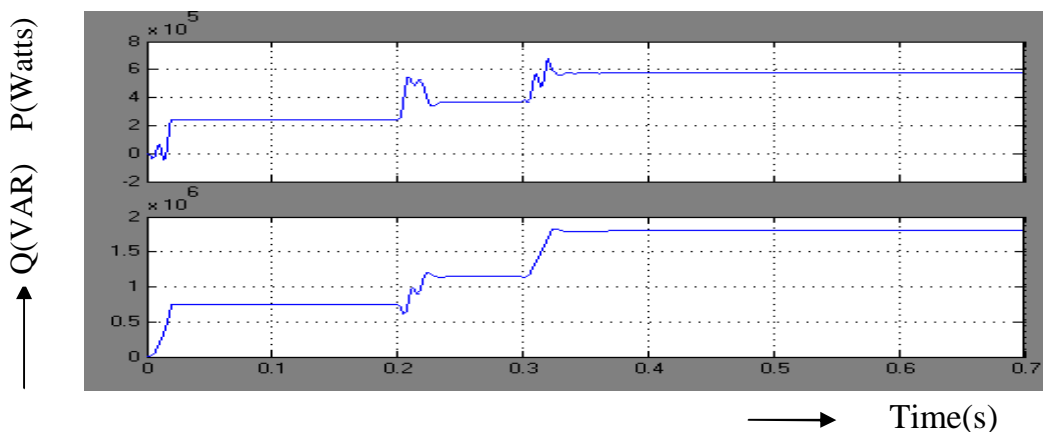


Fig.5.6. Real And Reactive Power Across Bus-3

Fig.5.7, shows the voltages across load 1 and 2. It is drawn with time on x-axis and voltages on y-axis. The voltages decreases at  $t = 0.2s$ . and resumes

its normal value at  $t = 0.3\text{s}$ . This is due to the voltage injected by the DVR part of UPQC. The injected voltage compensates the drop in the line impedance.

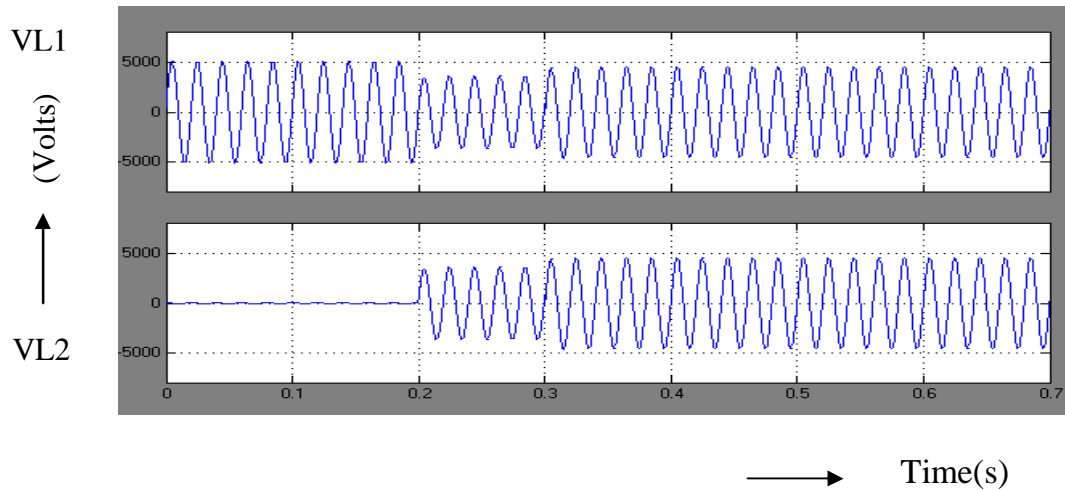


Fig.5.7. Voltage Across Load-1 And Load-2

The summary of real and reactive powers at various buses are shown in Table 5.1. The details of buses near the UPQC are presented. The changes in far end buses are negligible. The change in real and reactive power at bus 3 are predominant. This is due to the presence of UPQC near bus 3

**Table 5.1. Summary of Real and Reactive Power of 8 Bus System**

BUS NO	REAL POWER WITHOUT UPQC (MW)	REAL POWER WITH UPQC (MW)	REACTIVE POWER WITHOUT UPQC (MVAR)	REACTIVE POWER WITH UPQC (MVAR)
BUS-1	0.823	0.778	1.572	1.761
BUS-2	0.793	0.681	1.521	1.668
<b>BUS-3</b>	<b>0.0307</b>	<b>0.208</b>	<b>0.059</b>	<b>0.156</b>
BUS-4	0.289	0.381	0.825	0.978
BUS-5	0.358	0.423	0.958	1.278
BUS-6	0.268	0.378	1.237	1.132
BUS-7	0.248	0.513	0.981	1.478
BUS-8	0.456	0.574	1.432	1.641

### 5.3. Results and Discussions

It can be seen that the reactive power increases with the increase in the injected voltage. This is because the reactive power is proportional to squarer of the voltage. The increase in real power, reactive power and the voltage is higher near bus three than the other buses due the presence of UPQC. The real and reactive powers can be increased by connecting UPQC and they can be controlled by using the UPQC. Hence the desired power flow can be made to flow in a bus by providing suitable control to the UPQC.

### 5.4. Results comparison with desirables and analysis

Real and Reactive power at all the Eight Buses are shown. The reactive power is proportional to square of the voltage. Hence reactive power increases with the increase in the injected voltage. The increase in real, reactive power and the voltage is higher near bus three than the other buses due to the presence of UPQC. The simulation results are inline with the predictions.

### 5.5. Model of Fourteen Bus System using UPQC in power systems to improve power quality

Simulink model of 14 bus system is shown in Fig.5.6.1.

The specifications of the components used for simulation are as follows:

L and C are designed by assuming  $\Delta I = 0.4A$ ,  $f = 3kHz$  and  $R = 1K\Omega$ .

L and C for boost converter worksout to be 7.5mH and 12 $\mu$ F;

$T_{ON} = 0.25ms$  ;  $T_{OFF} = 0.08ms$ .

Scopes are connected to measure receiving end voltage, receiving end current, real power and reactive power. The generator is represented as series combination of R, L, and E. Each Line is represented by a series impedance. The load at the receiving end is series combination of resistance of 200 $\Omega$  and inductance of 100mH. The parameters of the additional load are 50 $\Omega$  and 50mH.



DC required by the UPQC is applied from a photo cell. The output of UPQC is injected using a series transformer.

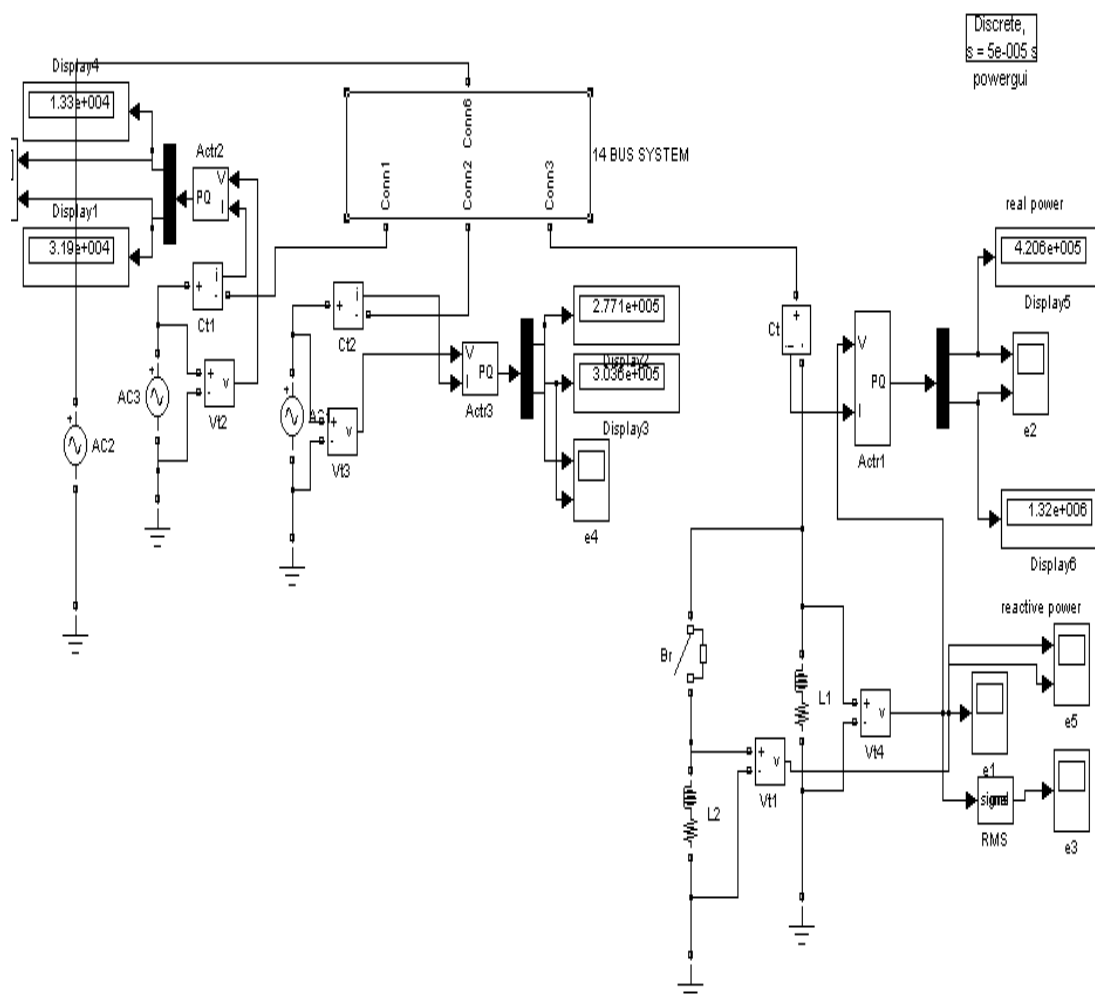


Fig.5.6.1. Fourteen Bus System without UPQC

The inverter of DVR used in the UPQC is triggered at 50Hz. All the switches are operated with puls of 10ms width. The puls given to the other two switches are displaced by 10ms. The output of the inverter is filtered by using a LC filter. This will reduce heating since harmonics are reduced. The inverter switches of active filter are triggered at 250Hz. The circuit of Fourteen bus system without UPQC is shown in Fig.5.6.1. Load 2 is connected in parallel with load 1. The breaker is connected in series with load 2. Additional load is applied by closing the breaker at  $t=0.2s$ .

Fig.5.6.2, shows the real and reactive power across bus 7. The graph is drawn with time on x-axis and power on y-axis. The real and reactive power increases at  $t=0.2s$ , since the current drawn is increased.

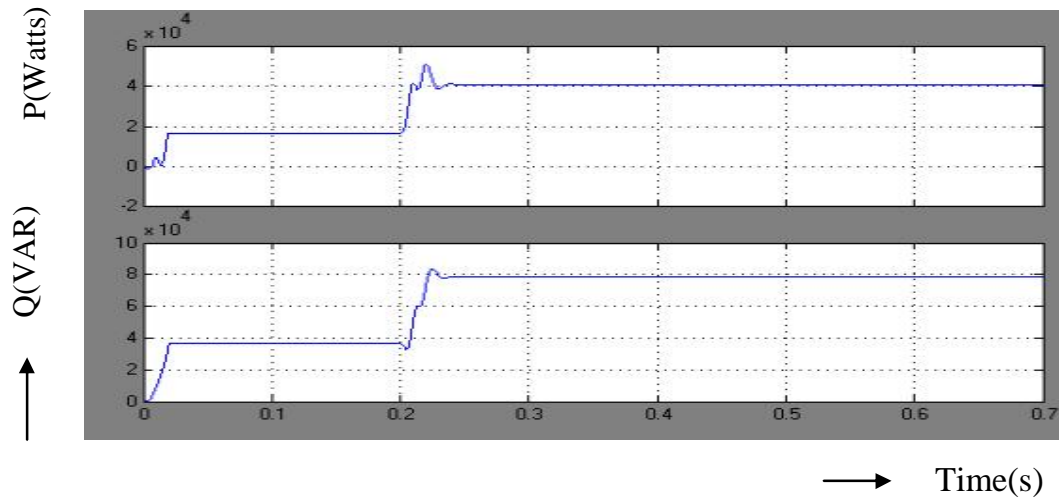


Fig. 5.6.2. Real and Reactive Power Across Bus-7

Fig. 5.6.3, shows the real and reactive power across bus 3. The graph is drawn with time on x-axis and power on y-axis. The real and reactive power increases at  $t=0.2s$ , since the current drawn is increased. This is due to the increase in the load at bus 3.

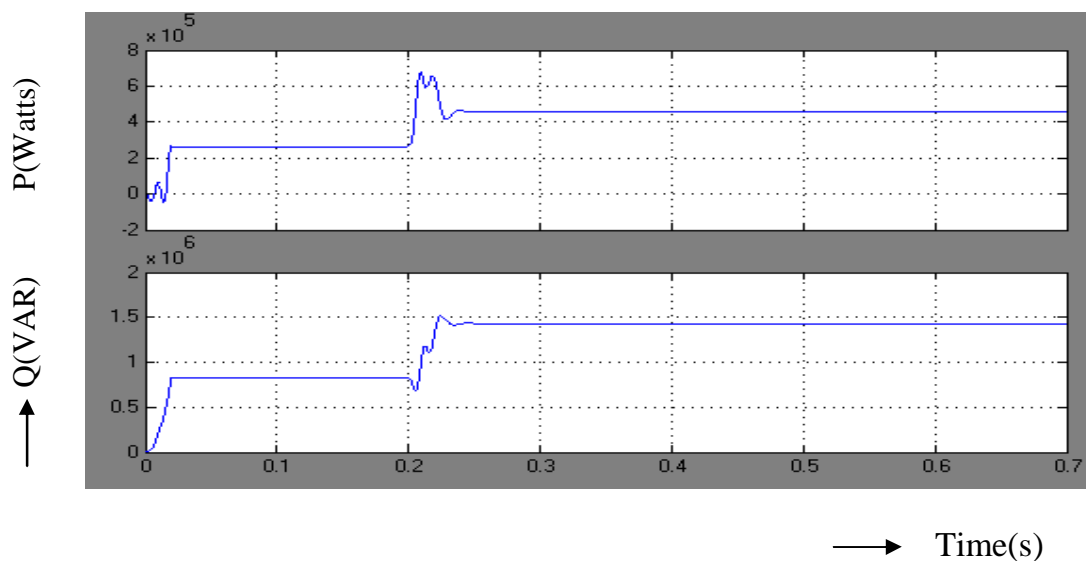


Fig. 5.6.3. Real and Reactive Power Across Bus-3

Fig. 5.6.4, shows the voltage across load 1 and load 2. The graph is drawn with time on x-axis and voltage on y-axis. At  $t=0.2s$ , the voltage across loads 1 and 2 decrease due to the addition of heavy load.

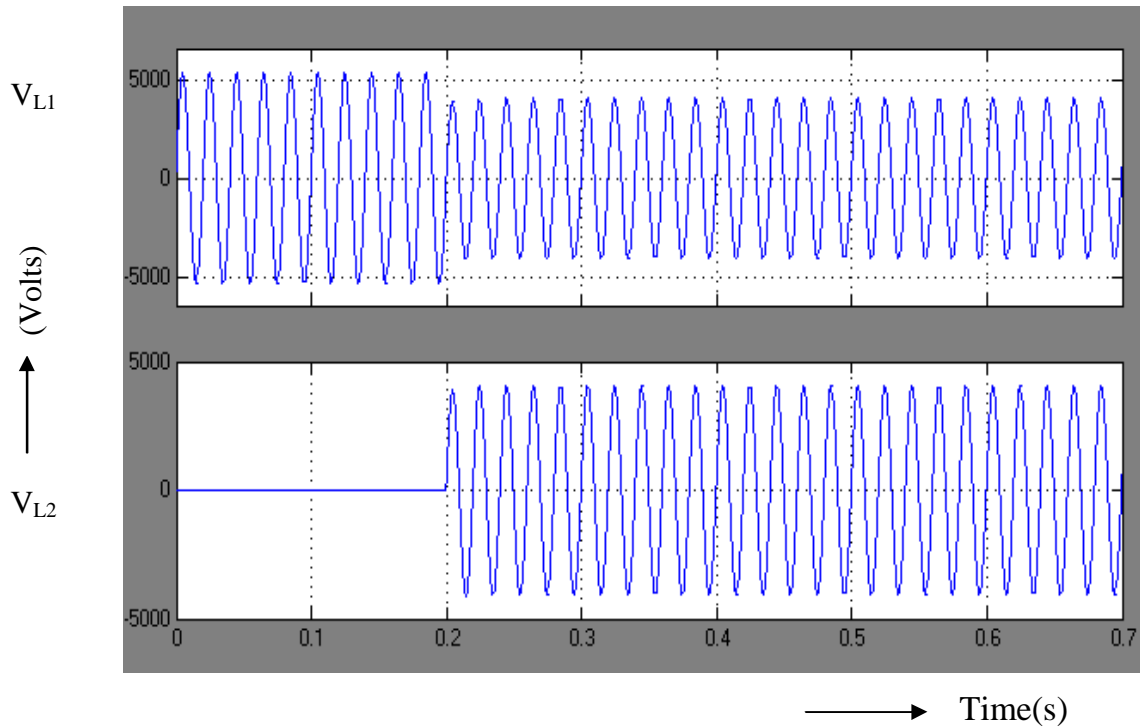


Fig. 5.6.4. Voltage Across Load-1 And Load-2

The circuit of Fourteen bus system with UPQC is shown in Fig. 5.6.5. The network of 14 bus system is represented as a sub-system and it is shown in Fig. 5.6.6.

Scopes are connected to measure receiving end voltage, receiving end current, real power and reactive power. The generator is represented as series combination of R, L, and E. Each Line is represented by a series impedance. The load at the receiving end is series combination of resistance of  $200\Omega$  and inductance of 100mH. The parameters of the additional load are  $50\Omega$  and 50mH. DC required by the UPQC is obtained from a photo cell. The output of UPQC is injected using a series transformer.



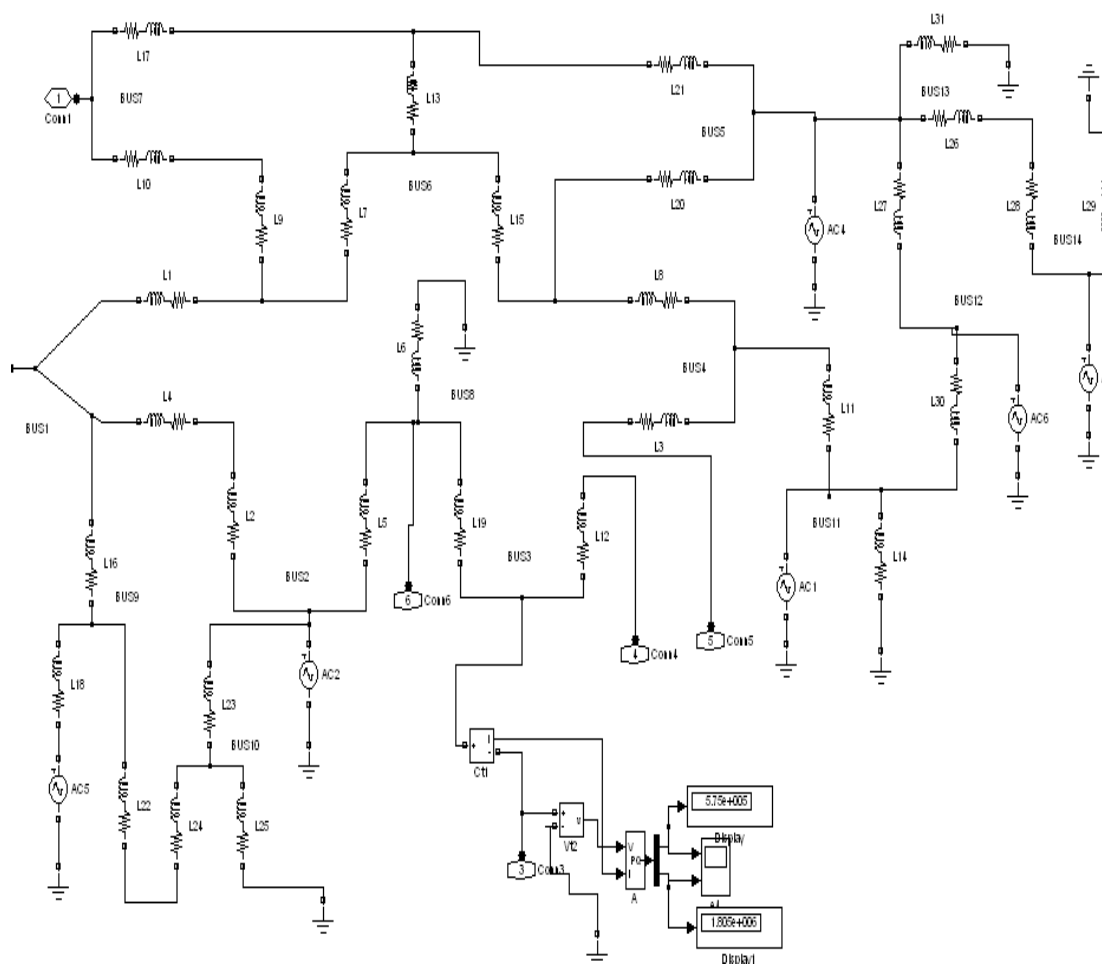


Fig. 5.6.6. Circuit model of 14 Bus System

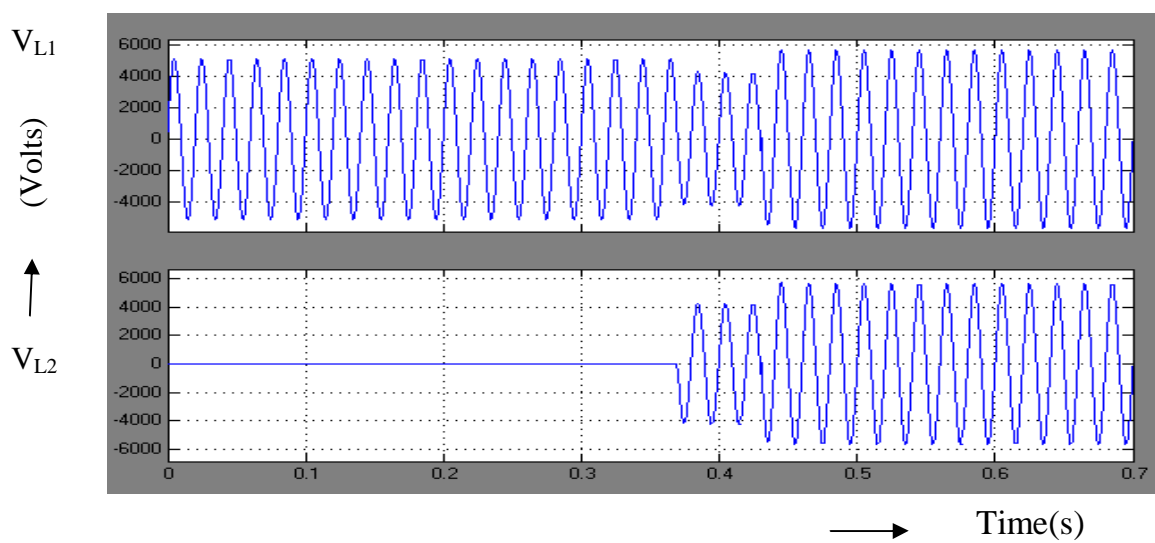


Fig. 5.6.7. Voltage Across Load-1 And Load-2

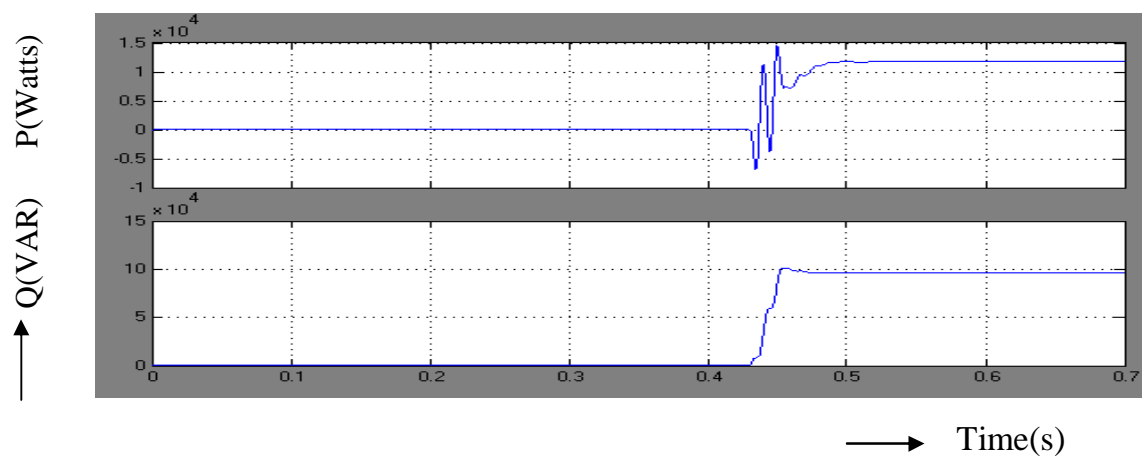


Fig. 5.6.8. Real and Reactive Power Across Bus-7

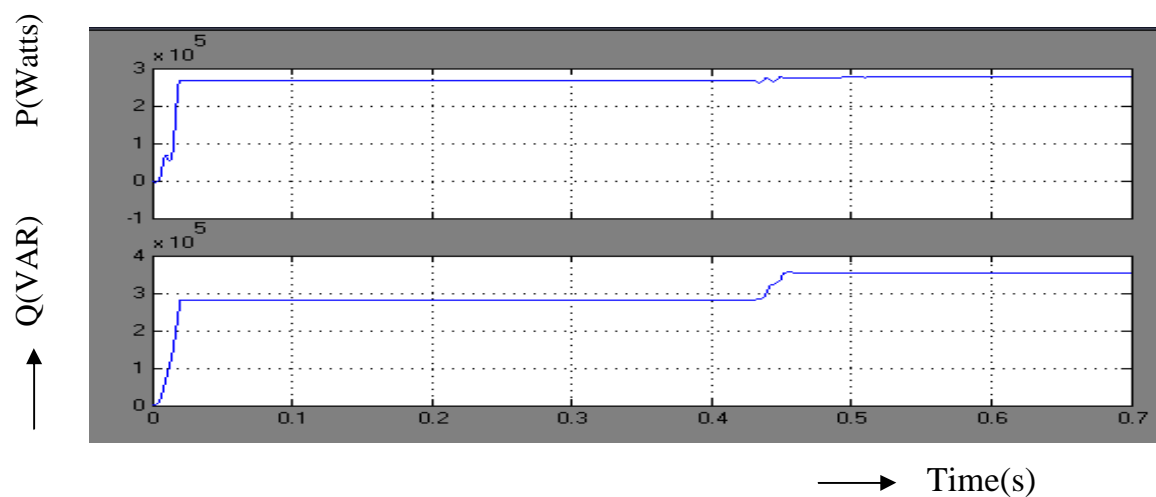


Fig. 5.6.9. Real and Reactive Power Across Bus-1

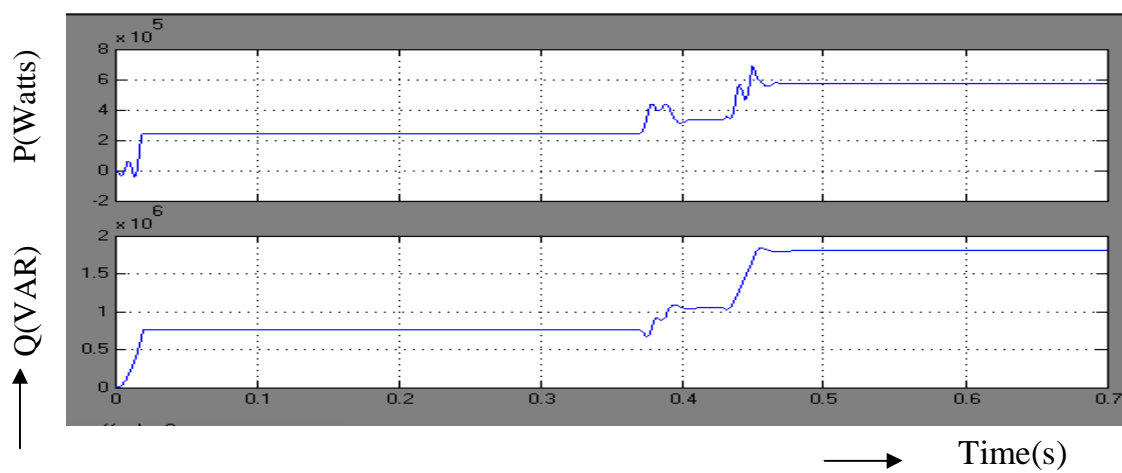


Fig. 5.6.10. Real and Reactive Power Across Bus-3

The voltages across load 1 and load 2 are shown in Fig. 5.6.7. The real and reactive power in buses 7, 1 and 3 are shown in Figs. 5.6.8, 5.6.9 and 5.6.10 respectively. The load is applied at  $t=0.2s$ . The DVR part of UPQC injects voltage at  $t=0.3s$ . The real and reactive power at bus 1 decreases and that of bus 3 increases due to the transfer of power from bus 1 to bus 3. The voltage decreases at  $t=0.2s$ . and resumes to its normal value at  $t=0.3s$ . This is due to the voltage injected by the UPQC.

The summary of real and reactive powers at various buses are shown in Table 5.2. The changes at the far end buses are neglected. The voltage injected by UPQC is increase at the bus voltage. Therefore increase in reactive power is enormous.

**Table 5.2. Summary of Real and Reactive Power of 14 Bus System**

BUS NO	REAL POWER WITHOUT UPQC (MW)	REAL POWER WITH UPQC (MW)	REACTIVE POWER WITHOUT UPQC (MVAR)	REACTIVE POWER WITH UPQC (MVAR)
BUS-1	0.277	0.377	0.303	0.323
BUS-2	0.267	0.356	0.297	0.316
BUS-3	0.420	0.678	1.320	2.127
BUS-4	0.389	0.587	1.182	1.891
BUS-5	0.365	0.538	1.452	1.678
BUS-6	0.313	0.428	1.284	1.385
BUS-7	0.110	0.338	0.989	1.258
BUS-8	0.231	0.278	0.897	1.182
BUS-9	0.348	0.3867	1.231	1.347
BUS-10	0.389	0.587	1.182	1.891
BUS-11	0.365	0.583	1.452	1.678
BUS-12	0.327	0.459	1.214	1.368
BUS-13	0.336	0.436	1.123	1.485
BUS-14	0.314	0.389	1.089	1.247

## 5.6. Results and Discussions

It can be seen that the reactive power increases with the increase in the injected voltage. The increase in real power, reactive power and the voltage is higher in buses near Bus 7 than the other buses due the presence of UPQC. The real and reactive powers can be increased by connecting UPQC and they can be controlled by using the UPQC.

## 5.7. Results comparison with desirables and analysis

Real and Reactive power at all the Fourteen Buses are shown. The reactive power is proportional to square of the voltage. Hence reactive power increases with the increase in the injected voltage. The increase in real, reactive power and the voltage is higher near bus seven than the other buses due to the presence of UPQC. The simulation results are inline with the predictions.

## 5.8. Model of Thirty Bus System using single UPQC in power systems to improve power quality

Thirty bus system is analyzed by using the single phase circuit model. The circuit model of thirty bus system is shown in Fig. 5.7.1a.

A Simulink model of 30 bus system is shown here. Thirty Bus System is modeled using the elements of Matlab Simulink and the simulation results are presented in this section.

The specifications of the components used for simulation are as follows:

L and C are designed by assuming  $\Delta I = 0.4A$ ,  $f = 3kHz$  and  $R = 1K \Omega$ .

L and C for boost converter workout to be 7.5mH and 12 $\mu$ F;

$T_{ON} = 0.25ms$  ;  $T_{OFF} = 0.08ms$ .

Scopes are connected to measure receiving end voltage, receiving end current, real power and reactive power. The generator is represented as series



combination of R, L, and E. Each Line is represented by series impedance. The load at the receiving end is series combination of resistance of  $200\Omega$  and inductance of  $100\text{mH}$ . The parameters of the additional load are  $50\Omega$  and  $50\text{mH}$ . DC required by the UPQC is applied from a photo cell. The output of UPQC is injected using a series transformer.

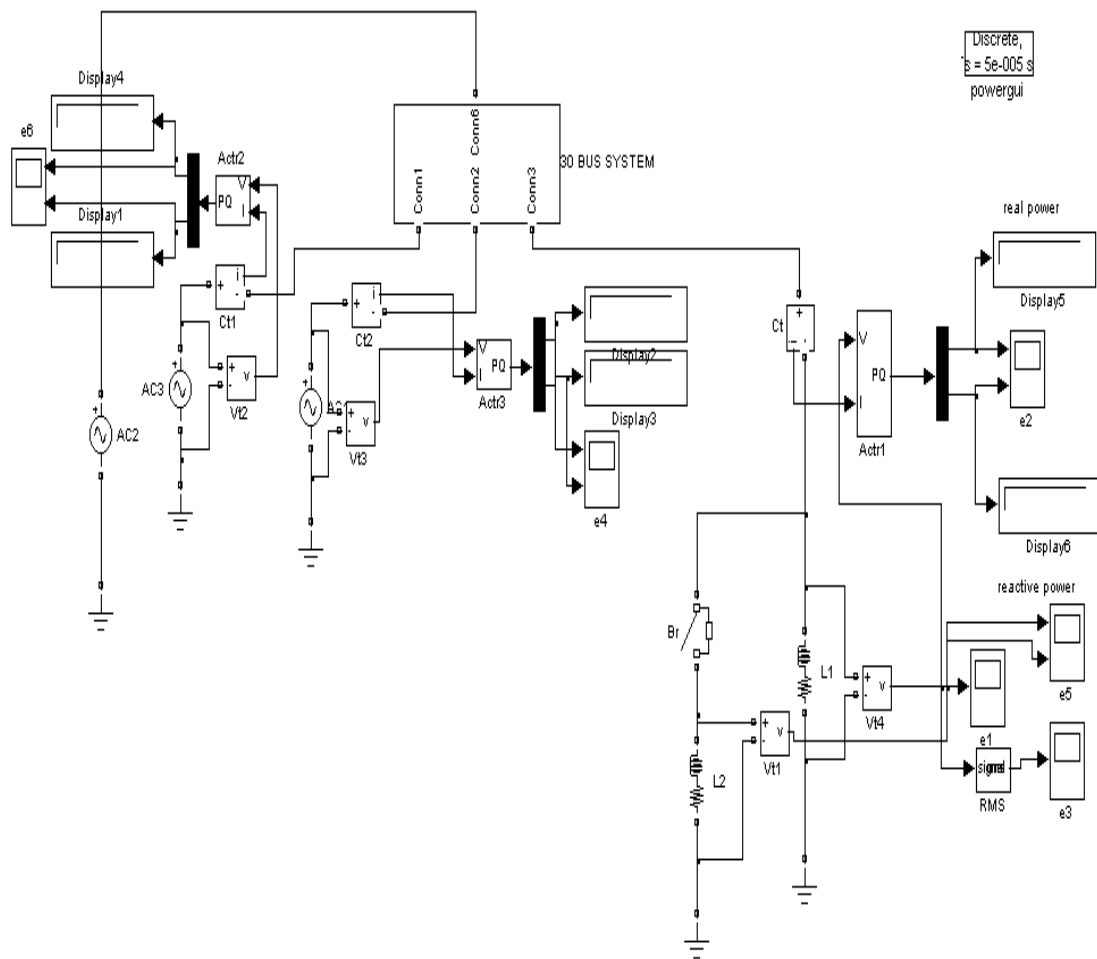


Fig. 5.7.1a. Thirty Bus system

The inverter of DVR used in the UPQC is triggered at  $50\text{Hz}$ . All the switches are operated with pulse of  $10\text{ms}$  width. The pulse given to the other two switches are displaced by  $10\text{ms}$ . The output of the inverter is filtered by using LC filter. This will reduce heating since harmonics are reduced. The inverter switches of active filter are triggered at  $250\text{Hz}$ .

Real and Reactive power display blocks are added to measure the true power and reactive power at buses nearer to the location of UPQC. The voltage sag is created by connecting an additional load in parallel with the existing load. The real and reactive power at the buses 7 and 3 are shown in Figs. 5.7.1b and 5.7.1c respectively. The real and reactive powers increase due to the increase in the load near these buses.

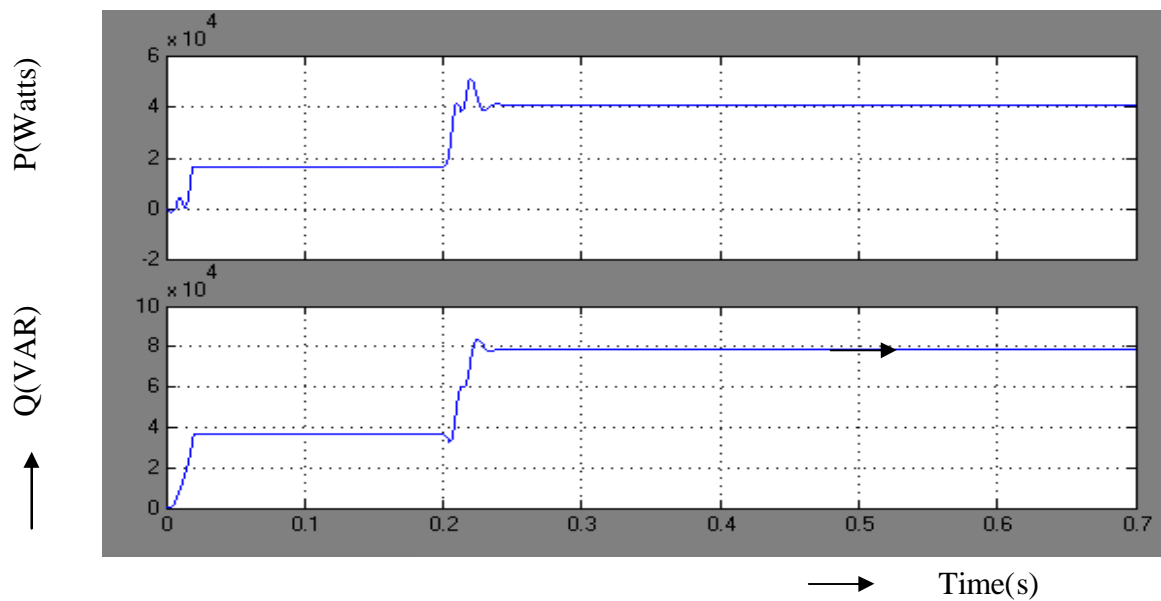


Fig. 5.7.1b. Real and Reactive Power Across Bus-7

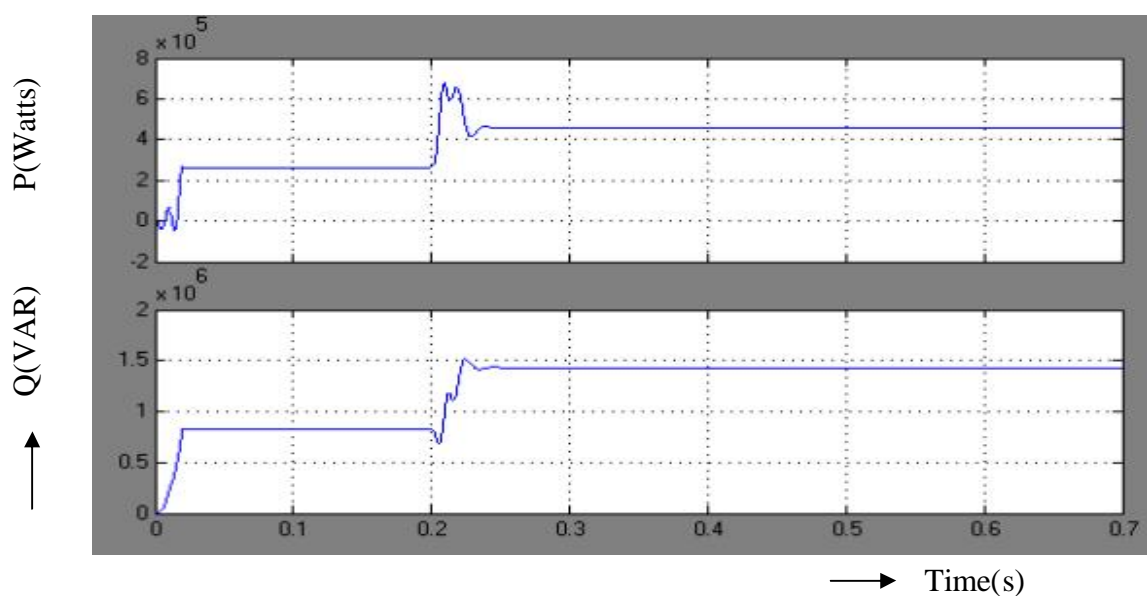


Fig. 5.7.1c. Real and Reactive Power Across Bus-3

The real and reactive power of bus 21 is shown in Fig. 5.7.1d. The powers in other buses remain the same since they are far from the point of change in load.

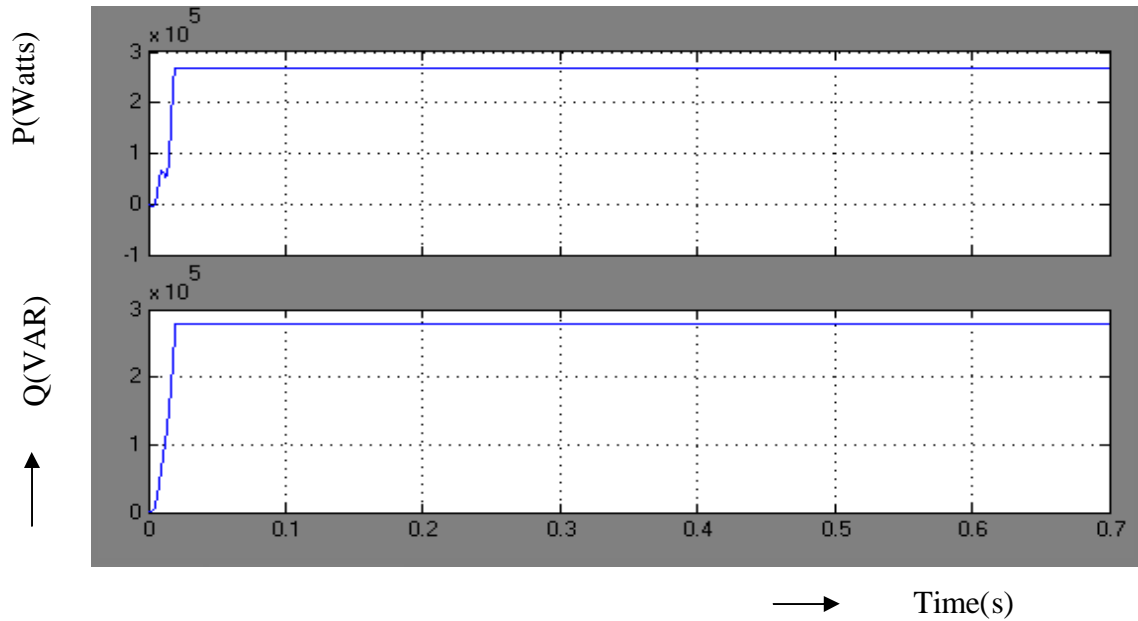


Fig. 5.7.1d. Real and Reactive Power Across Bus-21

The voltages across load 1 and load 2 are shown in Fig. 5.7.1(e). The amplitude of voltage decreases on the application of additional load. In the above figure voltage across load 1 and 2 is drawn with time on x-axis and time on y-axis. At  $t=0.2s$ , the voltage across 1 and 2 decreases due to addition of heavy load.

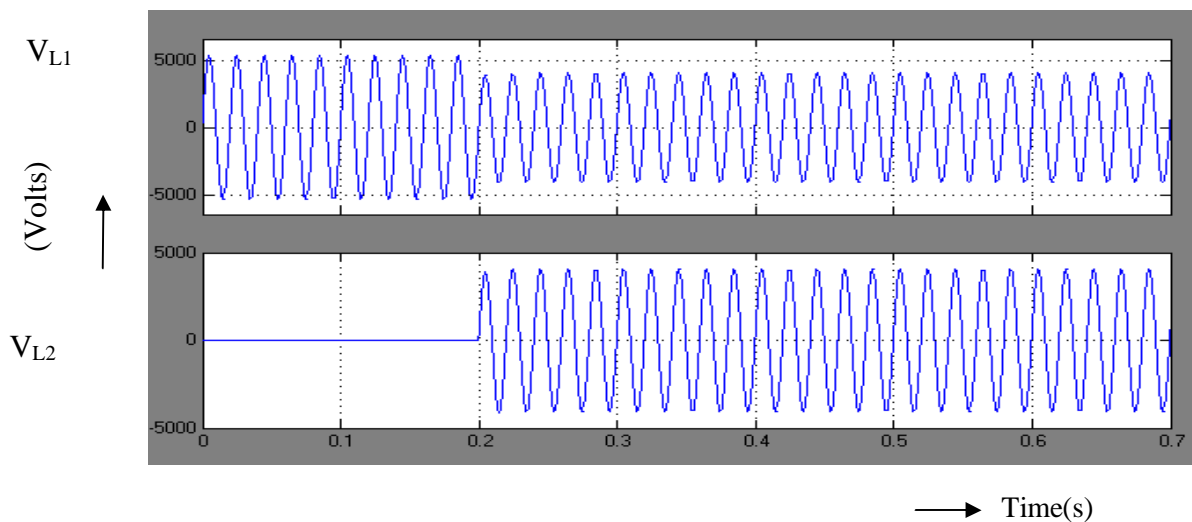


Fig. 5.7.1e. Voltage Across Load-1 and Load-2

Thirty bus system with UPQC is shown in Fig. 5.7.2.a. Existing load and additional load are shown in Fig. 5.7.2.a.

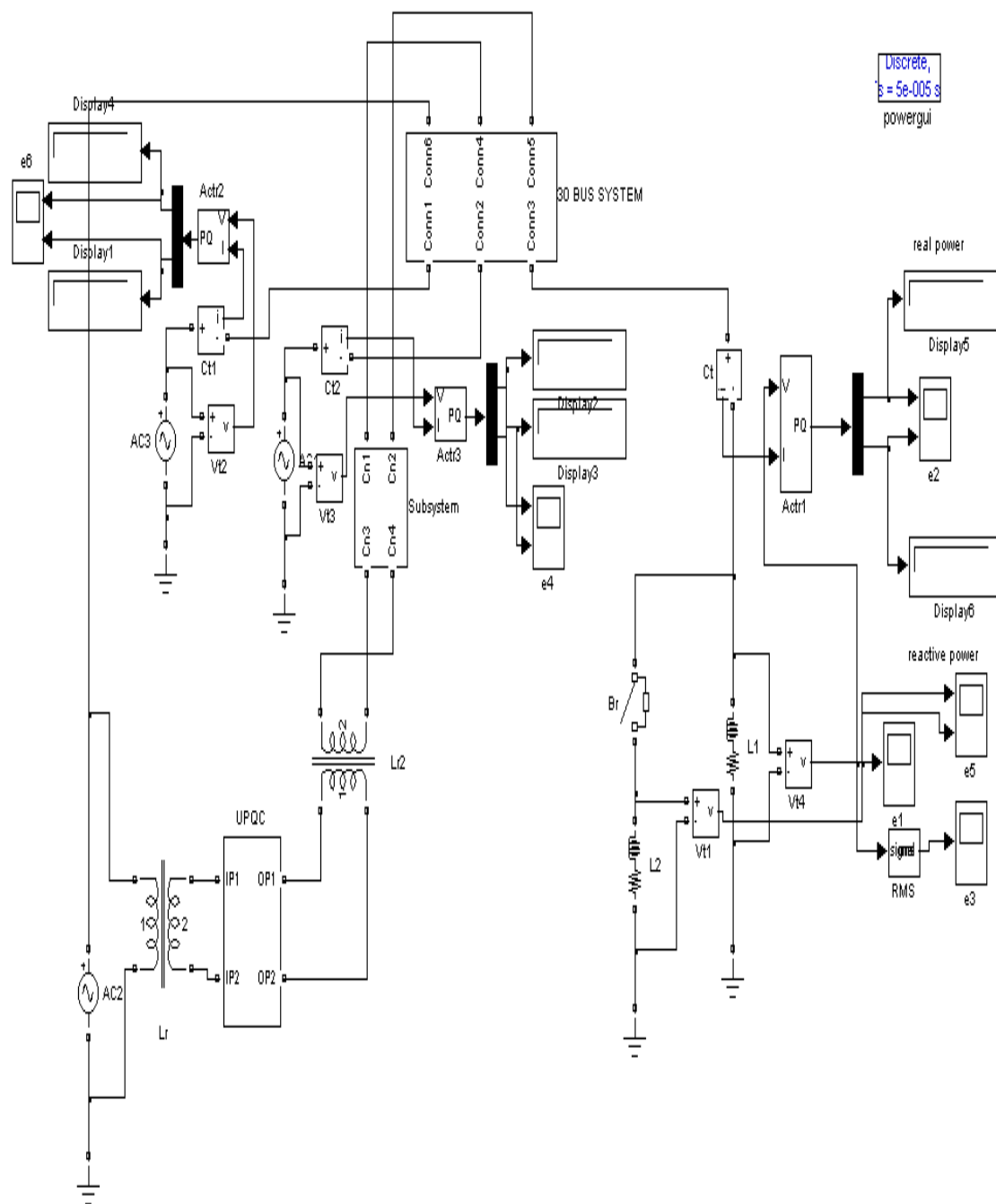


Fig. 5.7.2a. Thirty bus system with the UPQC

The UPQC circuit is introduced to improve the power quality of multi bus system. Thirty bus network is represented as a subsystem. This subsystem is shown in Fig. 5.7.2b.

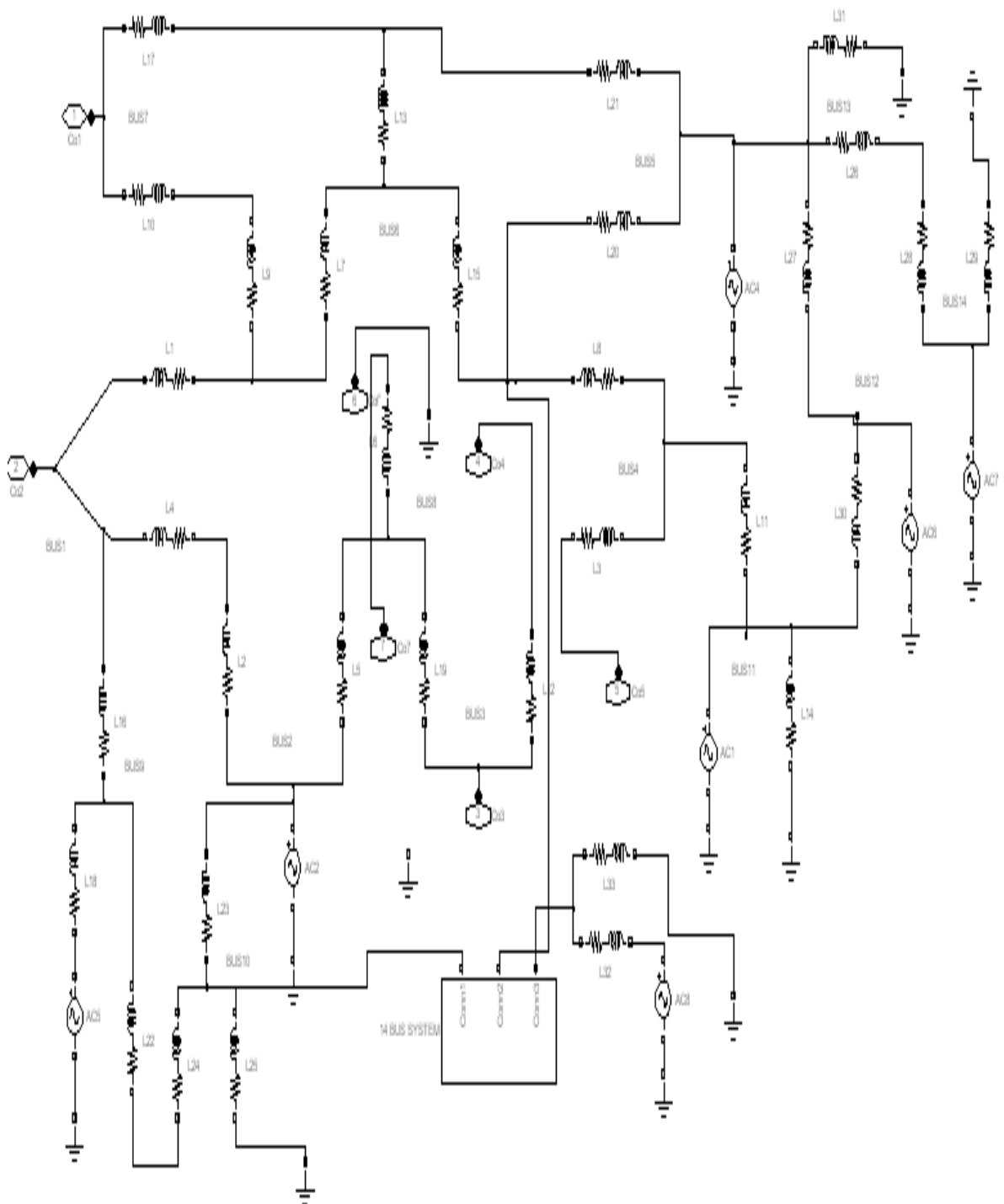


Fig. 5.7.2b. Thirty Bus Network

The Fig. 5.7.2c, represents the real and reactive power across bus 1. The graph is drawn between time on x-axis and power on y-axis. From origin real and reactive power starts to increase and maintains a constant value. After  $t=0.4s$  the real and reactive power increases and remains constant due to injection of emf by the UPQC.

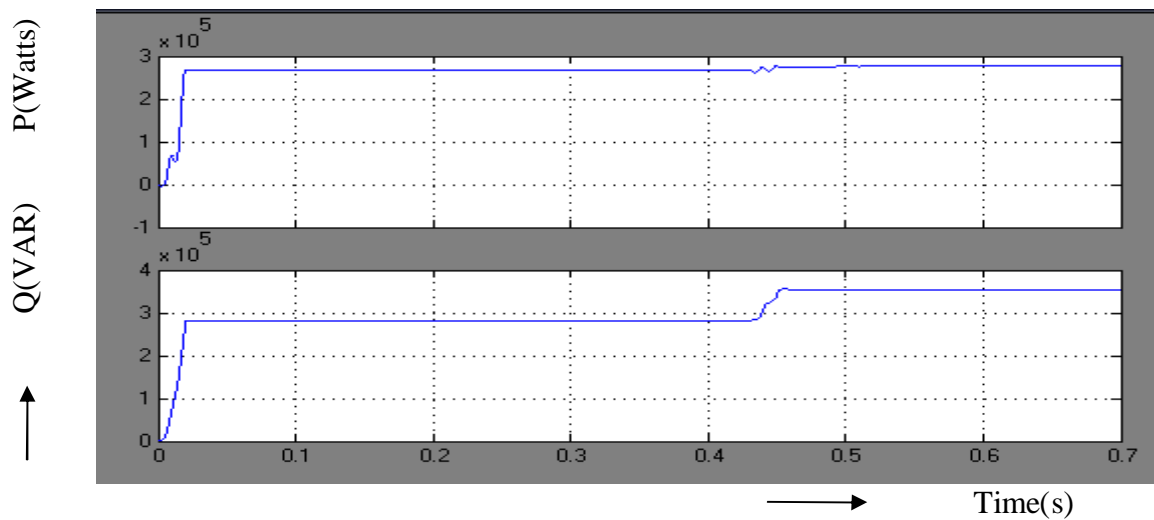


Fig. 5.7.2c. Real and Reactive Power Across Bus-1

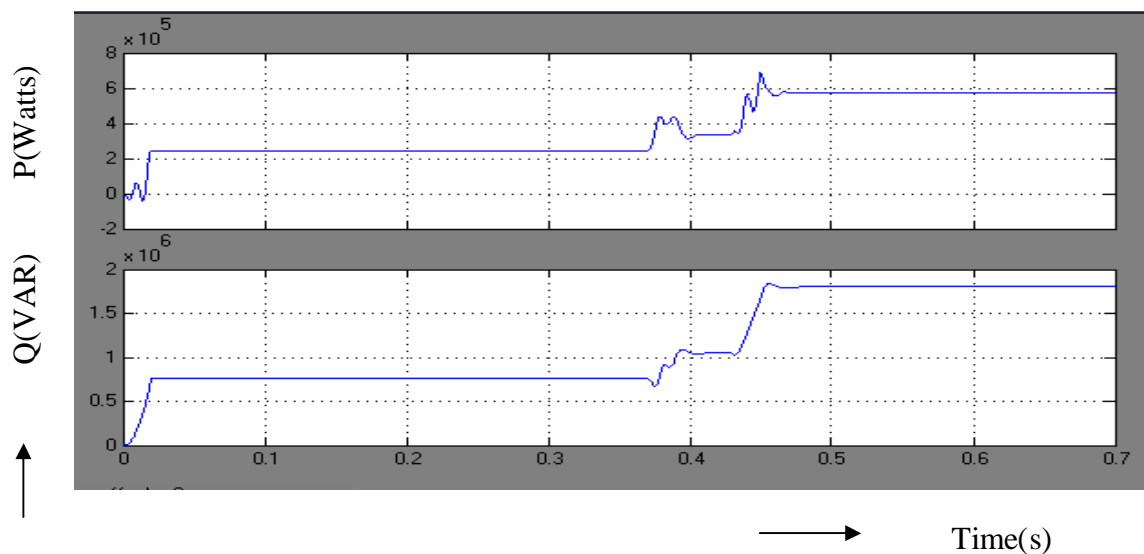


Fig. 5.7.2d. Real and Reactive Power Across Bus-7

The Fig. 5.7.2d, represents the real and reactive power across bus 7. The graph is drawn between time on x-axis and power on y-axis. From origin real and reactive power starts to increase and then it remains constant. Before  $t=0.4s$  the real and reactive power increases and maintains a constant value and again starts to increase and maintains a constant value after  $t=0.4s$ , due to injection of emf by the UPQC.

The Fig. 5.7.2e, represents the real power at bus 15. The graph is drawn between time on x-axis and the real power on y-axis. From the above wave form the real power increases and remains a constant.

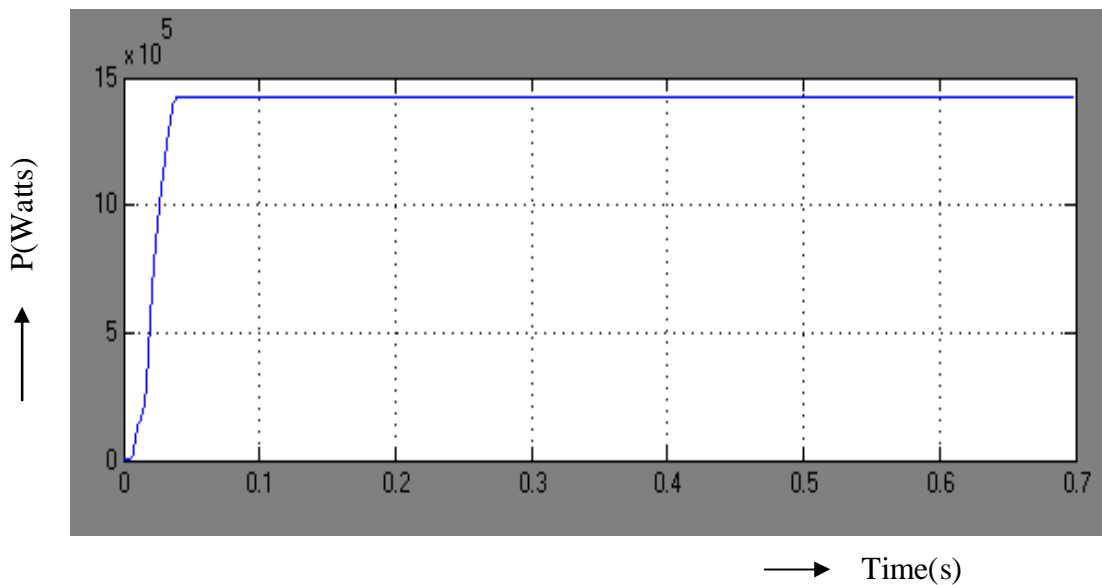


Fig. 5.7.2e. Real Power at Bus-15

The Fig. 5.7.2f, represents voltage across load 1 and 2. The graph is drawn between time on x-axis and voltage on y-axis. In the voltage across load 1, upto  $t=0.3s$  the voltage maintain a constant value and after  $t=0.3s$  the voltage starts to decreases, after  $t=0.4s$  the voltage starts to increases. The voltage decreases and then increases due to the action of UPQC. In voltage across load 2, upto  $t=0.4s$ , the voltage is not available and after  $t=0.4s$  the voltage decreases and then increases due the action of UPQC.

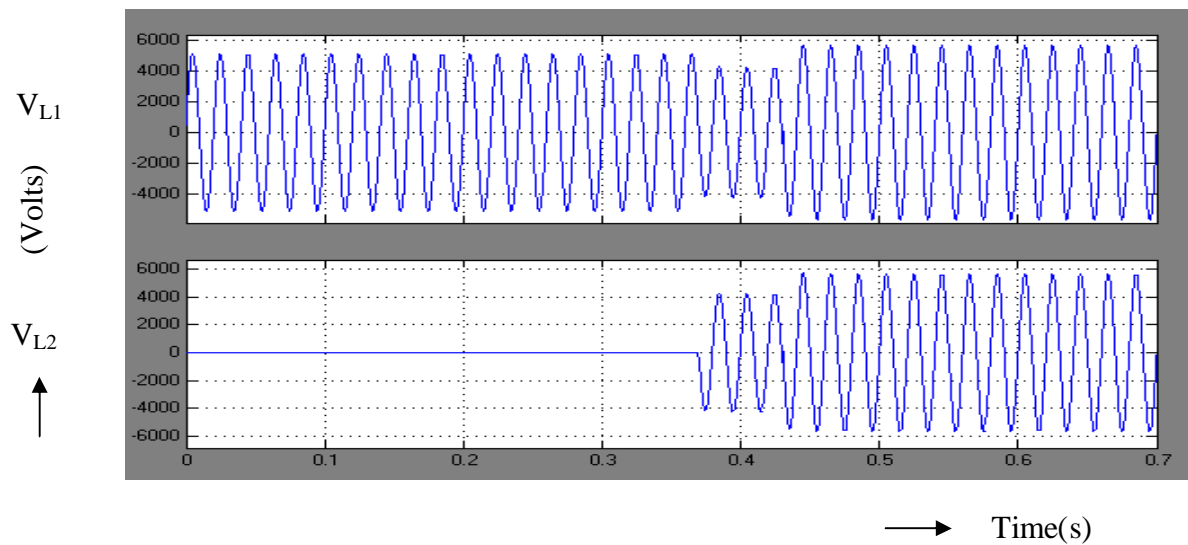


Fig. 5.7.2f. Voltage Across Load-1 and Load-2

The Fig.7.2g, represents the real and reactive power at bus 7. The graph is drawn between time on x-axis and the power on y-axis. From the above waveform the real power starts to decrease and again increases due to injection of emf by UPQC. The reactive power after  $t=0.4s$ , starts to increase and maintain a constant value due to injection of emf by UPQC.

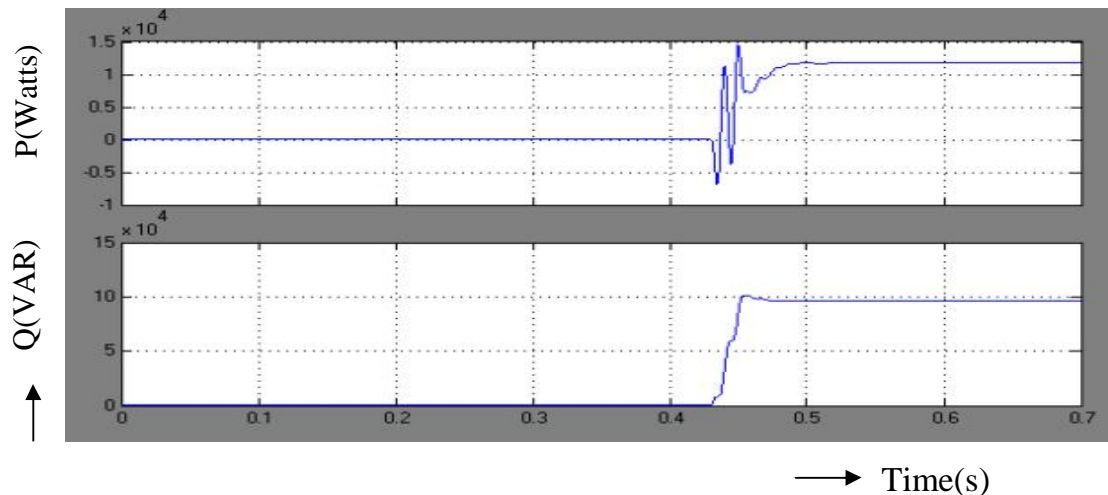


Fig. 5.7.2g. Real and Reactive Power Across Bus-7

The fig. 5.7.2h, represents the reactive power at bus 15. The graph is drawn between time on x-axis and reactive power on y-axis. The reactive power starts to increase from origin and maintain a constant value due to injection of emf by UPQC.



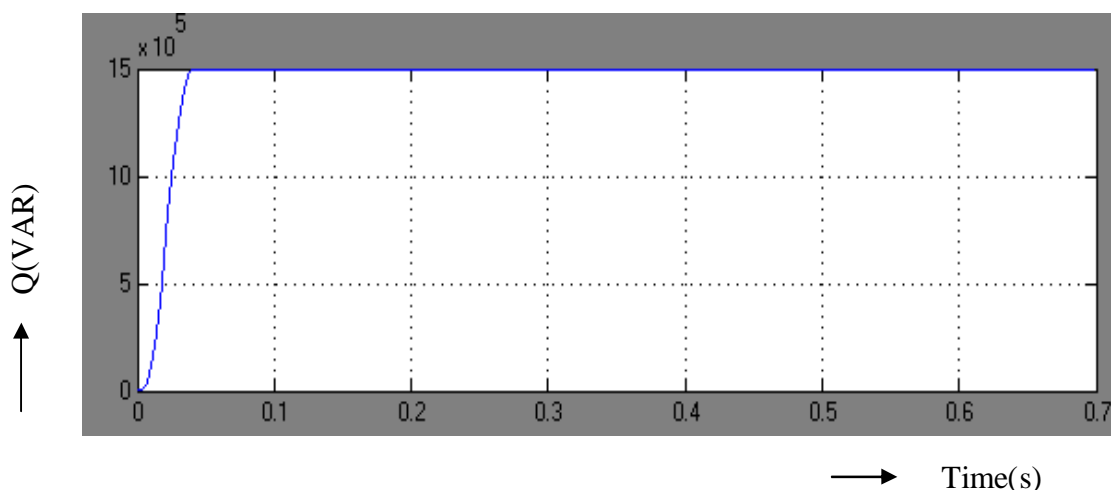


Fig. 5.7.2h. Reactive Power at Bus-15

The fig. 5.7.2i, represents real and reactive power at bus 21. The graph is drawn between time on x-axis and power on y-axis. From the above wave form the real and reactive power at bus 21 starts to increase from origin and maintains a constant value before  $t=0.4s$ . The real and reactive power again starts to increase and maintains a constant value due to the action of the UPQC.

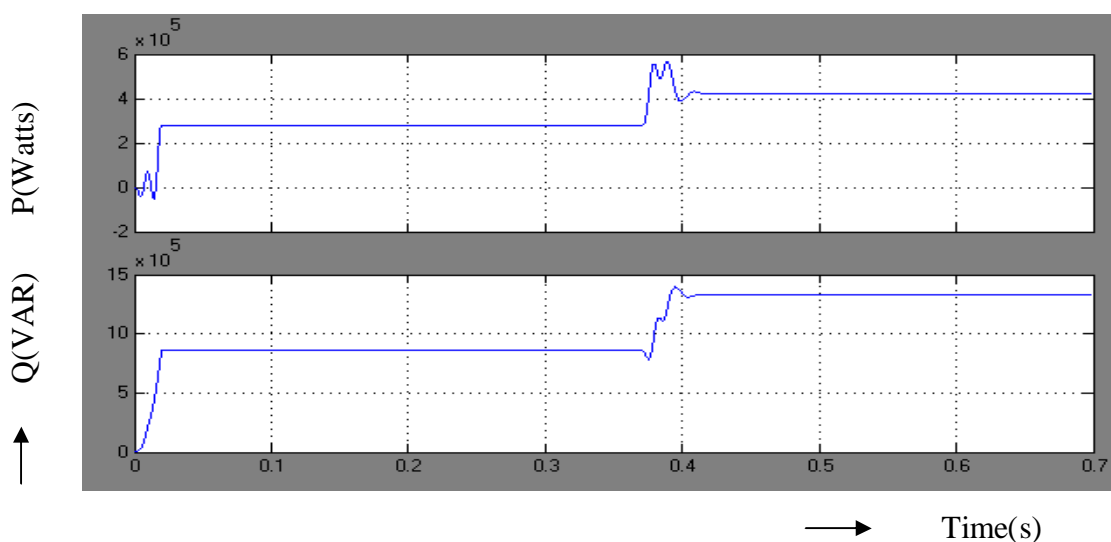


Fig. 5.7.2i. Real and Reactive Power Across Bus-21

The Figs. 5.7.2j and 5.7.2k, represents, the real and reactive power at bus 29. The graphs are drawn between time on x-axis and power on y-axis. From the above waveform the real and reactive power at bus 29 starts to increase from origin and maintains a constant value due to the action of UPQC.

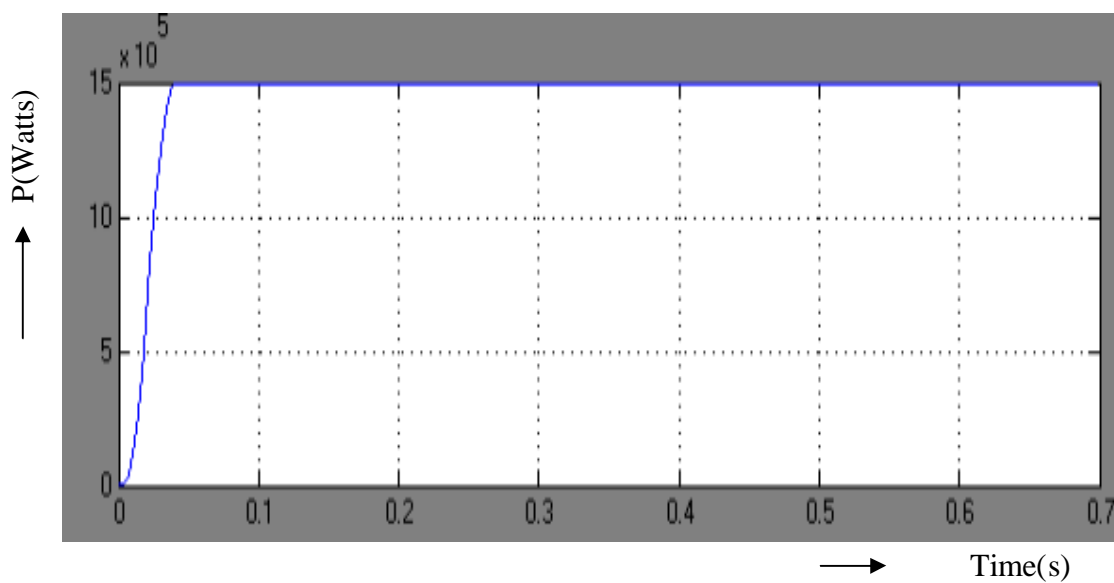


Fig. 5.7.2j. Real Power at Bus-29

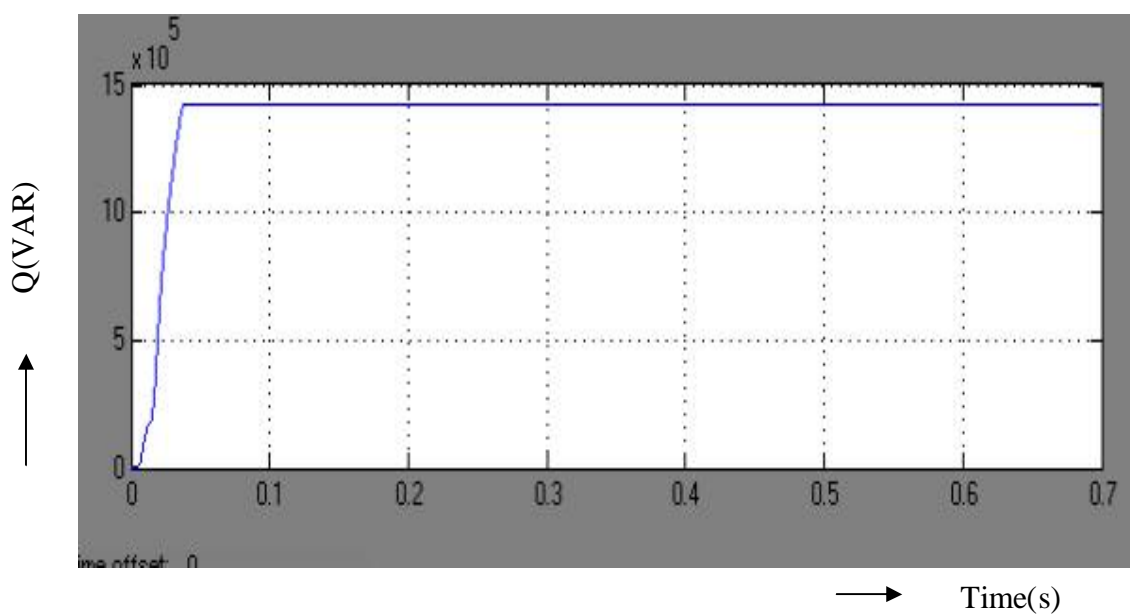


Fig. 5.7.2k. Reactive Power at Bus-29

The summary of real and reactive powers at various buses with and without UPQC are given in Table 5.3. It can be seen that there is an increase in real and reactive power due to the addition of UPQC. The increase in real and reactive power is due to the increase in the voltage.

**Table 5.3 Summary of Real and Reactive Powers of IEEE 30 Bus System**

BUS NO	REAL POWER WITHOUT UPQC (MW)	REAL POWER WITH UPQC (MW)	REACTIVE POWER WITHOUT UPQC (MVAR)	REACTIVE POWER WITH UPQC (MVAR)
BUS-1	0.367	0.360	0.115	0.113
BUS-2	0.294	0.278	0.922	0.901
BUS-3	0.277	0.267	0.108	0.105
BUS-4	<b>0.144</b>	<b>0.169</b>	<b>0.047</b>	<b>0.055</b>
BUS-5	0.63	0.917	0.237	0.346
BUS-6	0.364	0.377	1.14	1.185
BUS-7	0.218	0.257	0.685	0.807
BUS-8	<b>0.367</b>	<b>0.360</b>	<b>0.115</b>	<b>0.113</b>
BUS-9	0.294	0.287	0.922	0.901
BUS-10	0.277	0.267	0.108	0.105
BUS-11	0.144	0.169	0.074	0.055
BUS-12	0.63	0.917	0.237	0.346
BUS-13	0.364	0.377	1.14	1.185
BUS-14	0.218	0.257	0.685	0.807
BUS-15	0.367	0.360	0.922	0.901
BUS-16	0.294	0.287	0.922	0.901
BUS-17	0.277	0.267	0.108	0.105
BUS-18	0.144	0.169	0.047	0.055
BUS-19	0.63	0.917	0.237	0.346
BUS-20	0.364	0.377	1.14	1.185
BUS-21	0.218	0.257	0.685	0.807
BUS-22	0.364	0.377	1.14	1.185
BUS-23	0.218	0.257	0.685	0.807
BUS-24	0.367	0.360	0.115	0.113
BUS-25	0.144	0.169	0.047	0.055
BUS-26	0.63	0.917	0.237	0.346
BUS-27	0.364	0.377	1.14	1.185
BUS-28	0.218	0.257	0.685	0.807
BUS-29	0.63	0.917	0.237	0.346
BUS-30	0.364	0.377	1.14	1.185

### 5.9. Model of IEEE 30 Bus System with multiple UPQC

The thirty bus system with two UPQCs is simulated using Matlab and the results are presented in this section. Two UPQC's are connected in Thirty Bus Systems. The real and reactive powers are tabulated without connecting the UPQC and with the UPQC. The voltage sag compensation is made by the UPQC in a Thirty Bus System. For realizing the voltage sag additional load is added. The wave forms are observed by connecting the UPQC.

Simulink model of 30 bus system is shown here. Thirty Bus System is modeled using the elements of Matlab Simulink and the simulation results are presented in this section.

The specifications of the components used for simulation are as follows:

L and C are designed by assuming  $\Delta I = 0.4A$ ,  $f = 3kHz$  and  $R = 1K \Omega$ .

L and C for boost converter workout to be 7.5mH and 12 $\mu$ F;

$T_{ON} = 0.25ms$  ;  $T_{OFF} = 0.08ms$ .

Scopes are connected to measure receiving end voltage, receiving end current, real power and reactive power. The generator is represented as series combination of R, L, and E. Each Line is represented by a series impedance. The load at the receiving end is series combination of resistance of 200 $\Omega$  and inductance of 100mH. The parameters of the additional load are 50 $\Omega$  and 50mH. DC required by the UPQC is applied from a photo cell. The output of UPQC is injected using a series transformer.

The inverter of DVR used in the UPQC is triggered at 50Hz. All the switches are operated with pulses of 10ms width. The pulses given to the other two switches are displaced by 10ms. The output of the inverter is filtered by using LC filter. This will reduce heating since harmonics are reduced. The inverter switches of active filter are triggered at 250Hz.

The circuit model of thirty bus system without UPQC is shown in Fig. 5.7.3.1. Voltage sag across at three buses i.e., bus 4, bus 12 and bus 26.

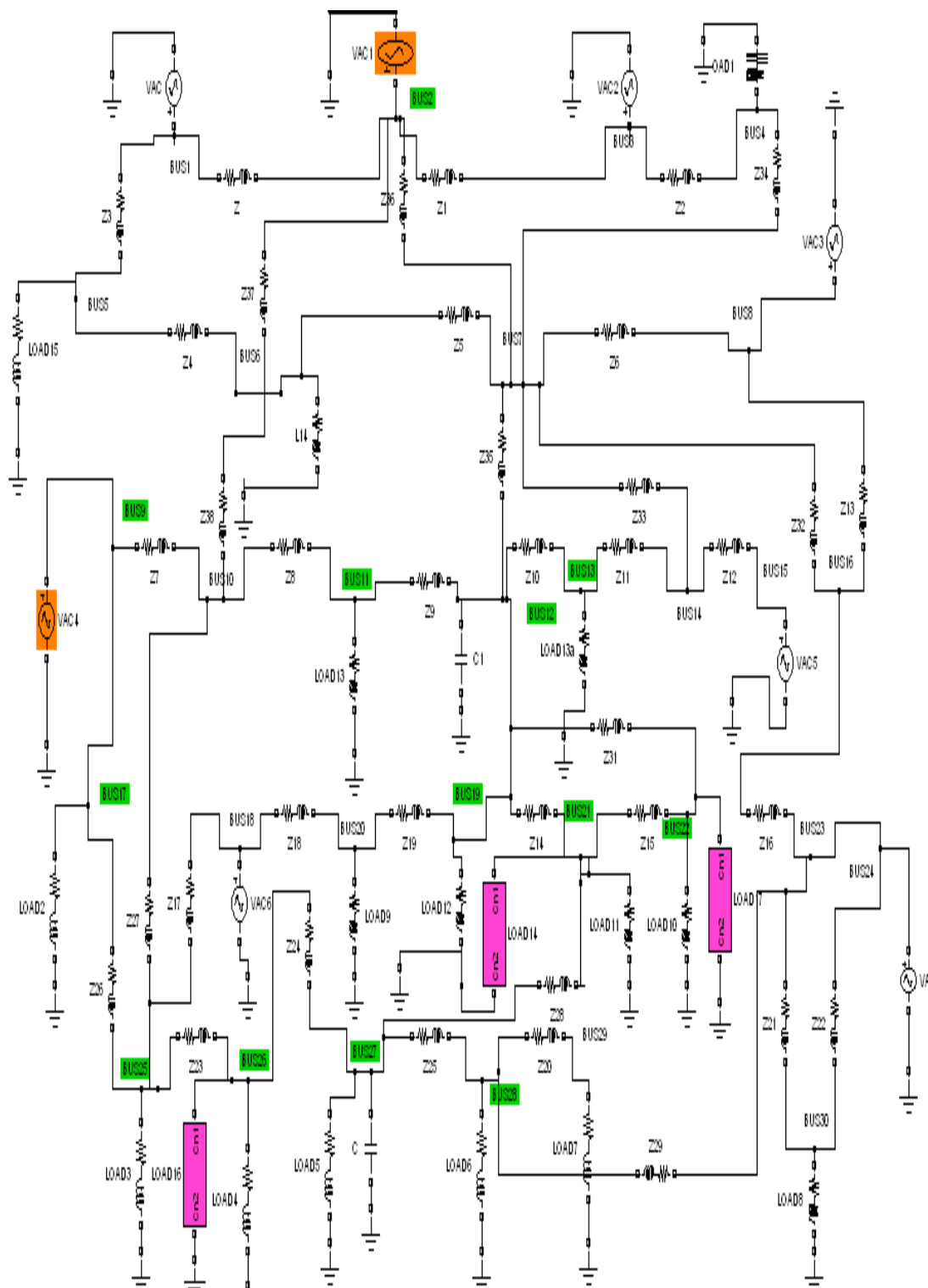


Fig. 5.7.3.1. 30 Bus System without UPQC

The Fig. 5.7.3.2, represents the voltage at bus 4. The graph is drawn between time on x-axis and voltage on y-axis. From the above waveform the voltage at bus 4 maintains a constant value upto  $t=0.2s$ . After that the amplitude of voltage level decreases due to addition of load.

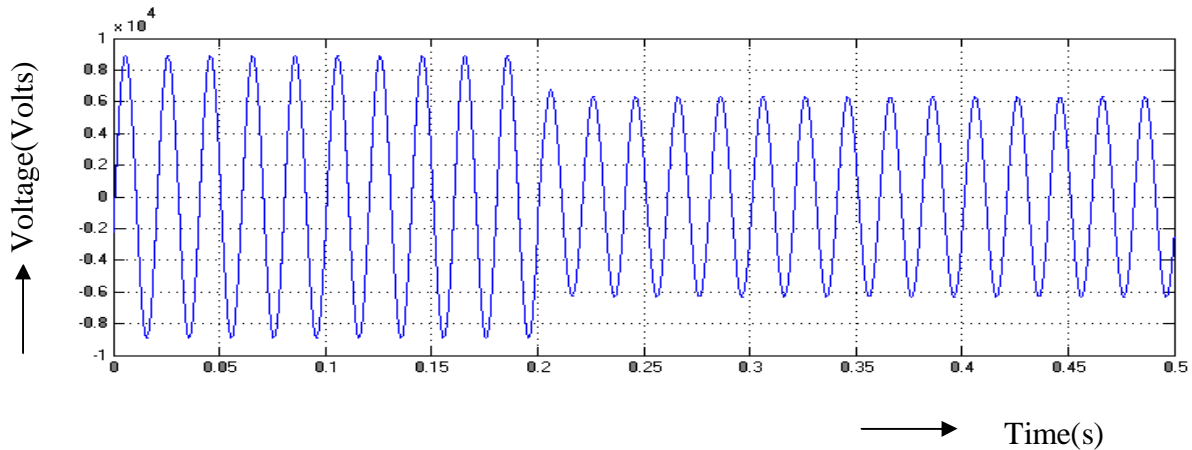


Fig. 5.7.3.2. Voltage at Bus-4

The Figs. 5.7.3.3 and 5.7.3.4, represents the real and reactive power at bus 4. The graph is drawn between time on x-axis and power on y-axis. From the above waveform the real and reactive power starts to increase from origin and maintain a constant value upto  $t=0.2s$  after that starts to decrease, again maintain a constant value. This action takes place since voltage sag created at bus 4.

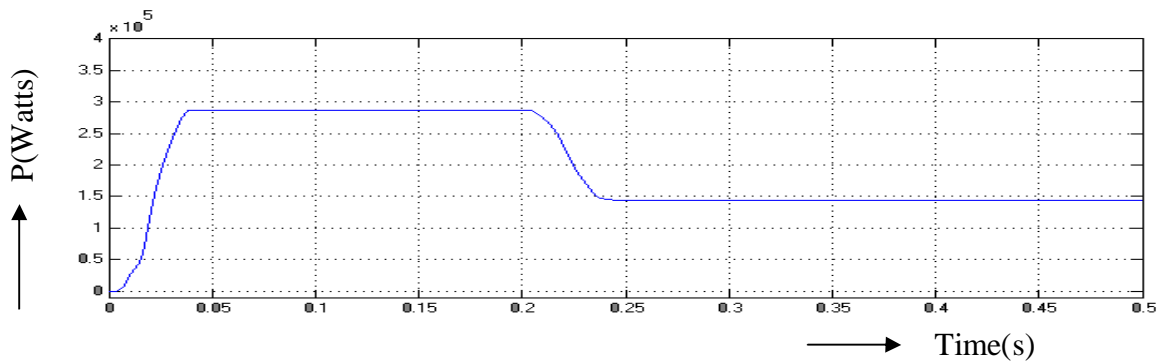


Fig. 5.7.3.3. Real Power at Bus-4

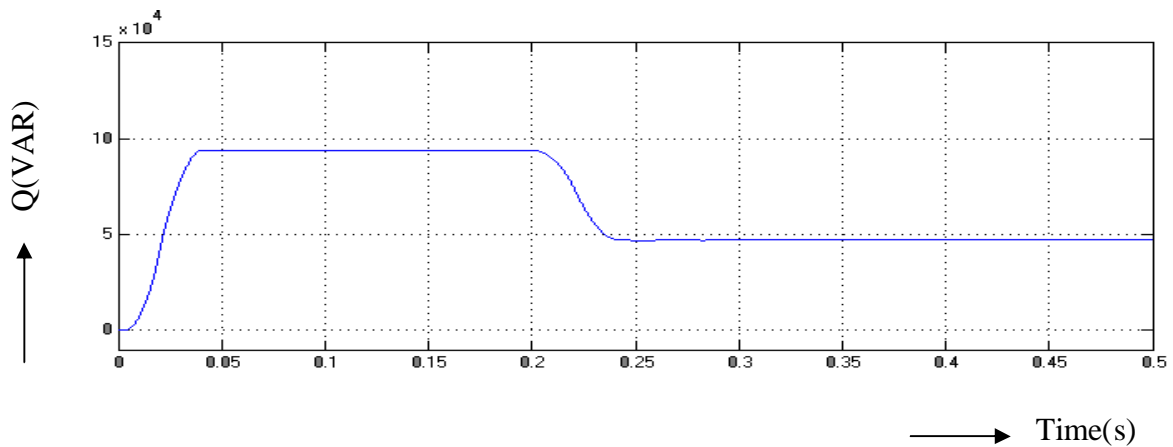


Fig. 5.7.3.4. Reactive Power at Bus-4

The Fig. 5.7.3.5, represents the voltage at bus 12. The graph is drawn between time on x-axis and voltage on y-axis. From the above waveform the voltage at bus 12 maintains a constant value upto  $t=0.2s$ . After that the amplitude of voltage level decreases due to addition of load.

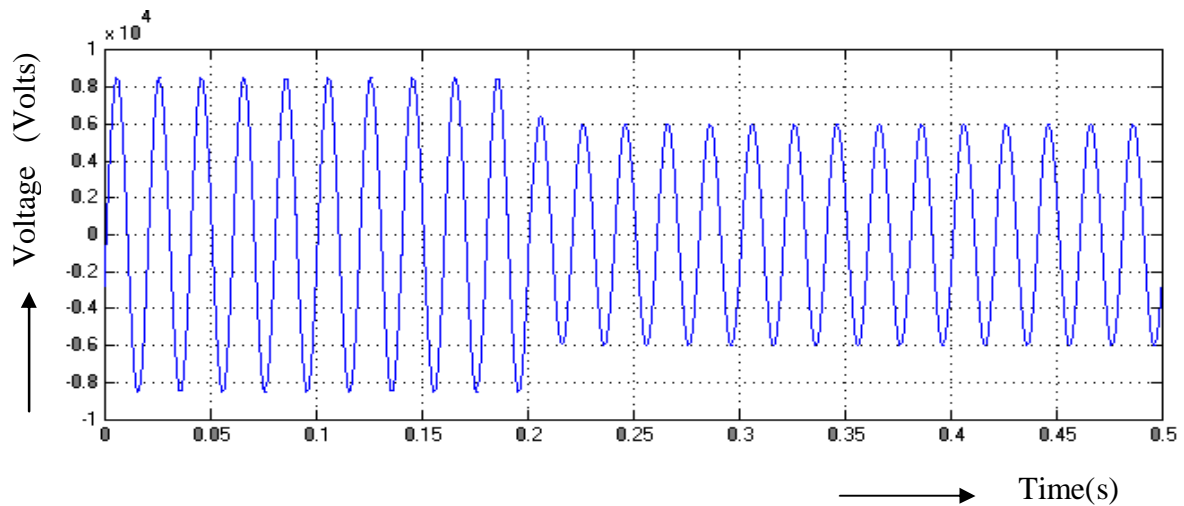


Fig. 5.7.3.5. Voltage at Bus-12

The Figs. 5.7.3.6. and 5.7.3.7, represents the real and reactive power at bus 12. The graph is drawn between time on x-axis and power on y-axis. From the above waveform the real and reactive power starts to increase from origin and maintain a constant value upto  $t=0.2s$  after that starts to decrease, again maintain a constant value. This action takes place since voltage sag created at bus 12.

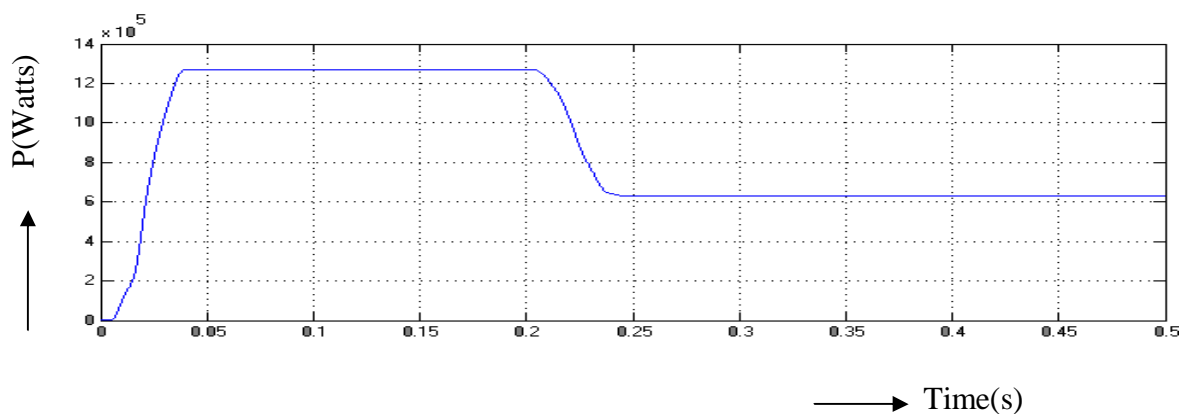


Fig. 5.7.3.6. Real Power at Bus-12

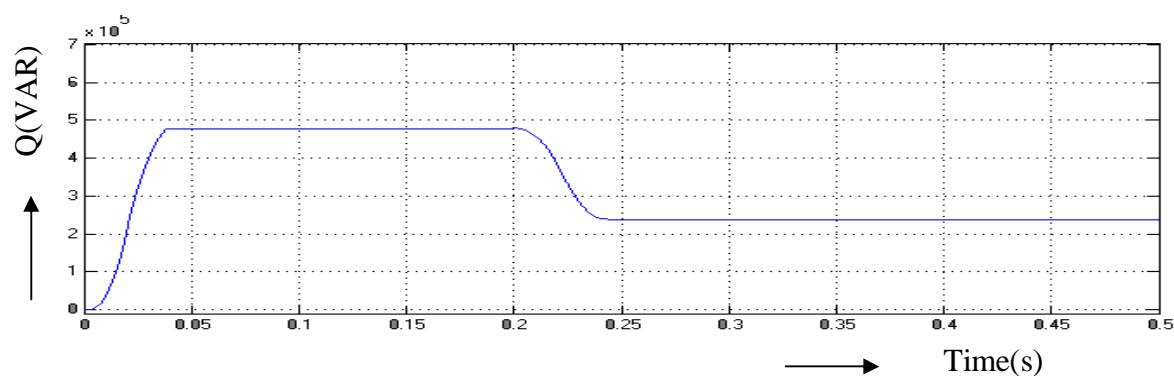


Fig. 5.7.3.7. Reactive Power at Bus-12

The Fig. 5.7.3.8, represents the voltage at bus 26. The graph is drawn between time on x-axis and voltage on y-axis. From the above waveform the voltage at bus 26 maintains a constant value upto  $t=0.2$ s. After that the amplitude of voltage level decreases due to addition of load.

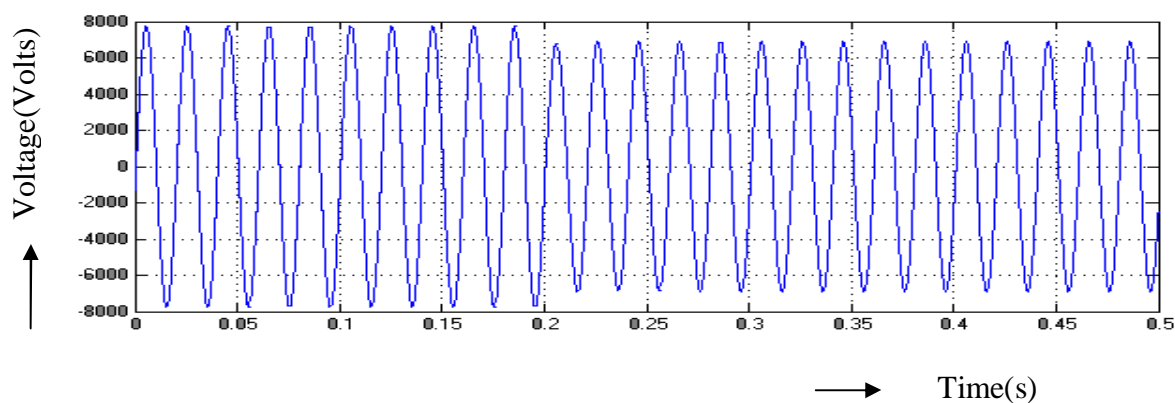


Fig. 5.7.3.8. Voltage at Bus-26



The Figs. 5.7.3.9 and 5.7.3.10, represents the real and reactive power at bus 26. The graph is drawn between time on x-axis and power on y-axis. From the above waveform the real and reactive power starts to increase from origin and maintain a constant value upto  $t=0.2s$  after that starts to decrease, again maintain a constant value. This action takes place since voltage sag is created at bus 26.

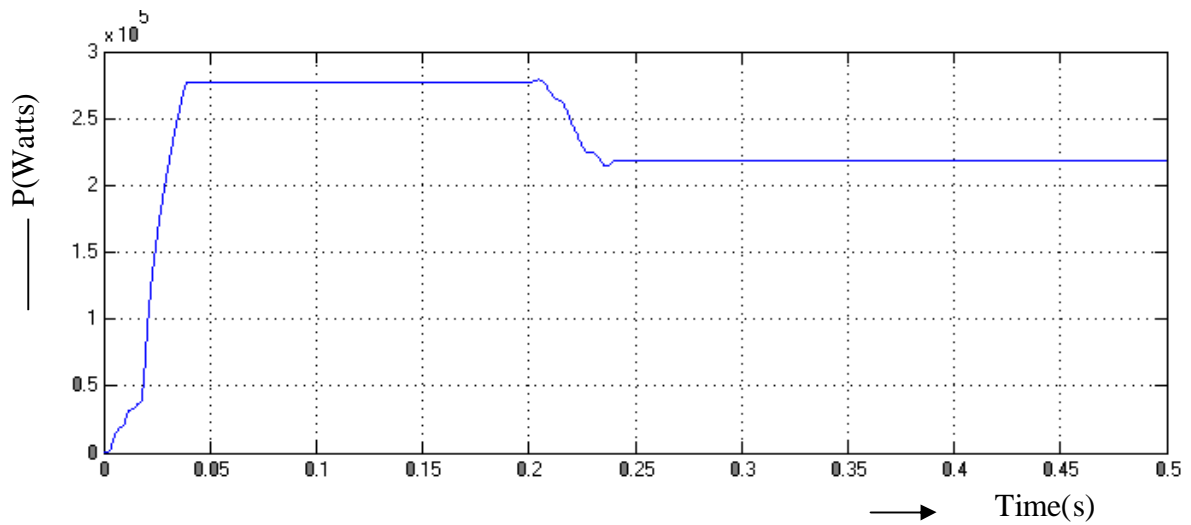


Fig. 5.7.3.9. Real Power at Bus-26

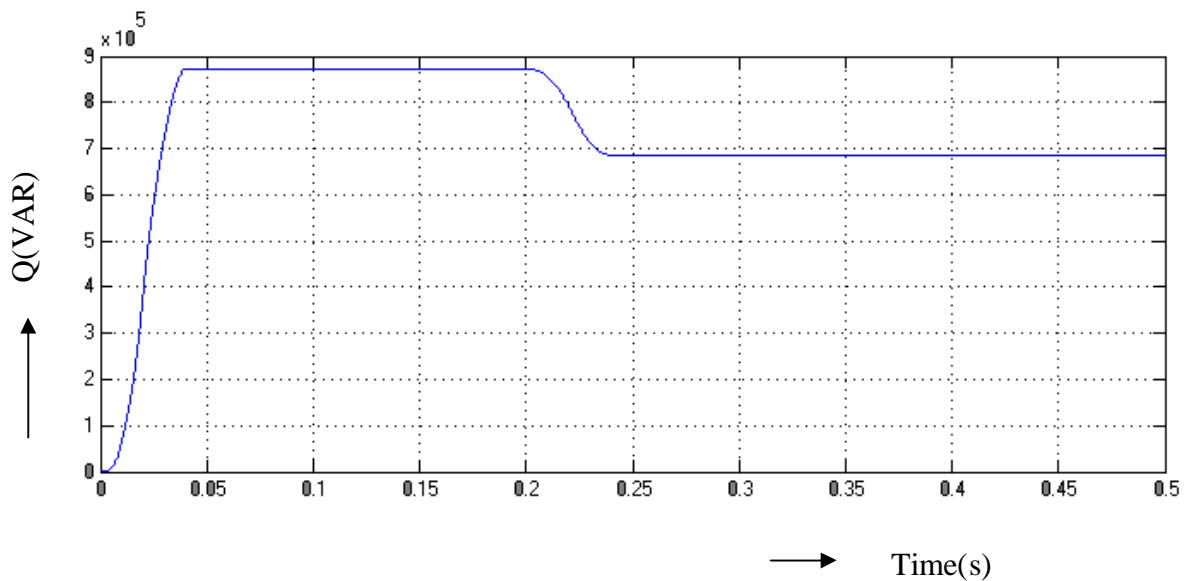


Fig. 5.7.3.10. Reactive Power at Bus-26

Thirty bus system with UPQC is shown in Fig. 5.7.3.11. Two UPQCs are introduced to improve the power quality. They are placed near buses 12 and 27.

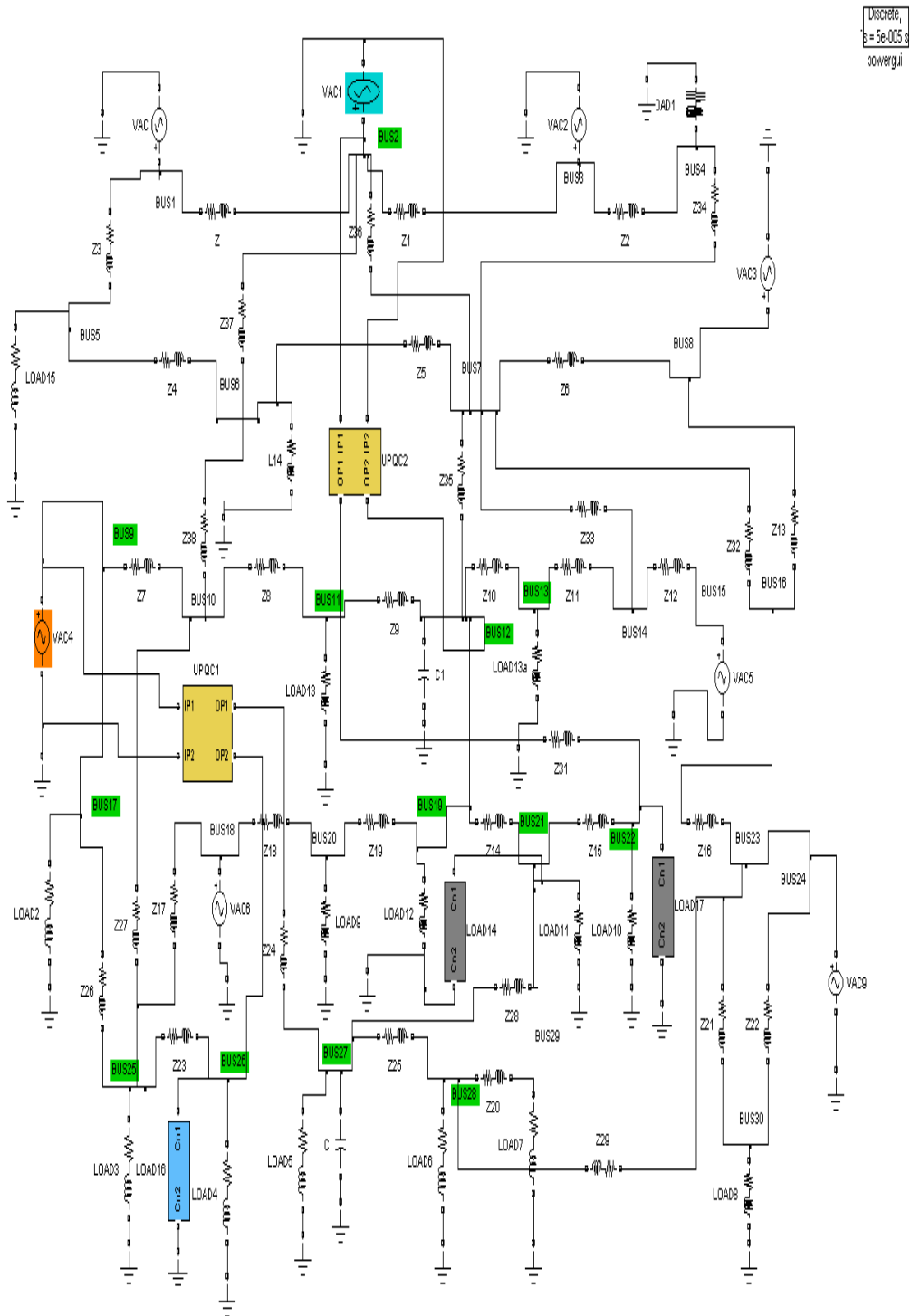


Fig. 5.7.3.11. 30 Bus Systems with multiple UPQCs

The circuit of UPQC is shown in Fig. 5.7.3.12.

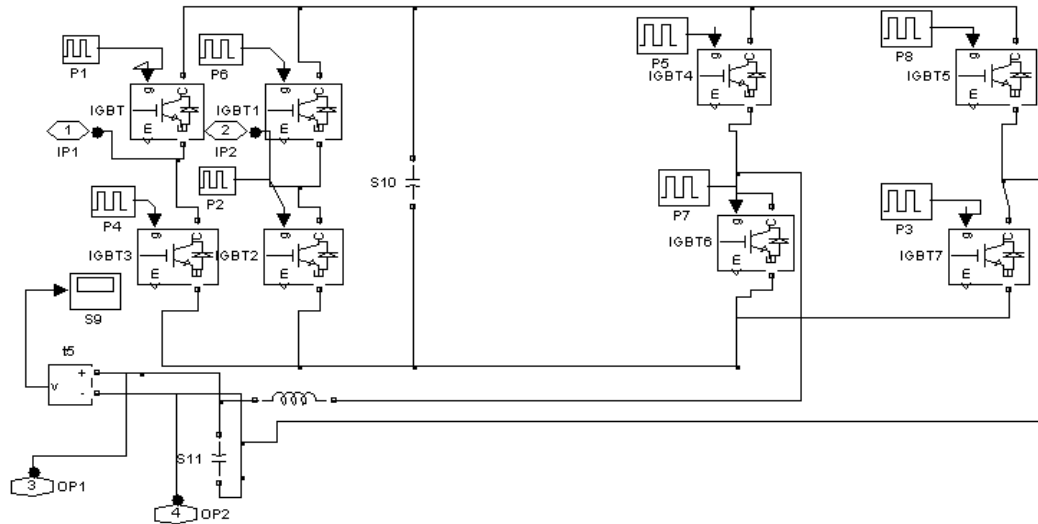


Fig. 5.7.3.12. Circuit of UPQC

The fig 5.7.3.13, represents the voltage at bus 4. The graph is drawn between time on x-axis and voltage on y-axis. From the above waveform it shows that, upto  $t=0.2s$ , the amplitude of voltage maintains as a constant and after that from  $t=0.2s$  to  $t=0.25s$  the amplitude of the voltage decreases. After  $t=0.25s$ , the voltage recovers to the normal value due to the injection of voltage.

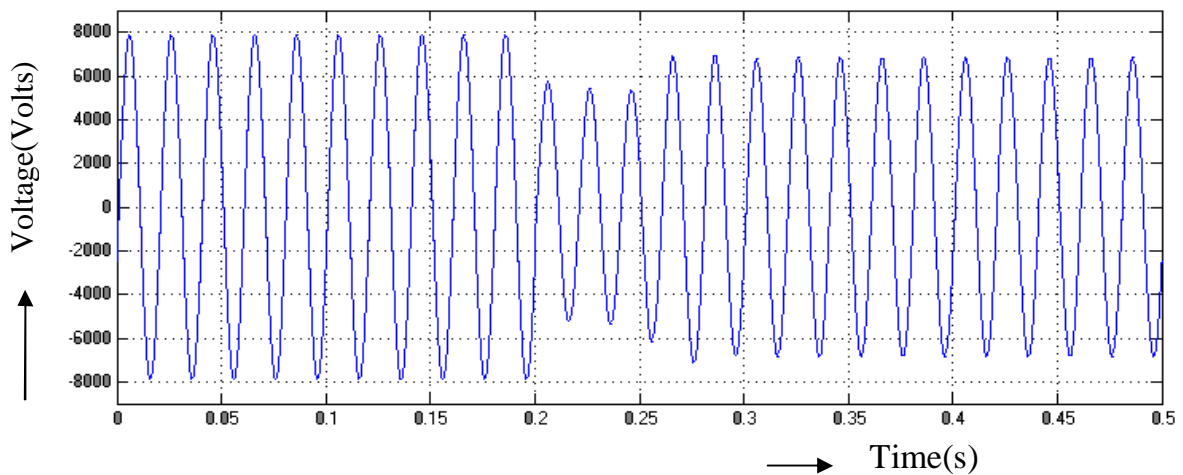


Fig. 5.7.3.13. Voltage at Bus-4

The Fig. 5.7.3.14 and 5.7.3.15, represents the real and reactive power at bus 4. The graph is drawn between time on x-axis and power on y-axis. From the above waveform it shows that, the real and reactive power starts to increase from origin and maintains a constant value upto  $t=0.2s$ . After that the real and reactive power starts to decrease and again increases. The real and reactive power decreases due to the addition of load at the bus 4. It is observed that the real and reactive powers increase due to the addition of UPQC.

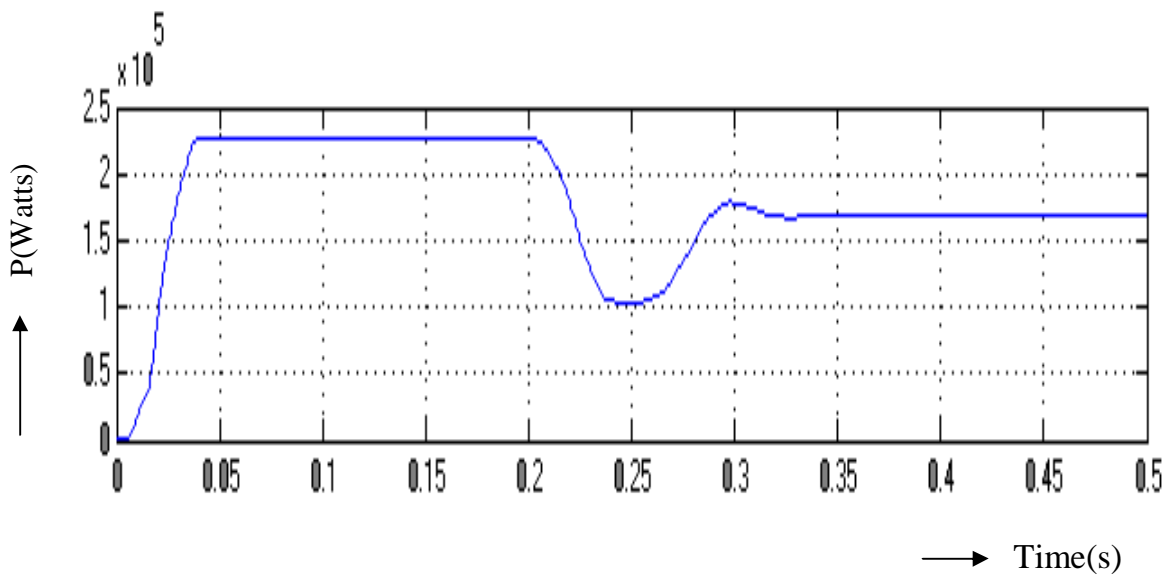


Fig. 5.7.3.14. Real Power at Bus-4

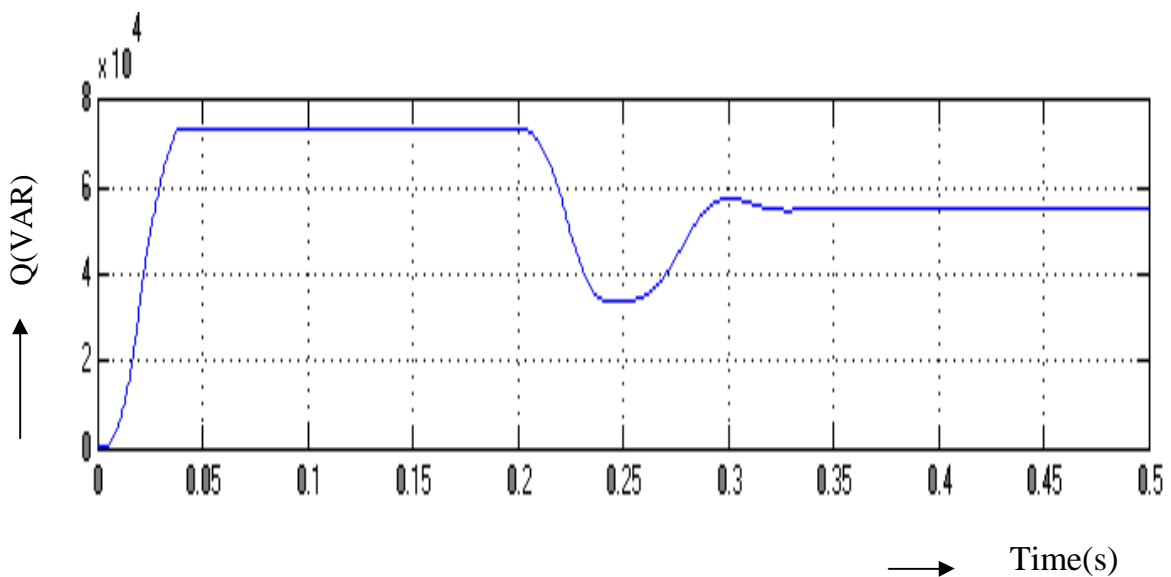


Fig. 5.7.3.15. Reactive Power at Bus-4

### **5.10. Results comparison with desirables and analysis**

Real and Reactive power at all the thirty Buses are shown. The reactive power is proportional to square of the voltage. Hence reactive power increases with the increase in the injected voltage. The voltage profile is also improved by adding UPQC in multiple system.

### **5.11. Fifty Bus System with UPQC**

Standard IEEE-50 bus system is considered for power flow Analysis. The fifty bus system with and without UPQC is studied and the results of simulation are presented in this chapter. The effect of multiple UPQC in fifty bus system is also studied.

In a transmission system, the independent control of real power and reactive power is essential to maintain the desired voltage level in a transmission system. In this chapter Fifty bus system is considered and it is modeled by using the blocks of simulink. The UPQC is connected in this system to achieve the independent control of real and reactive power. The real power is independently controlled by varying the angle of voltage injection of the UPQC. The reactive power is controlled by varying the magnitude of shunt voltage injected by the UPQC.

Harmonic distortion originates in the nonlinear characteristics of devices and loads on the power system. The harmonic distortion is measured in single quantity as Total Harmonic Distortion (THD). Voltages and currents having frequency components that are not integer multiples of the frequency at which the supply system is designed to operate are called interharmonics. It can be found in networks of all voltage levels. The main sources of interharmonics waveform distortion are power electronic circuits such as static frequency converters, cycloconverters, induction furnaces and arcing devices. Power line

carrier signals are also coming in this category. These harmonics result in failure or misoperation of consumer equipment.

The output of inverter contains odd harmonics. PWM is considered such that lower order harmonics are eliminated. Higher order harmonics are harmless since their magnitude is negligible. The output does not contain even harmonics since the output has odd symmetry. THD is the ratio of harmonic voltage to the fundamental voltage.

### **5.12. Model of IEEE Fifty Bus System with Multiple UPQC**

Simulink model of 50 bus system is shown here. Fifty Bus System is modeled using the elements of Matlab Simulink and the simulation results are presented in this section.

Scopes are connected to measure receiving end voltage, receiving end current, real power and reactive power. The generator is represented as series combination of R, L, and E. Each Line is represented by a series impedance. The load at the receiving end is series combination of resistance of  $200\Omega$  and inductance of 100mH. The parameters of the additional load are  $50\Omega$  and 50mH. DC required by the UPQC is applied from a photo cell. The output of UPQC is injected using a series transformer.

The inverter of DVR used in the UPQC is triggered at 50Hz. All the switches are operated with pulse of 10ms width. The pulse given to the other two switches are displaced by 10ms. The output of the inverter is filtered by using LC filter. This will reduce heating since harmonics are reduced. The inverter switches of active filter are triggered at 250Hz.

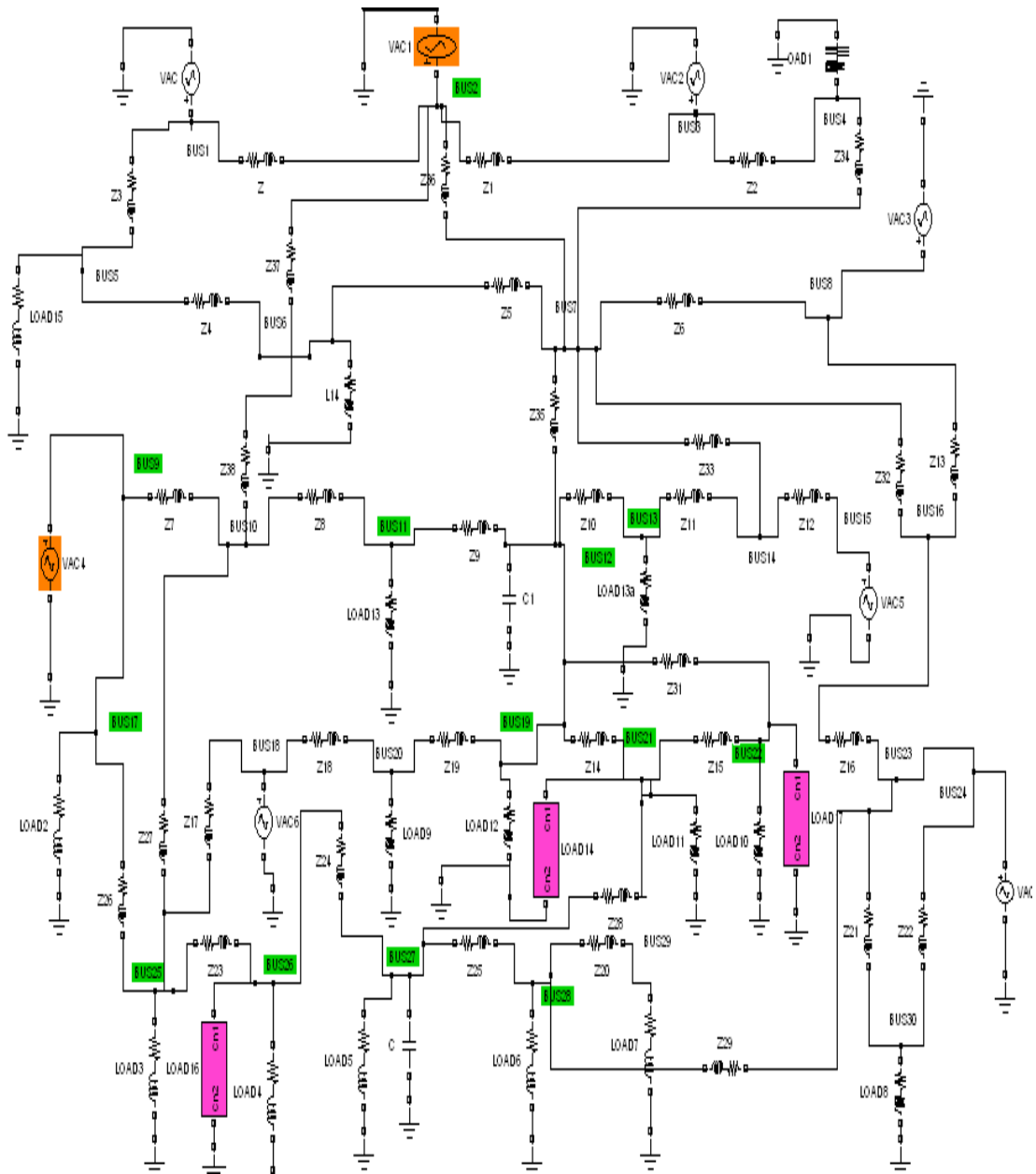


Fig. 5.8.2.1. 50 Bus System Without the UPQC

Fifty bus system is represented using single line diagram to perform simulation steadies. There are 8 generator buses and 42 load buses. The shunt capacitance of the wires is neglected. The 50 bus system without UPQC is shown in Fig. 5.8.2.1. Additional load is connected at buses 4 and 12.

The Fig.5.8.2.2, represents the voltage at bus 4. The graph is drawn between time on x-axis and voltage on y-axis. From  $t=0s$  to  $t=0.2s$  the amplitude of the voltage maintains as a same value. At  $t=0.2s$  the amplitude of the voltage decreases by adding additional load at bus 4.

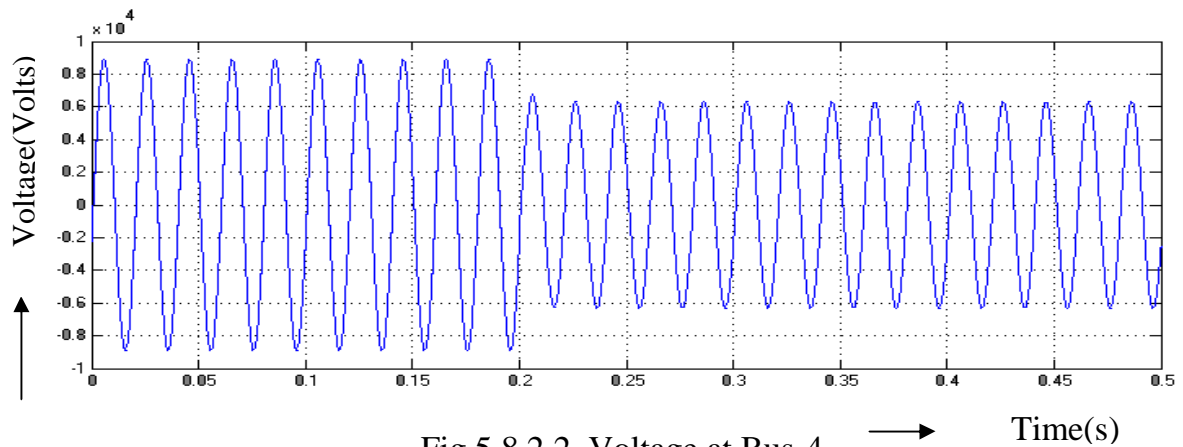


Fig.5.8.2.2. Voltage at Bus-4

The Fig.5.8.2.3 and 5.8.2.4, represents the real and reactive power at bus 4. The graph is drawn between time on x-axis and power on y-axis. From the above waveform it shows that, the real and reactive power starts to increases from origin and maintains a constant value upto  $t=0.2s$ . After that the real and reactive power decreases and setteles. The real and reactive power decreases due to the addition of load at the bus 4.

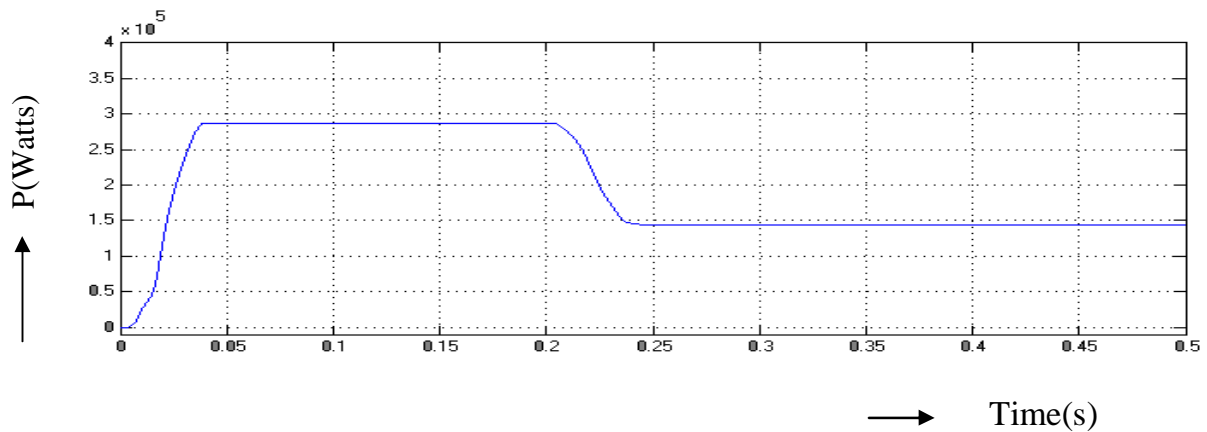


Fig.5.8.2.3. Real Power at Bus-4



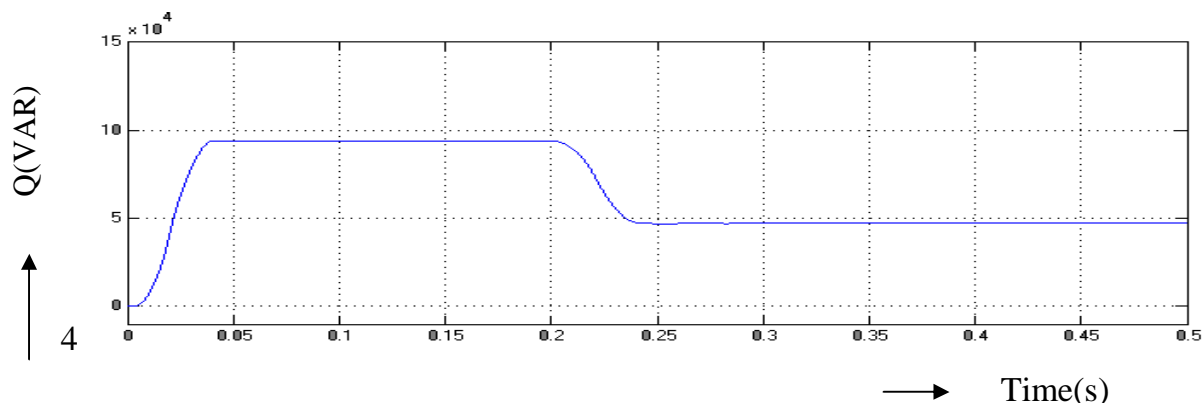


Fig.5.8.2.4. Reactive Power at Bus-4

The fig.5.8.2.5 represents the voltage at bus 12. The graph is drawn between time on x-axis and voltage on y-axis. From  $t=0$ s to  $t=0.2$ s the amplitude of the voltage maintains as a same value. At  $t=0.2$ s the amplitude of the voltage decreases by adding additional load at bus 12.

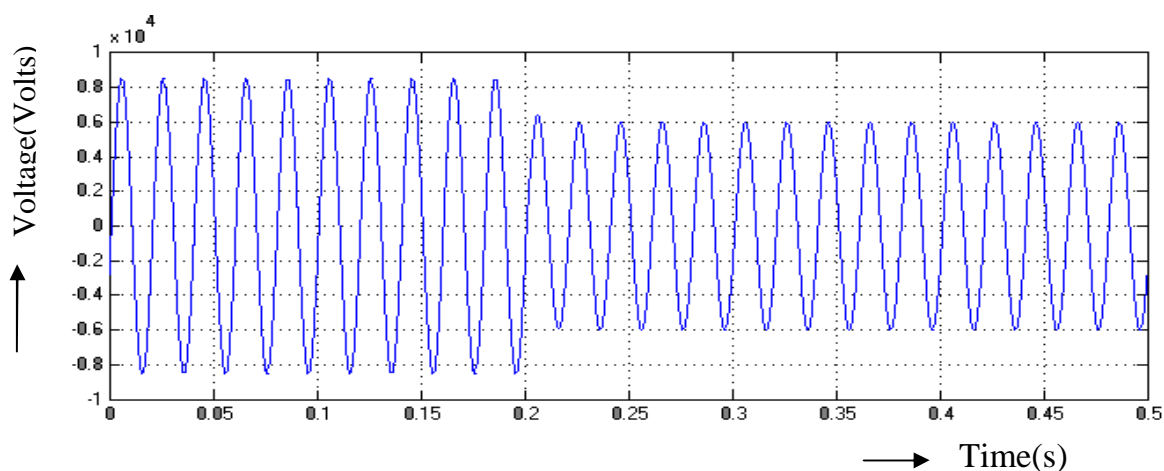


Fig.5.8.2.5. Voltage at Bus-12

The Figs.5.8.2.6 and 5.8.2.7, represents the real and reactive power at bus 12. The graph is drawn between time on x-axis and power on y-axis. From the above waveform it shows that, the real and reactive power starts to increases from origin and maintains a constant value upto  $t=0.2$ s. After that the real and reactive power starts to decreases and again increases. The real and reactive power decreases due to the addition of load at the bus 12.

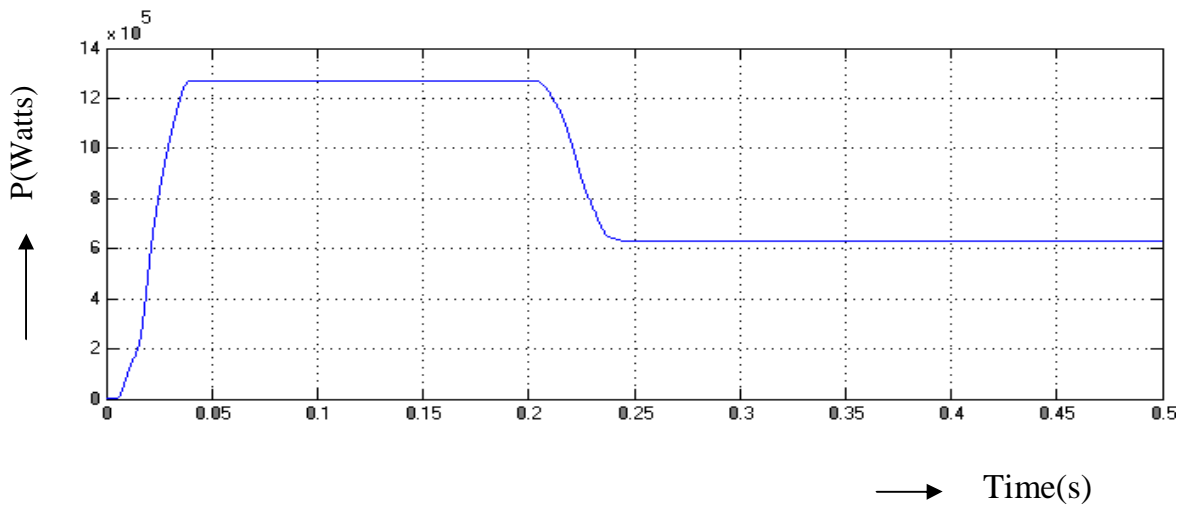


Fig.5.8.2.6. Real Power at Bus-12

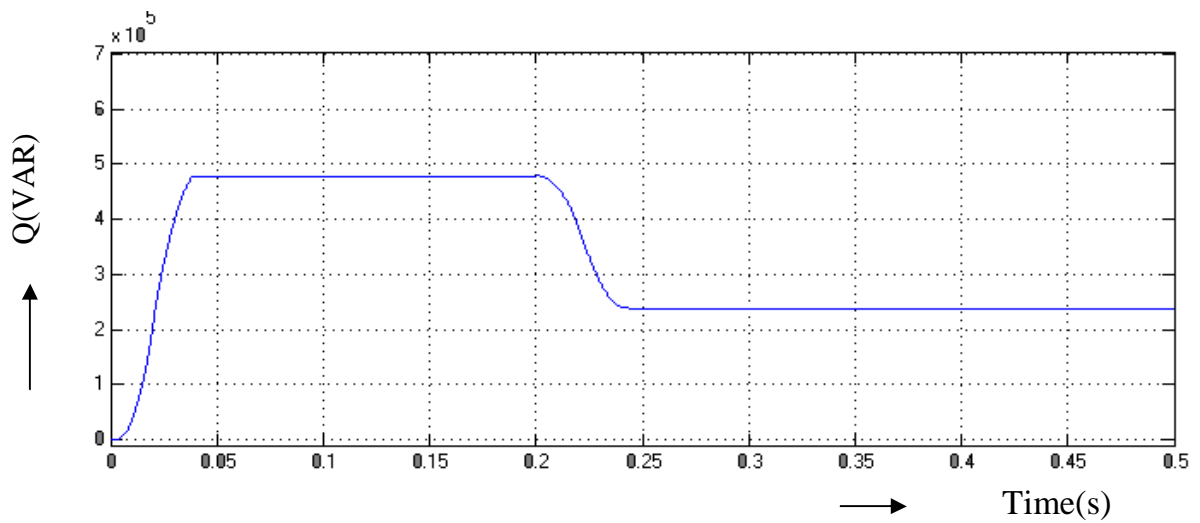


Fig.5.8.2.7. Reactive Power at Bus-12

The Fig.5.8.2.8, represents the voltage at bus 26. The graph is drawn between time on x-axis and voltage on y-axis. From  $t=0s$  to  $t=0.2s$  the amplitude of the voltage maintains as a same value. At  $t=0.2s$  the amplitude of the voltage decreases by adding additional load at bus 26.

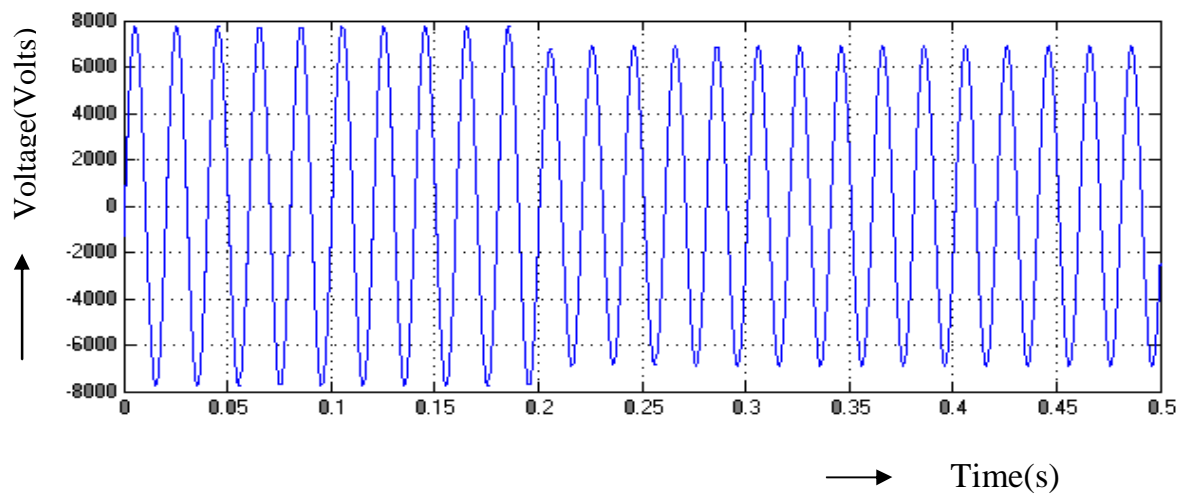


Fig.5.8.2.8. Voltage at Bus-26

The Fig.5.8.2.9 and 5.8.2.10, represents the real and reactive power at bus 26. The graph is drawn between time on x-axis and power on y-axis. From the above waveform it shows that, the real and reactive power starts to increase from origin and maintains a constant value upto  $t=0.2$ s. After that the real and reactive power decreases and settles. The real and reactive power decreases due to the addition of load at the bus 26.

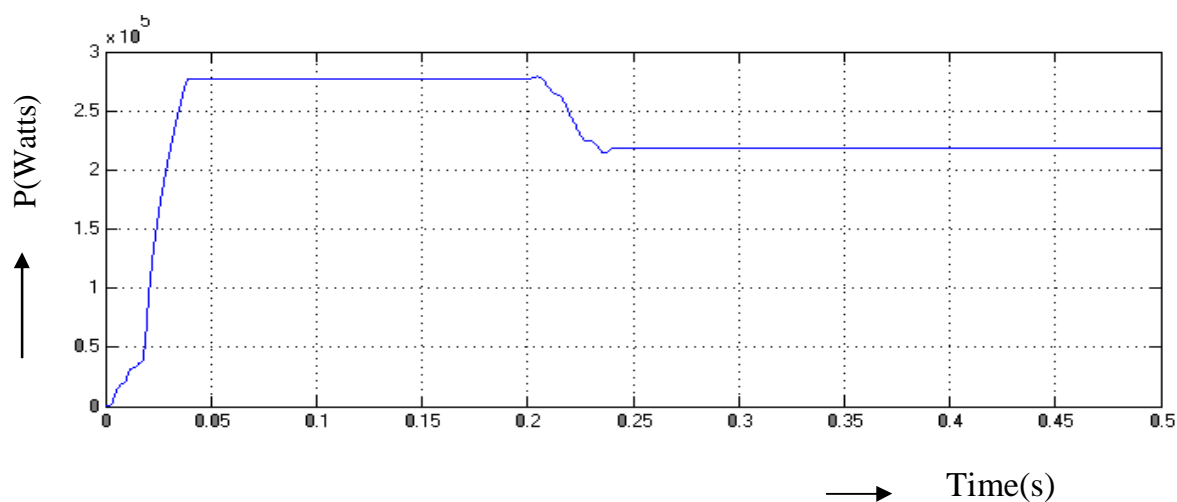


Fig.5.8.2.9. Real Power at Bus-26

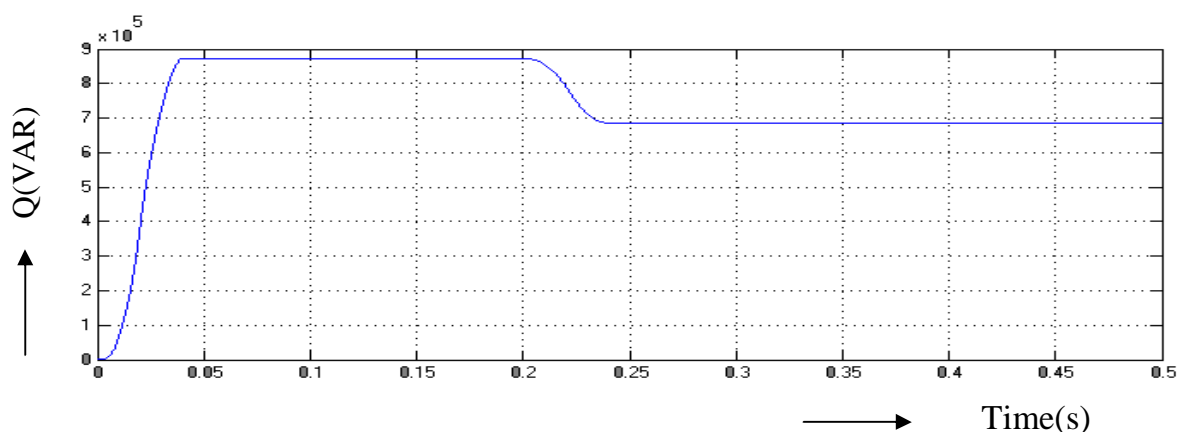


Fig.5.8.2.10. Reactive Power at Bus-26

The frequency spectrum for current is shown in Fig.5.8.2.11. The frequency spectrum is drawn with frequency on x-axis and magnitude of voltage on y-axis. The magnitude of higher order harmonics are negligible. The height decreases with the increase in the order of harmonics. This is due to the increased impedance at high frequency. The THD is 14.2%.

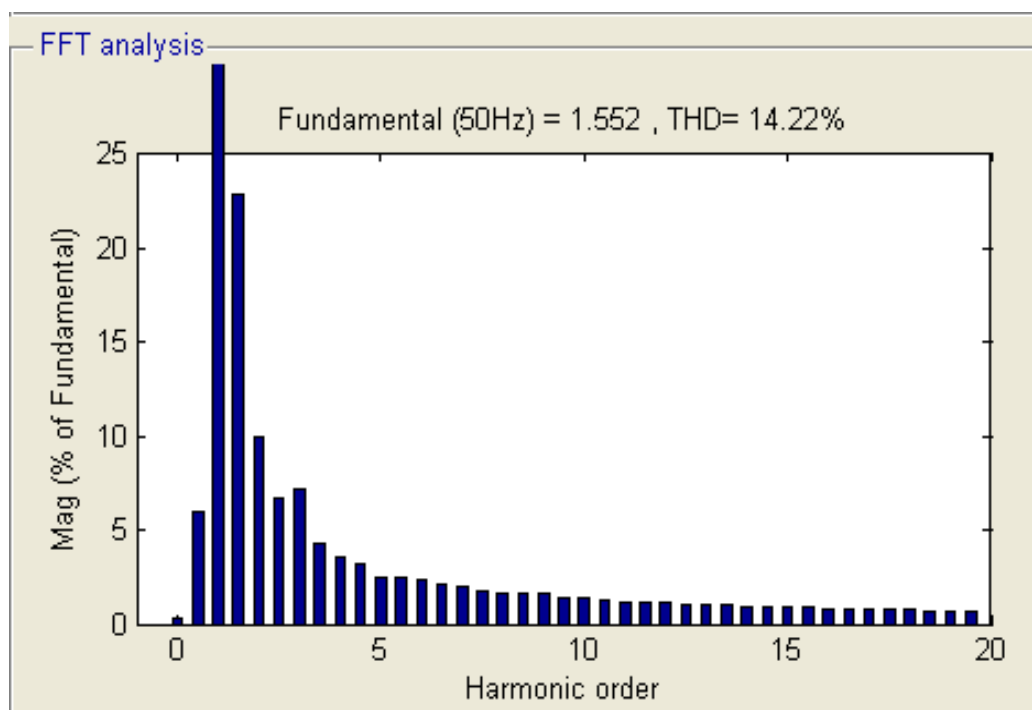


Fig. 5.8.2.11. THD

Fifty bus system with UPQC is shown in Fig.5.8.2.12. The UPQCs are introduced near buses 4 and 12.

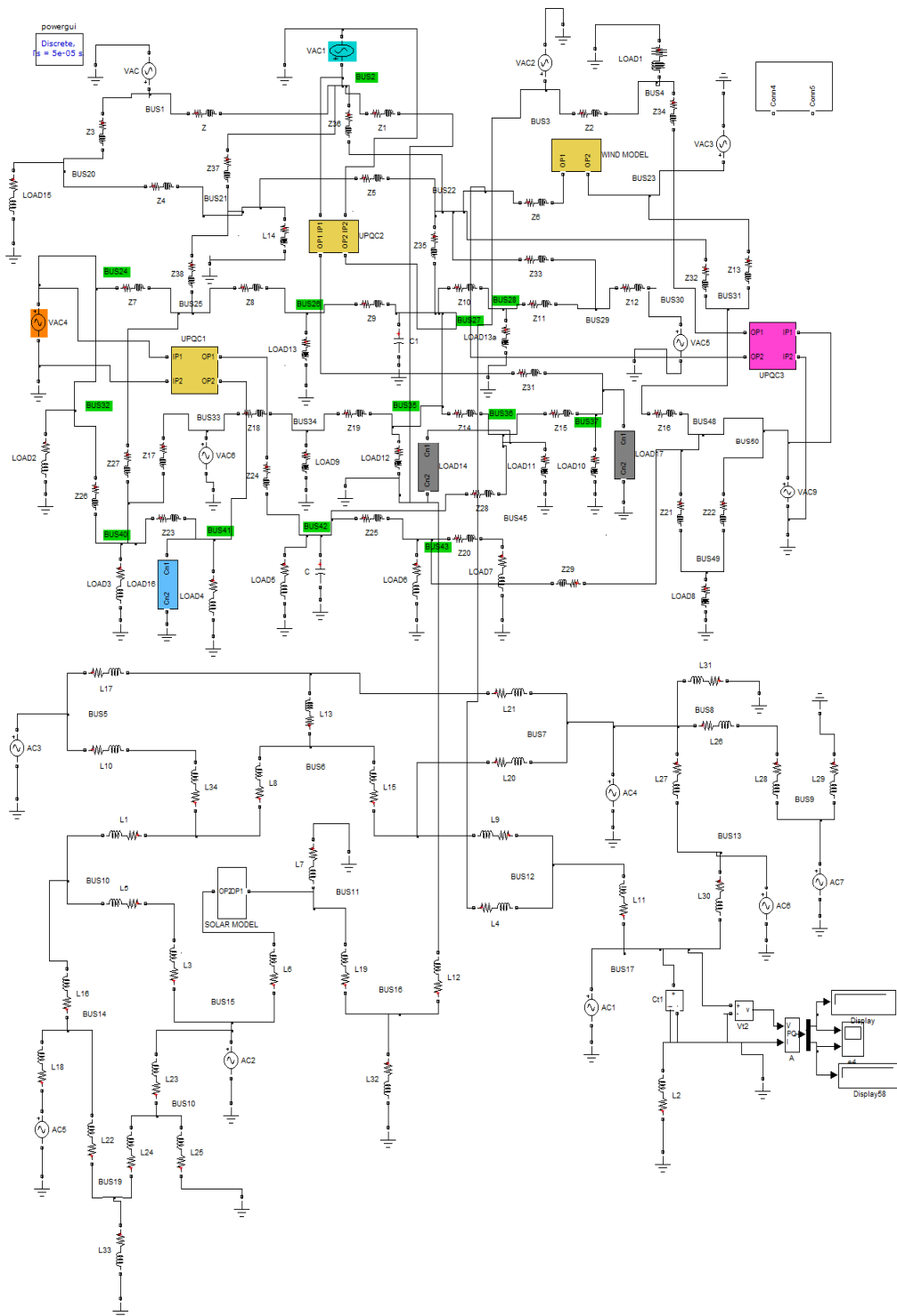


Fig.5.8.2.12. 50 Bus Systems with UPQC

The circuit of UPQC is shown in Fig.5.8.2.13. The bus voltage, real power and reactive power at buses 4,12,18,26,45 and 48 are shown in Fig.5.8.2.14 to 5.8.2.31. The spectrum for the current with UPQC is shown in Fig.5.8.2.32. The THD reduces to 3.2%. From the summary of real and reactive powers at various Buses with and without UPQC it can be seen that there is an increase in real and reactive power due to the addition of UPQC. The increase in real and reactive power is due to the increase in the voltage.

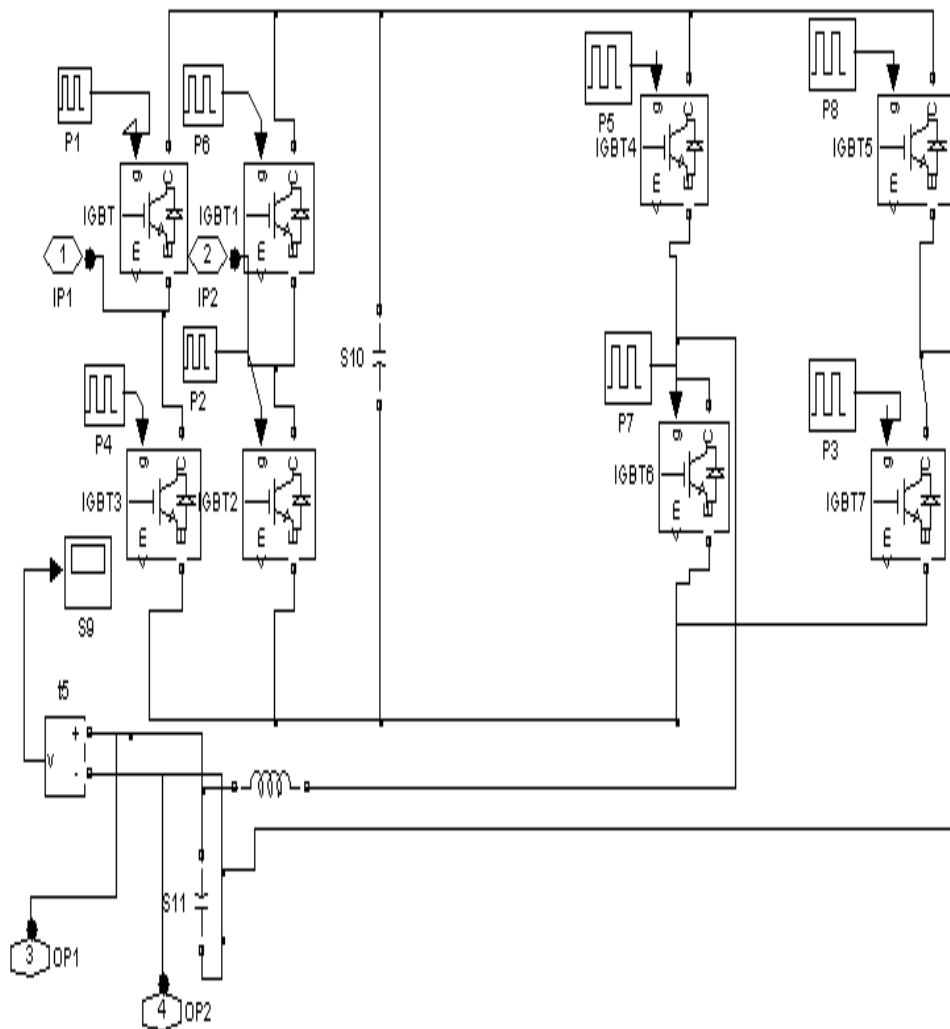


Fig.5.8.2.13. Circuit of UPQC

The Fig.5.8.2.14, represents the voltage at bus 4. The graph is drawn between time on x-axis and voltage on y-axis. From  $t=0\text{s}$  to  $t=0.2\text{s}$  the amplitude of the voltage maintains as a same value. At  $t=0.2\text{s}$  the amplitude of the voltage decreases by adding additional load at bus 4. From  $t=0.25\text{s}$ , the voltage recovers to the normal value due to the injection of voltage.

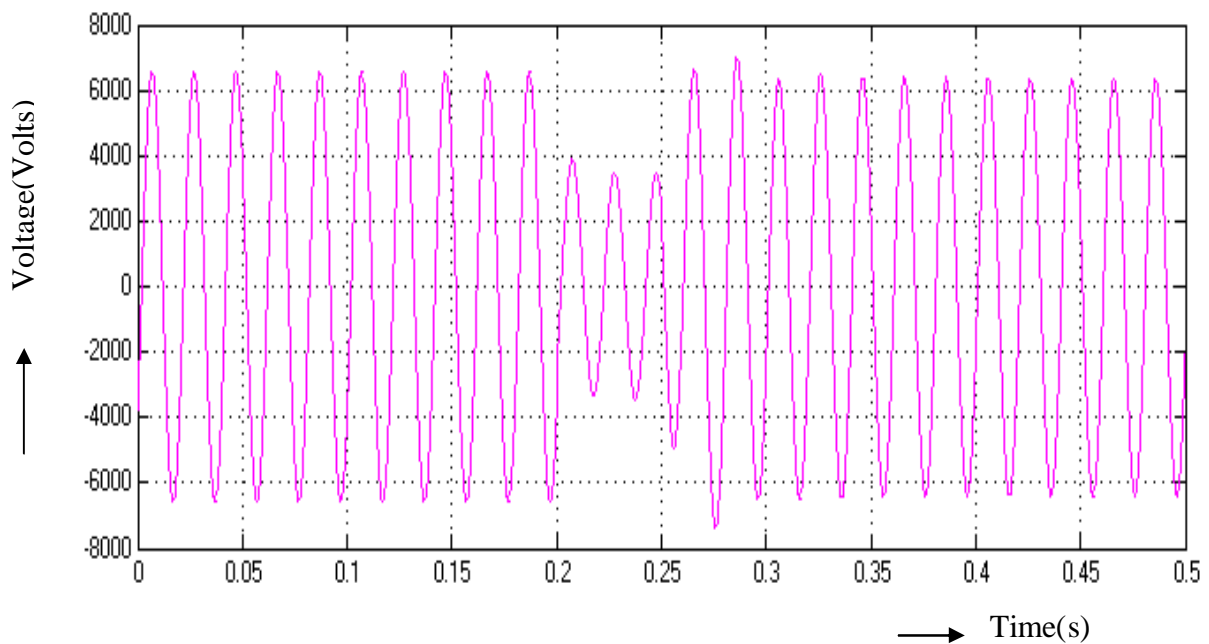


Fig.5.8.2.14 Voltage at Bus-4

The Fig.5.8.2.15 and 5.8.2.16, represents the real and reactive power at bus 4. The graph is drawn between time on x-axis and power on y-axis. From the above waveform it shows that, the real and reactive power starts to increase from origin and maintains a constant value upto  $t=0.2\text{s}$ . After that the real and reactive power starts to decrease and again increases. The real and reactive power decreases due to the addition of load at the bus 4, and again it starts to increase due to the addition of UPQC.

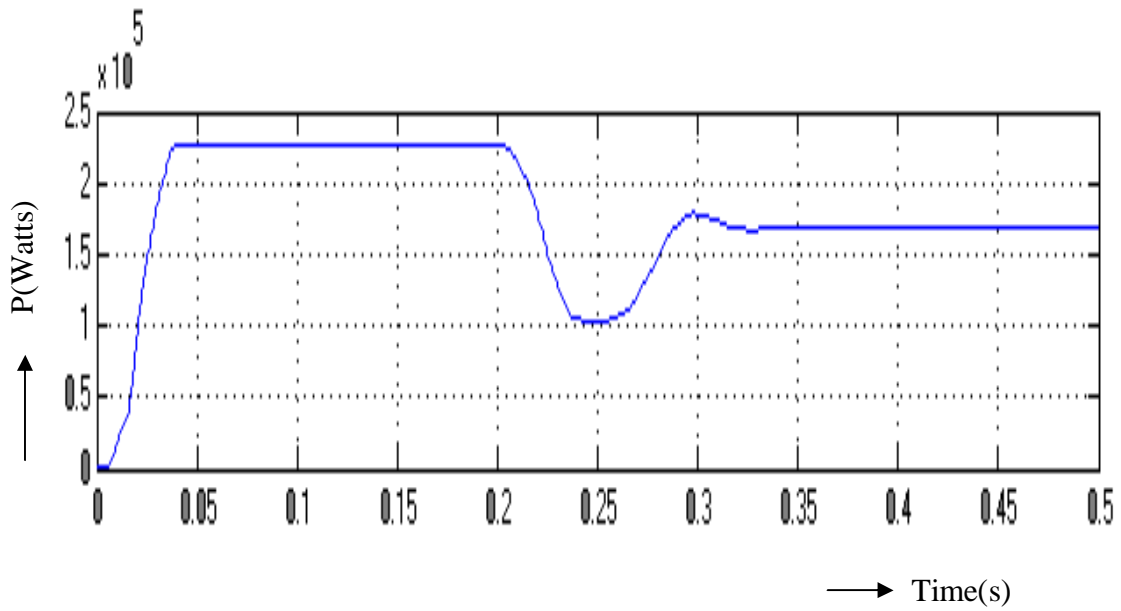


Fig.5.8.2.15. Real Power at Bus-4

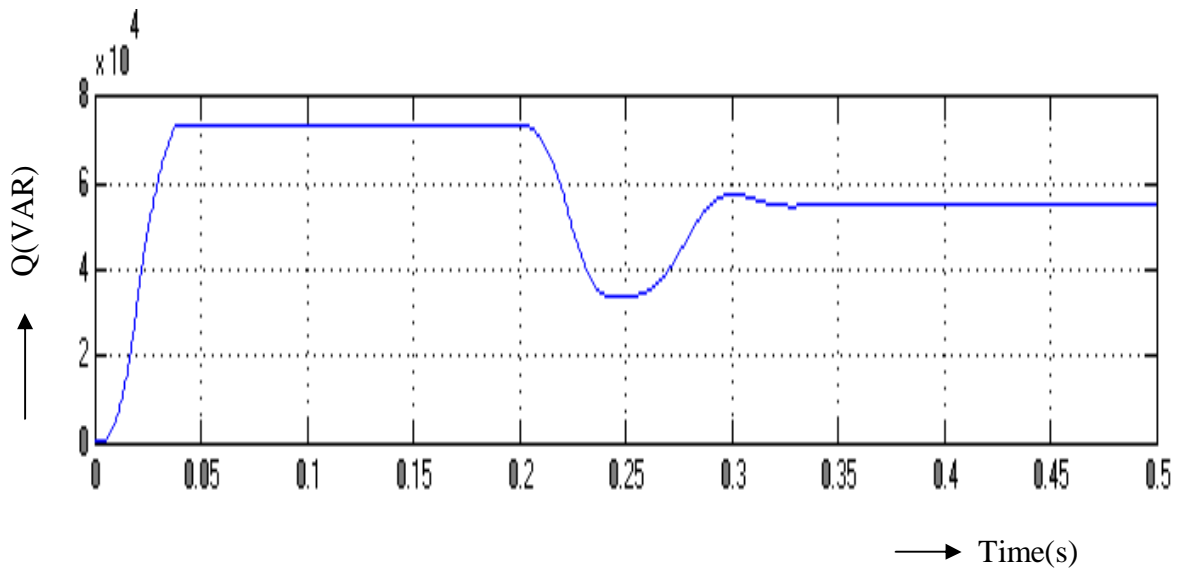


Fig.5.8.2.16. Reactive Power at Bus-4

The Fig.5.8.2.17, represents the voltage at bus 12. The graph is drawn between time on x-axis and voltage on y-axis. From  $t=0s$  to  $t=0.2s$  the amplitude of the voltage maintains as a same value. At  $t=0.2s$  the amplitude of the voltage decreases by adding additional load at bus 12. From  $t=0.25s$ , the voltage recovers to the normal value due to the injection of voltage.



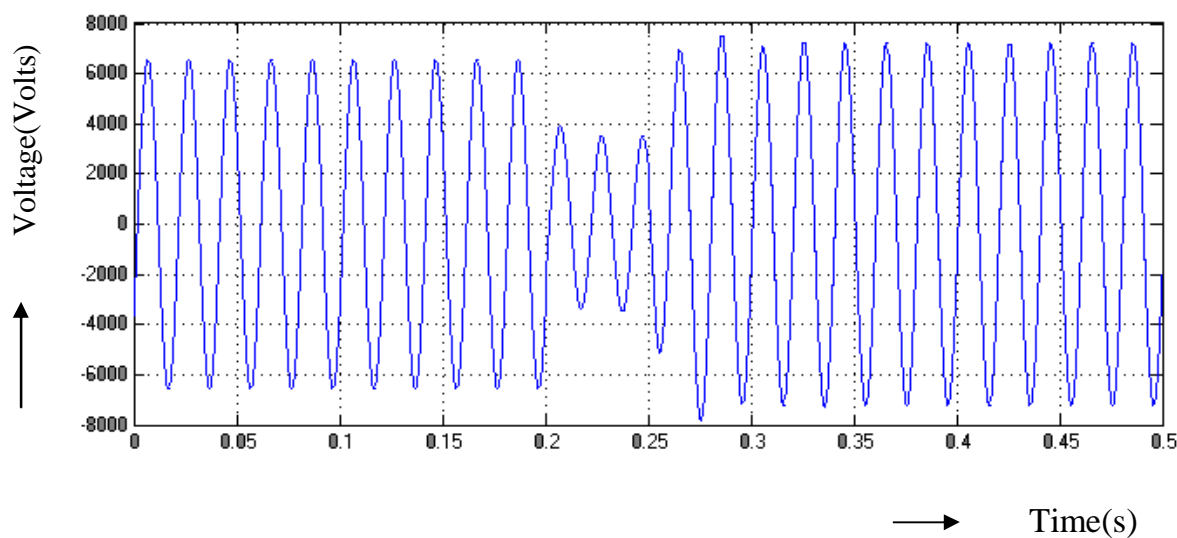


Fig.5.8.2.17. Voltage at Bus-12

The Figs.5.8.2.18 and 5.8.2.19, represents the real and reactive power at bus 12. The graph is drawn between time on x-axis and power on y-axis. From the above waveform it shows that, the real and reactive power starts to increase from origin and maintains a constant value upto  $t=0.2s$ . After that the real and reactive power starts to decrease and again increases. The real and reactive power decreases due to the addition of load at the bus 12. And again it starts to increase due to the addition of UPQC.

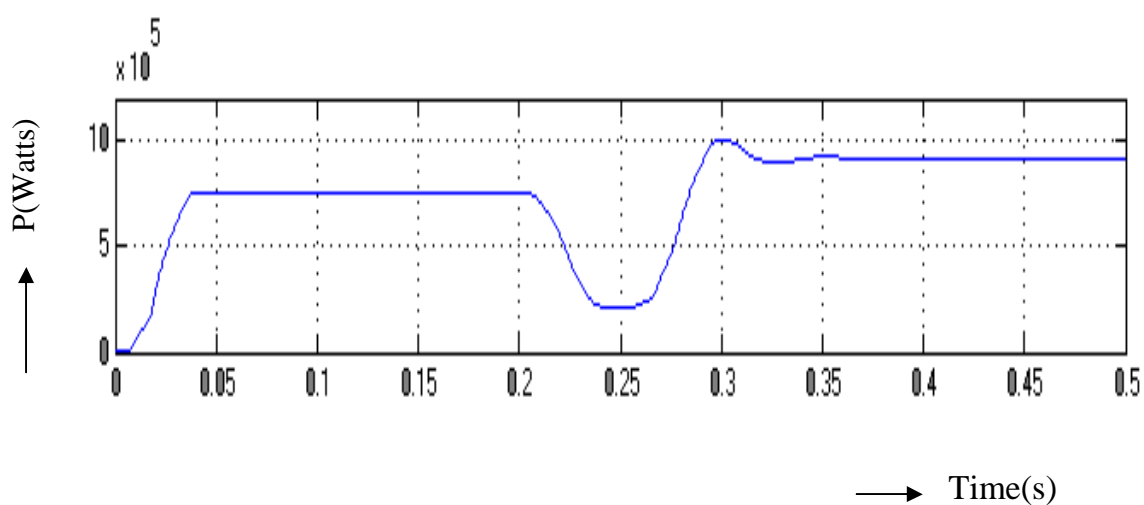


Fig. 5.8.2.18. Real Power at Bus-12

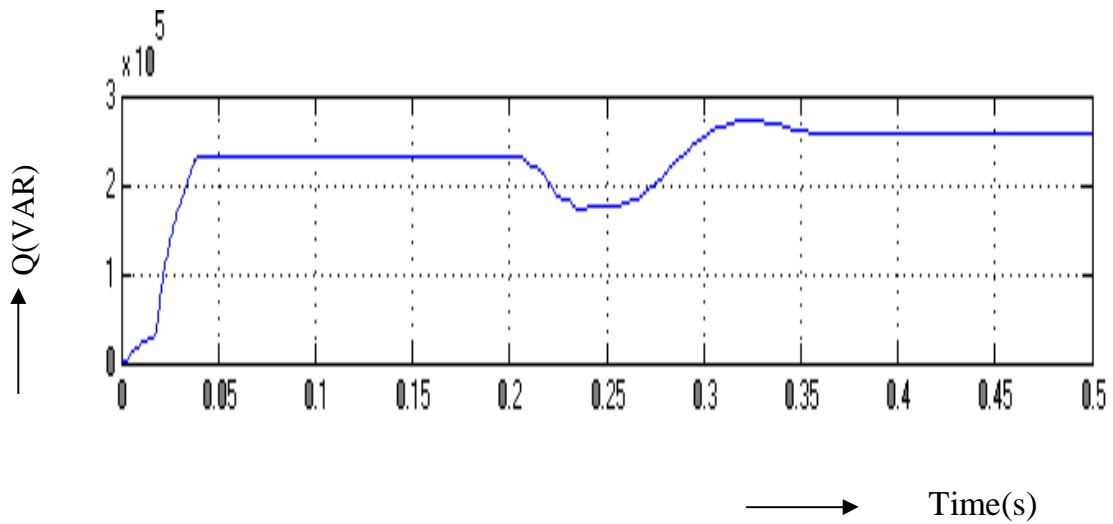


Fig.5.8.2.19. Reactive Power at Bus-12

The Fig.5.8.2.20, represents the voltage at bus 18. The graph is drawn between time on x-axis and voltage on y-axis. After  $t=0.25s$ , the amplitude of the voltage starts increases due to action of UPQC.

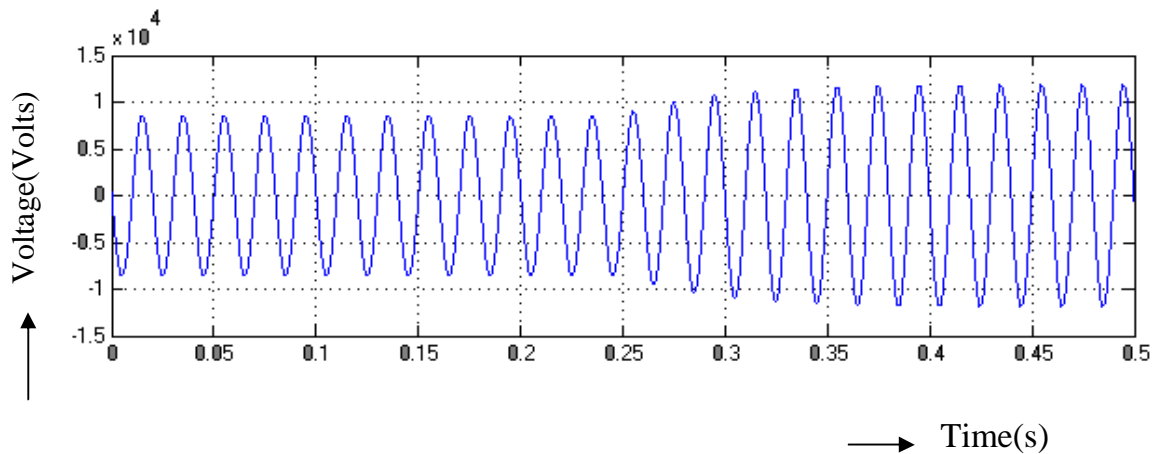


Fig.5.8.2.20. Voltage at Bus-18

The Figs.5.8.2.21 and 5.8.2.22, represents the real and reactive power at bus 18. The graph is drawn between time on x-axis and power on y-axis. From the above waveform it shows that, the real and reactive power starts to increases from origin and maintains a constant value upto  $t=0.25s$ . After that the real and reactive power starts to increases due to the addition of UPQC.

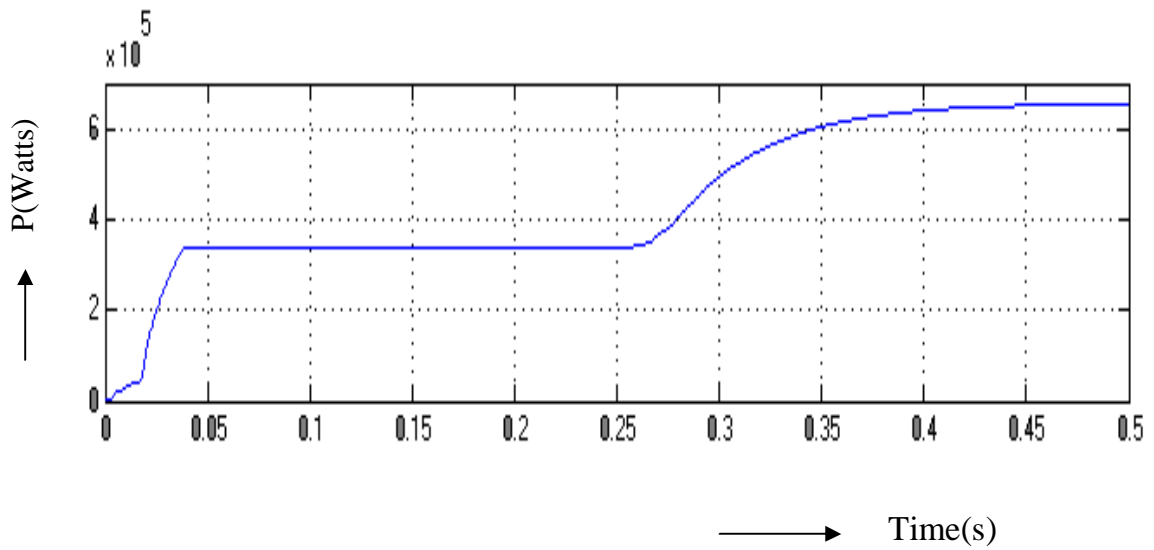


Fig.5.8.2.21. Real Power at Bus-18

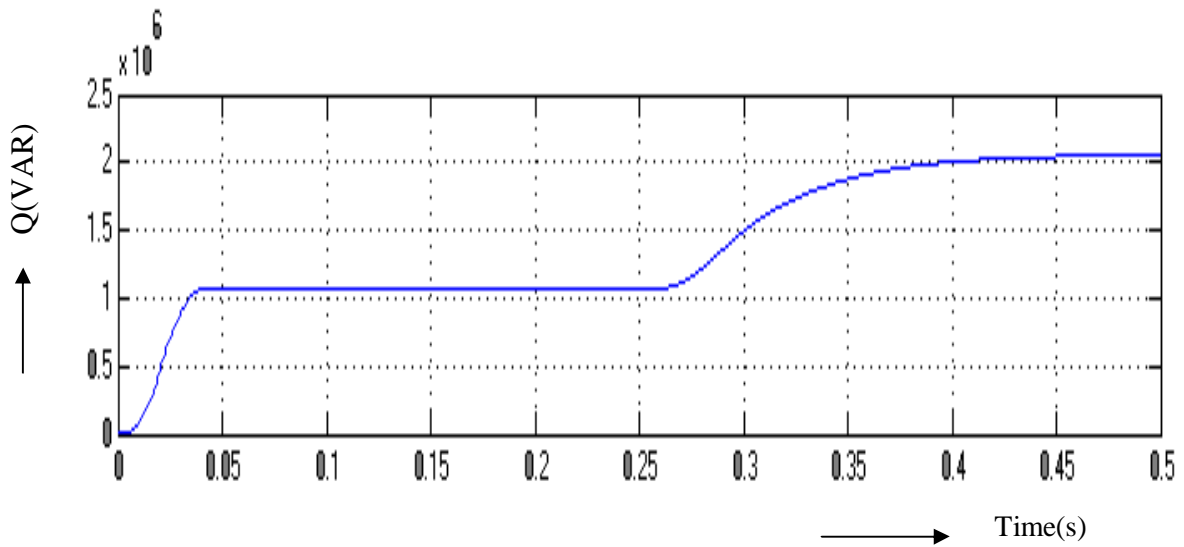


Fig.5.8.2.22. Reactive Power at Bus-18

The Fig.5.8.3.23, represents the voltage at bus 26. The graph is drawn between time on x-axis and voltage on y-axis. From the above waveform it shows that, upto  $t=0.2s$ , the amplitude of voltage maintains as a constant and after that from  $t=0.2s$  to  $t=0.25s$  the amplitude of the voltage decreases. After  $t=0.25s$ , the voltage recovers to the normal value due to the injection of voltage.

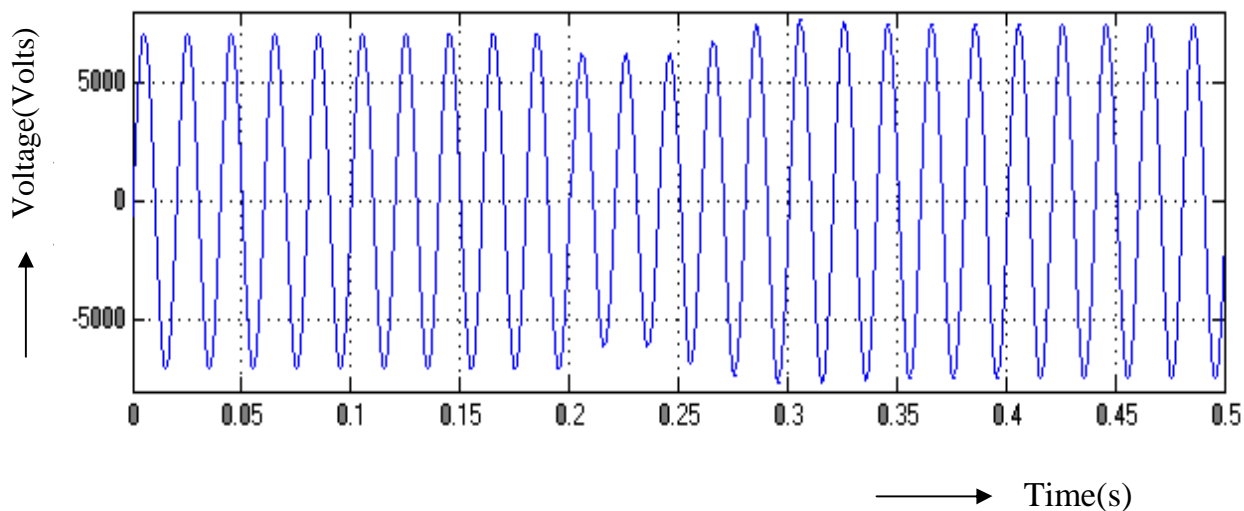


Fig.5.8.2.23. Voltage at Bus-26

The Fig.5.8.2.24 and 5.8.2.25, represents the real and reactive power at bus 26. The graph is drawn between time on x-axis and power on y-axis. From the above waveform it shows that, the real and reactive power starts to increase from origin and maintains a constant value upto  $t=0.2s$ . After that the real and reactive power starts to decrease and again increases. The real and reactive power decreases due to the addition of load at the bus 26. And again it starts to increase due to the addition of UPQC.

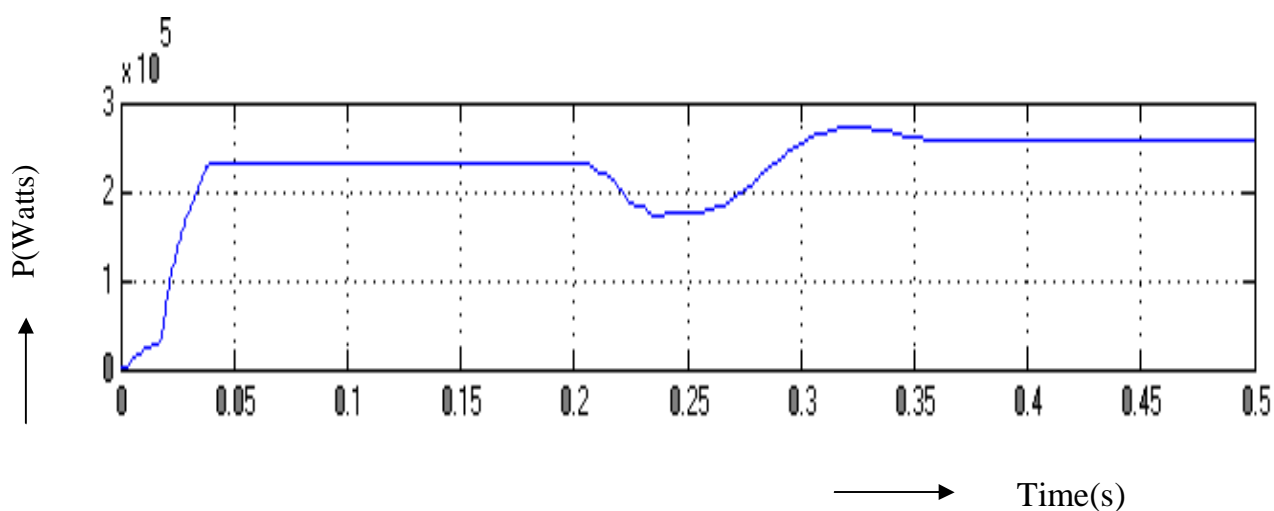


Fig.5.8.2.24. Real Power at Bus-26

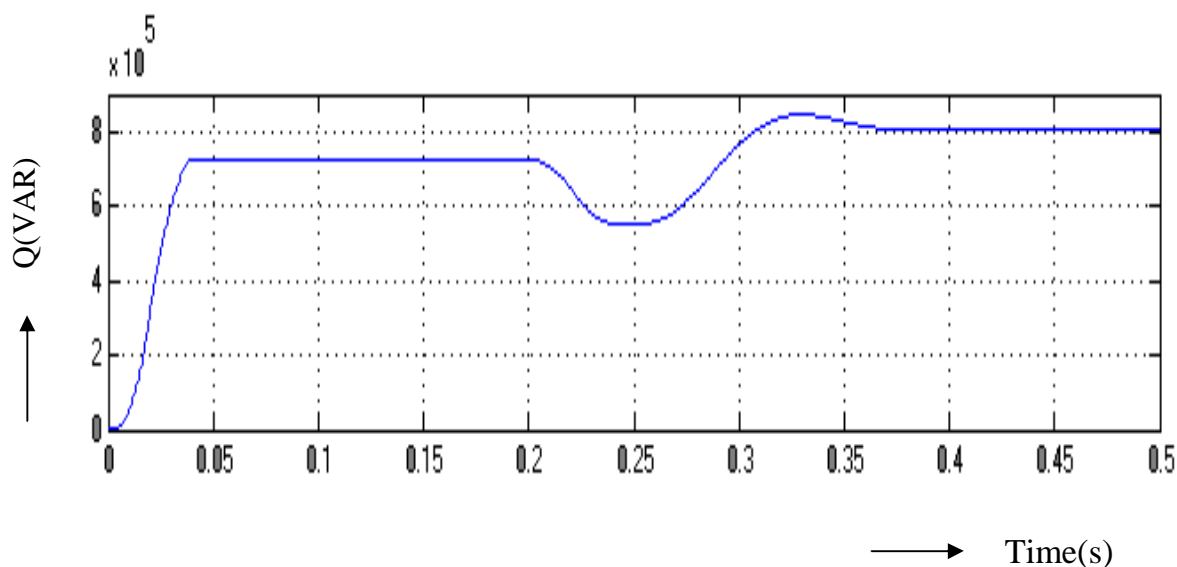


Fig.5.8.2.25. Reactive Power at Bus-26

The Fig.5.8.2.26, represents the voltage at bus 45. The graph is drawn between time on x-axis and voltage on y-axis. After  $t=0.25s$ , the amplitude of the voltage starts increases due to action of UPQC.

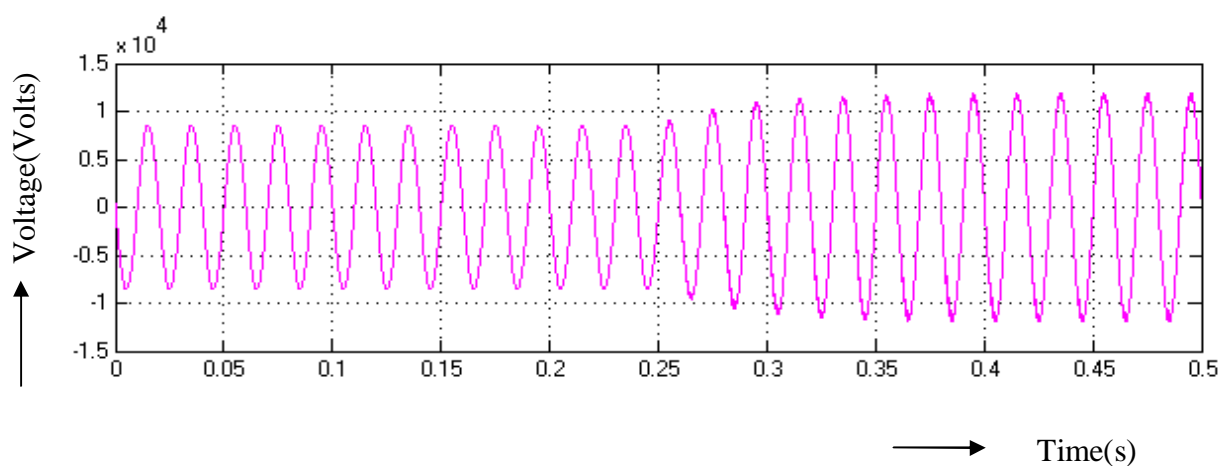


Fig.5.8.2.26. Voltage at Bus-45

The Figs.5.8.2.27 and 5.8.2.28, represents the real and reactive power at bus 45. The graph drawn between time on x-axis and power on y-axis. From the above waveform it shows that, the real and reactive power starts to increases from origin and maintains a constant value upto  $t=0.25s$ . After that the real and reactive power starts to increases due to the addition of UPQC.

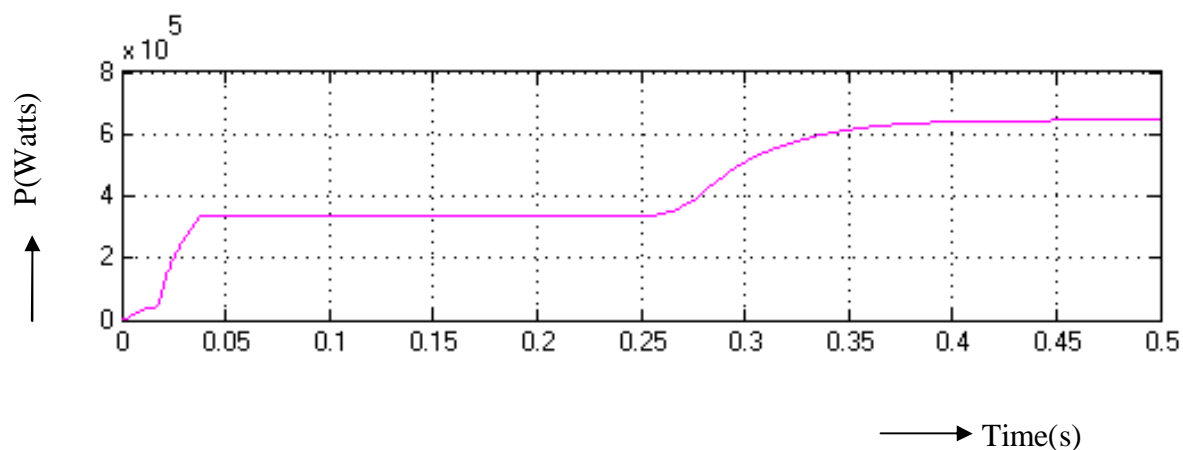


Fig.5.8.2.27. Real Power at Bus-45

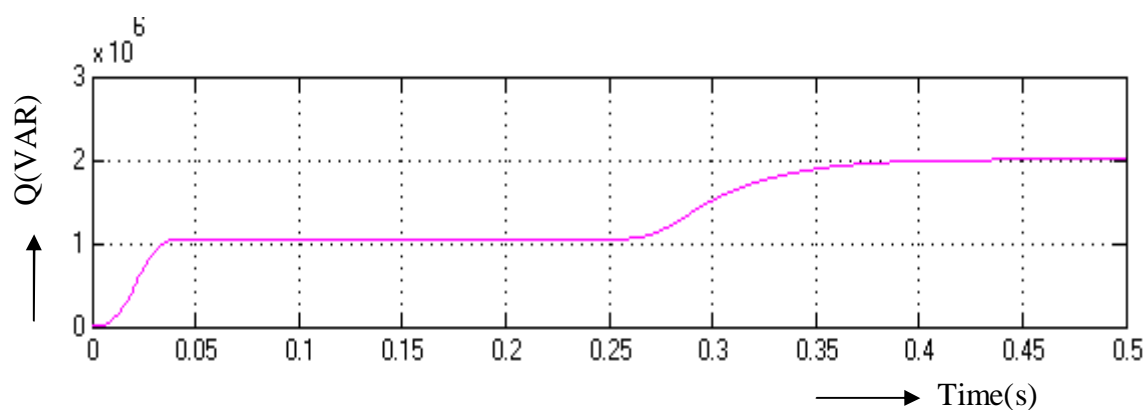


Fig.5.8.2.28. Reactive Power at Bus-45

The Fig.5.8.2.29, represents the voltage at bus 48. The graph is drawn between time on x-axis and voltage on y-axis. After  $t=0.25$ s, the amplitude of the voltage maintains a constant value due to action of UPQC.

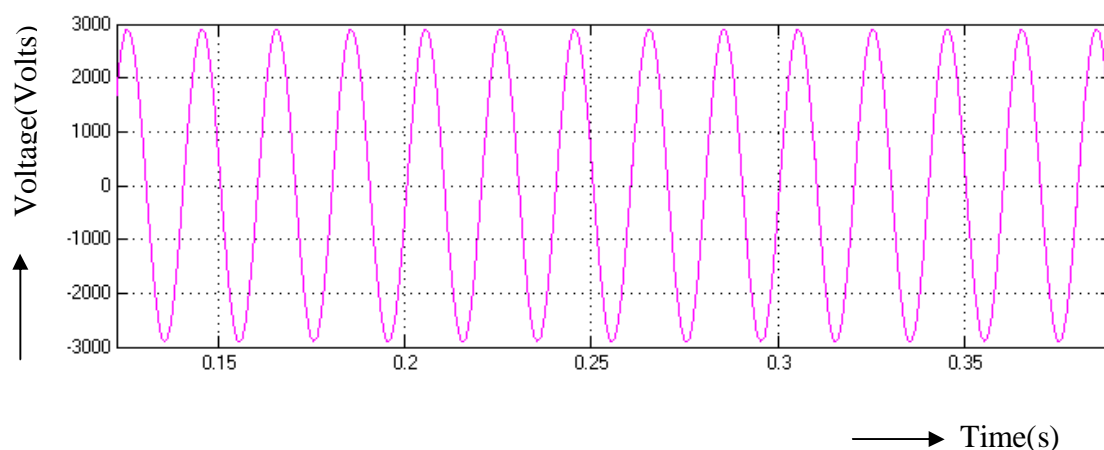


Fig.5.8.2.29. Voltage at Bus-48

The Figs.5.8.2.30 and 5.8.2.31, represents the real and reactive power at bus 48. The graph is drawn between time on x-axis and power on y-axis. From the above waveform it shows that, the real and reactive power starts to increases from origin and maintains a constant value due to the addition of UPQC.

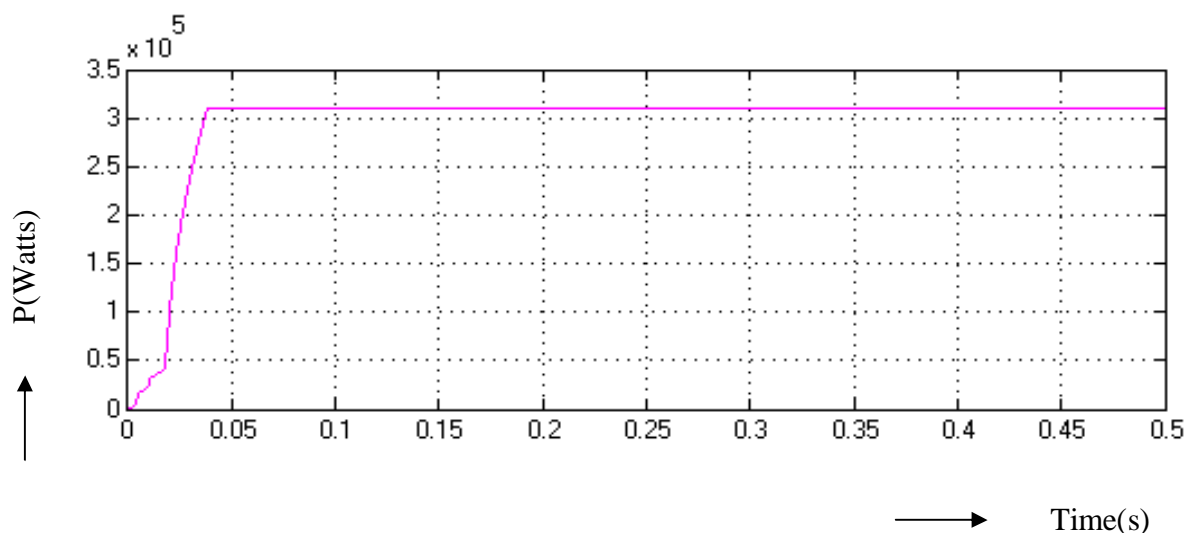


Fig.5.8.2.30. Real Power at Bus-48

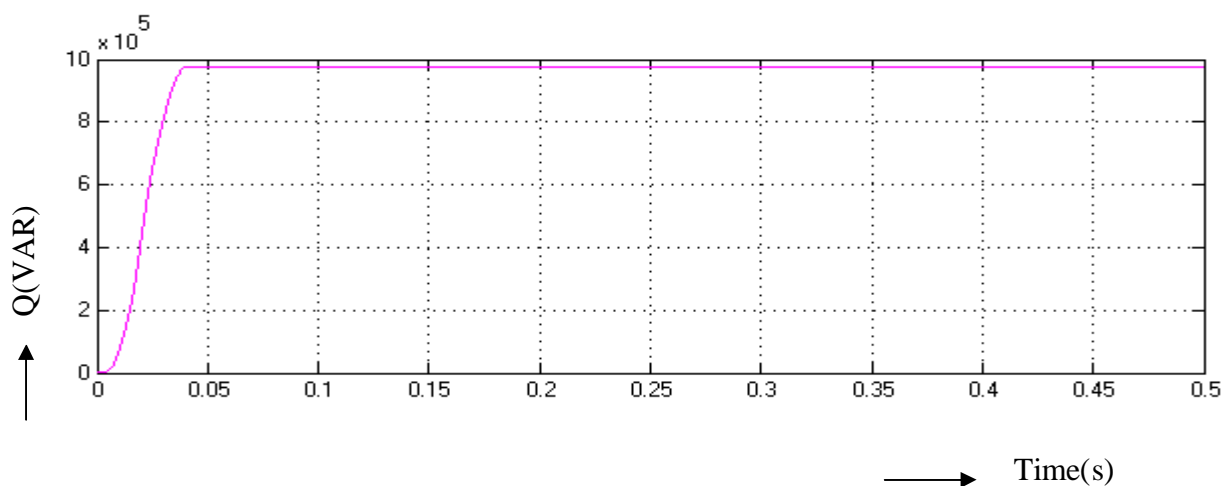


Fig.5.8.2.31. Reactive Power at Bus-48

The frequency spectrum for current with UPQC is shown in Fig.5.8.2.32. The frequency spectrum is drawn with frequency on x-axis and magnitude of voltage on y-axis. The magnitude of higher order harmonics are negligible. The height decreases with the increase in the order of harmonics. This is due to the increased impedance at high frequency. The THD is 3.2%.

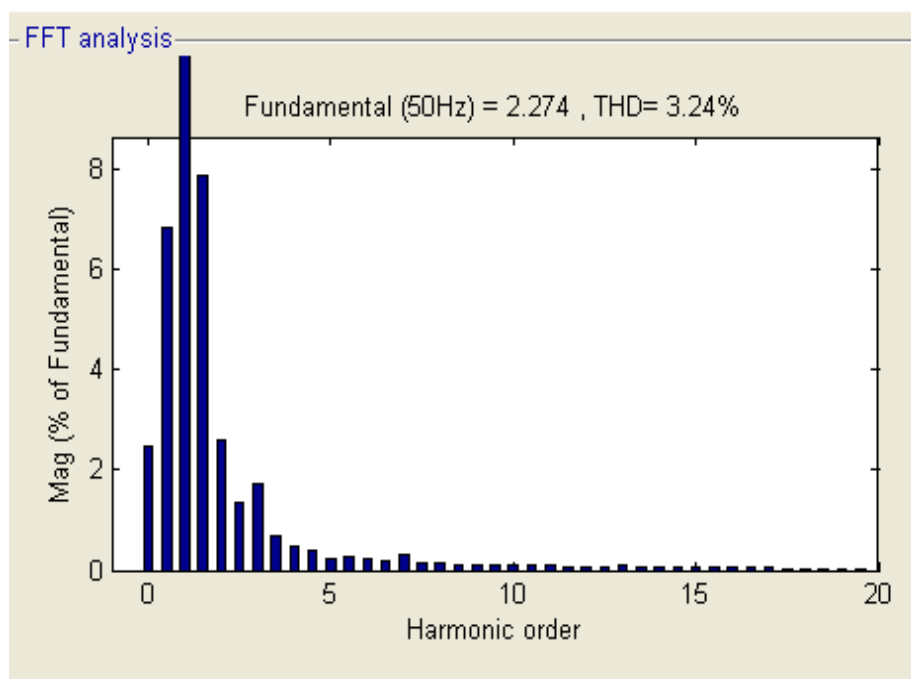


Fig.5.8.2.32. Frequency Spectrum for Current.

The Summary of real and reactive power with and without UPQC are shown in Table 5.4. The change in real and reactive power is more predominant in the buses in the nearer to UPQC 1 and to UPQC 2.

**Table 5.4. Summary of Real and Reactive Power of 50 Bus System**

BUS NO	REAL POWER WITHOUT UPQC (MW)	REAL POWER WITH UPQC (MW)	REACTIVE POWER WITHOUT UPQC (MVAR)	REACTIVE POWER WITH UPQC (MVAR)
BUS-1	0.277	0.275	0.304	0.352
BUS-2	0.263	0.272	0.301	0.348
BUS-3	0.42	0.575	1.32	1.801
<b>BUS-4</b>	<b>0.378</b>	<b>2.431</b>	<b>2.210</b>	<b>2.788</b>
BUS-5	0.321	0.442	2.23	2.791



**Read Table 5.4 (continued)**

BUS-6	0.311	0.378	2.27	2.810
BUS-7	0.321	0.358	2.26	2.842
BUS-8	0.318	0.346	2.241	2.846
BUS-9	0.309	0.336	2.238	2.832
BUS-10	0.356	0.373	2.861	2.989
BUS-11	3.20	3.21	3.35	3.36
<b>BUS-12</b>	<b>3.11</b>	<b>3.12</b>	<b>3.23</b>	<b>3.25</b>
BUS-13	2.13	2.18	2.29	2.28
BUS-14	1.89	1.982	1.971	1.998
BUS-15	1.25	1.45	1.38	1.57
BUS-16	1.069	1.76	1.86	1.89
BUS-17	1.089	2.087	2.879	2.978
BUS-18	1.068	2.042	2.798	2.861
BUS-19	1.863	2.456	2.388	2.458
BUS-20	1.861	2.452	2.386	2.451
BUS-21	0.378	2.431	2.210	2.788
BUS-22	3.26	3.351	3.612	3.629
BUS-23	1.089	2.087	2.879	2.978
BUS-24	1.89	1.982	1.971	1.998
BUS-25	2.891	2.958	3.121	3.221
<b>BUS-26</b>	<b>2.812</b>	<b>2.859</b>	<b>2.843</b>	<b>2.856</b>
BUS-27	0.42	0.575	1.32	1.801
BUS-29	3.20	3.21	3.35	3.36
BUS-30	0.378	2.431	2.210	2.788
BUS-31	0.321	0.442	2.23	2.791
BUS-32	0.311	0.378	2.27	2.810
BUS-33	0.321	0.358	2.26	2.842
BUS-34	0.318	0.346	2.241	2.846
BUS-35	1.89	1.982	1.971	1.998
BUS-36	0.42	0.575	1.32	1.801
BUS-37	0.311	0.378	2.27	2.810
BUS-38	0.321	0.358	2.26	2.842

**Read Table 5.4 (continued)**

BUS-39	0.318	0.346	2.241	2.846
BUS-40	0.309	0.336	2.238	2.832
BUS-41	0.356	0.373	2.861	2.989
BUS-42	3.20	3.21	3.35	3.36
BUS-43	3.11	3.12	3.23	3.25
BUS-44	2.13	2.18	2.29	2.28
<b>BUS-45</b>	<b>1.89</b>	<b>1.982</b>	<b>1.971</b>	<b>1.998</b>
BUS-46	1.25	1.45	1.38	1.57
BUS-47	1.069	1.76	1.86	1.89
BUS-48	1.089	2.087	2.879	2.978
BUS-49	1.58	2.56	2.98	2.97
BUS-50	1.681	2.781	2.89	2.987

### 5.13. Results and Discussions

The fifty bus system is modeled and simulated using the blocks and elements of simulink. From the above wave forms and table it is cleared that the following things are noticed.

From the bus voltage wave forms it can be seen that , The decrease due to addition of the extra load. The voltage recovers to the normal value due to the injection of voltage.

- From the summary of real and reactive powers at various Buses with and without UPQC, it can be seen that there is an increase in real and reactive power due to the addition of UPQC. The increase in real and reactive power is due to the increase in the voltage.

- From the current spectrum wave forms with UPQC THD reduces from 14.2% to 3.2%.

#### **5.14. Results comparison with desirables and analysis**

Real and Reactive power at all the fifty Buses are shown. The reactive power is proportional to square of the voltage. Hence reactive power increases with the increase in the injected voltage. The voltage profile is also improved by adding UPQC in multiple system.

#### **5.15. Conclusion**

The Eight, Fourteen, Thirty and Fifty Bus Systems are modeled and simulated using the blocks and elements of Simulink. The above Systems with UPQC are also simulated. It is observed that the real and reactive powers increase due to the addition of UPQC. The voltage profile is also improved by adding UPQC in multiple system. The simulation results agree with the theoretical results.

## CHAPTER 6

### CONCLUSION AND FUTURE WORK

#### 6.1. Conclusion

An UPQC system is successfully designed and modeled using the circuit elements of simulink. The sag in the voltage is created by applying an additional heavy load at the receiving end. This sag is compensated by using the DVR part of UPQC. The simulation results are in line with the predictions. The THD in the output is reduced by operating the inverter at 250Hz. The hardware is fabricated and tested using PIC micro controller. The experimental results closely agree with the simulation results.

The eight bus system with UPQC is successfully designed and modeled using the circuit elements of simulink. The sag in the voltage is created by applying an additional heavy load at the receiving end. This sag is compensated by using DVR. The simulation results are in line with the predictions. The THD in the output is reduced by UPQC. The increase in real power was 18% and the increase in reactive power was 15% by introducing UPQC.

The fourteen bus system is drawn by using the corresponding data. This is simulated and the results are presented. The results indicate that the power quality is improved by introducing UPQC. The thirty bus system is simulated and the corresponding results are given. Multiple UPQCs are proposed to maintain the required voltage. The increase in real power was 36% and the increase in reactive power was 6% by introducing UPQC.

The fifty bus system is also simulated and the corresponding results are given. Multiple UPQCs are proposed to maintain the required voltage. The increase in real and reactive powers were high at the buses close to the UPQC.

UPQC system has advantages like improvement in voltage of load buses, sag compensation and reduction in losses. The disadvantages of UPQC is that it requires two three phase inverters operating at different frequencies. UPQC is a viable alternative to the existing FACTS devices since they have more advantages.

## **6.2. Scope for further work**

The scope of this work is the modeling and simulation of eight, fourteen, thirty and fifty bus systems. Simulation of sixty four bus system is yet to be done.

The simulation is done using Matlab. The simulation can be repeated with PSCAD or PSIM for comparison purpose. The hardware is done using PIC. The hardware may be implemented using DSP processor.

## APPENDIX

### TWO BUS SYSTEM

**Comparison Table-1 PV PARAMETERS**

<b>Open circuit voltage(Voc)</b>	<b>120V</b>
<b>Short circuit current(ISC)</b>	<b>2.5A</b>
<b>Voltage at maximum power(Vmp)</b>	<b>115V</b>
<b>Current at maximum power(Imp)</b>	<b>2.31A</b>
<b>Maximum system voltage</b>	<b>2000VDC</b>
<b>Maximum reverse current</b>	<b>5A</b>
<b>Nominal operating temperature</b>	<b>47° C</b>
<b>Maximum power(Pmax)</b>	<b>300W</b>

**Comparison Table-2 line Parameters**

<b>Bus</b>	<b>Voltage</b>	<b>Load impedance</b>		<b>Line impedance</b>	
		<b>Resistance</b>	<b>Inductance</b>	<b>Resistance</b>	<b>Inductance</b>
<b>BUS 1</b>	<b>11.3kv</b>	<b>200Ω</b>	<b>100mH</b>	<b>0.001Ω</b>	<b>30mH</b>
<b>BUS 2</b>	<b>–</b>	<b>50Ω</b>	<b>50mH</b>	<b>0.1Ω</b>	<b>30mH</b>

**Comparison Table-3 IGBT & Diode details**

<b>IGBT(150N)</b>	<b>1700V/150A</b>
<b>DIOED</b>	<b>230V/1A</b>

**THD for bus-2**  
**Comparison Table-4 Bus Voltage & THD**

<b>Bus No</b>	<b>Voltage</b>	<b>THD</b>
<b>Bus-1</b>	<b>6.11kv</b>	<b>4.17%</b>
<b>Bus -2</b>	<b>6.25kv</b>	<b>1.59%</b>

**TWO BUS SYSTEM**  
**SIMULATION PARAMETERS**

<b>S. No.</b>	<b>Simulation value</b>	<b>Hardware value</b>
<b>Vin</b>	<b>48v</b>	<b>48v</b>
<b>C1</b>	<b>3500UF</b>	<b>3500UF</b>
<b>Co</b>	<b>220UF</b>	<b>2200UF</b>
<b>L0</b>	<b>100MH</b>	<b>100MH</b>
<b>RL</b>	<b>15K</b>	<b>10K</b>
<b>IGBT(150N)</b>	<b>500V/8A</b>	<b>500V/8A</b>
<b>DIOED</b>	<b>230V/1A</b>	<b>230V/1A</b>
<b>V0</b>	<b>130V</b>	<b>126V</b>

### 8-bus system line parameters

BUS	VOLTAGE	LOAD IMPEDANCE	
		RESISTANCE	INDUCTANCE
bus 1	6350	-	-
bus 2	-	35Ω	48mH
bus 3	6350	-	-
bus 4	-	12Ω	23mH
bus 5	6350	-	-
bus 6	-	20Ω	63mH
bus 7	6350	-	-
bus 8	-	56Ω	86mH

Bus	LINE IMPEDANCE	
	RESISTANCE	INDUCTANCE
bus 1-2	3Ω	50mH
bus 2-3	3Ω	18mH
bus 3-4	11Ω	24mH
bus 4-5	19Ω	26mH
bus 5-6	21Ω	37mH
bus 6-7	16Ω	72mH
bus 7-8	46Ω	58mH
bus 8-L	65Ω	92mH



### 14 Bus system line parameters

BUS	VOLTAGE	LOAD IMPEDANCE	
		RESISTANCE	INDUCTANCE
bus 1	6350	-	-
bus 2	-	8Ω	23mH
bus 3	-	5Ω	14mH
bus 4	-	9Ω	9mH
bus 5	6350	-	-
bus 6	-	10Ω	40mH
bus 7	-	18Ω	25mH
bus 8	6350	-	-
bus 9	-	45Ω	55mH
bus 10	-	33Ω	65mH
bus 11	6350	-	-
bus 12	-	62Ω	42mH
bus 13	-	45Ω	59mH
bus 14	6350	5Ω	-

BUS	LINE IMPEDANCE	
	RESISTANCE	INDUCTANCE
bus 1-2	5Ω	22mH
bus 2-3	3Ω	15mH
bus 3-4	13Ω	8mH
bus 4-5	15Ω	26mH
bus 5-6	25Ω	32mH
bus 6-7	10Ω	22mH
bus 7-8	26Ω	17mH
bus 8-9	45Ω	32mH
bus 9-10	35Ω	28mH
bus 10-11	43Ω	11mH
bus 11-12	90Ω	36mH
bus 12-13	32Ω	10mH
bus 13-14	26Ω	15mH
bus 14-1	20Ω	40mH

### 30 bus system line parameters

BUS	Voltage	load Impedance	
		Resistance	Inductance
bus 1	11kv	-	-
bus 2	-	10Ω	50mH
bus 3	-	25Ω	40mH
bus 4	11kv	-	-
bus 5	-	85Ω	110mH
bus 6	-	95Ω	125mH
bus 7	-	125 Ω	180mH
bus 8	11kv	-	-
bus 9	-	135 Ω	167mH
bus 10	-	58 Ω	127mH
bus 11	-	100Ω	100mH
bus 12	11kv	-	-
bus 13	-	48Ω	100mH
bus 14	-	67 Ω	97mH
bus 15	11kv	-	-
bus 16	-	33Ω	65mH
bus 17	-	78 Ω	125mH
bus 18	11kv	-	-
bus 19	-	120Ω	150mH
bus 20	-	120Ω	168mH
bus 21	-	125Ω	130mH
bus 22	-	25Ω	90mH
bus 23	-	110 Ω	138mH
bus 24	11kv	-	-
bus 25	-	10Ω	100mH
bus 26	-	10Ω	100mH
bus 27	11kv	-	-
bus 28	-	10Ω	100mH
bus 29	-	89Ω	189mH
bus 30	-	115Ω	198mH

BUS	LINE IMPEDANCE	
	RESISTANCE	INDUCTANCE
bus 1-2	8 $\Omega$	30mH
bus 2-3	3 $\Omega$	38mH
bus 3-4	6 $\Omega$	40mH
bus 4-5	13 $\Omega$	37mH
bus 5-6	15 $\Omega$	30mH
bus 6-7	23 $\Omega$	26mH
bus 7-8	45 $\Omega$	56mH
bus 8-9	54 $\Omega$	63mH
bus 9-10	43 $\Omega$	100mH
bus 10-11	36 $\Omega$	113mH
bus 11-12	24 $\Omega$	55mH
bus 12-13	36 $\Omega$	85mH
bus 13-14	78 $\Omega$	125mH
bus 14-15	85 $\Omega$	79mH
bus 15-16	96 $\Omega$	150mH
bus 16-17	110 $\Omega$	138mH
bus 17-18	108 $\Omega$	124mH
bus 18-19	89 $\Omega$	119mH
bus 19-20	76 $\Omega$	106mH
bus 20-21	79 $\Omega$	98mH
bus 21-22	86 $\Omega$	110mH
bus 22-23	55 $\Omega$	103mH
bus 23-24	40 $\Omega$	75mH
bus 24-25	55 $\Omega$	69mH
bus 25-26	64 $\Omega$	78mH
bus 26-27	81 $\Omega$	93mH
bus 27-28	112 $\Omega$	97mH
bus 28-29	106 $\Omega$	136mH
bus 29-30	93 $\Omega$	131mH
bus 30-31	89 $\Omega$	124mH

### 50 bus system line parameters

BUS	Voltage	Load impedance	
		Resistance	Inductance
bus 1	11kv	-	-
bus 2	-	10 $\Omega$	50mH
bus 3	-	25 $\Omega$	40mH
bus 4	11kv	-	-
bus 5	-	85 $\Omega$	110mH
bus 6	-	95 $\Omega$	125mH
bus 7	-	125 $\Omega$	180mH
bus 8	11kv	-	-
bus 9	-	135 $\Omega$	167mH
bus 10	-	58 $\Omega$	127mH
bus 11	-	100 $\Omega$	100mH
bus 12	11kv	-	-
bus 13	-	48 $\Omega$	100mH
bus 14	-	67 $\Omega$	97mH
bus 15	11kv	-	-
bus 16	-	33 $\Omega$	65mH
bus 17	-	78 $\Omega$	125mH
bus 18	11kv	-	-
bus 19	-	120 $\Omega$	150mH
bus 20	-	120 $\Omega$	168mH
bus 21	-	125 $\Omega$	130mH
bus 22	-	25 $\Omega$	90mH
bus 23	-	110 $\Omega$	138mH
bus 24	11kv	-	-
bus 25	-	10 $\Omega$	100mH

<b>bus 26</b>	-	<b>10Ω</b>	<b>100mH</b>
<b>bus 27</b>	<b>11kv</b>	-	-
<b>bus 28</b>	-	<b>10Ω</b>	<b>100mH</b>
<b>bus 29</b>	-	<b>89Ω</b>	<b>189mH</b>
<b>bus 30</b>	-	<b>115Ω</b>	<b>198mH</b>
<b>bus 31</b>	-	<b>48Ω</b>	<b>100mH</b>
<b>bus 32</b>	-	<b>67 Ω</b>	<b>97mH</b>
<b>bus 33</b>	<b>11kv</b>	-	-
<b>bus 34</b>	-	<b>33Ω</b>	<b>65mH</b>
<b>bus 35</b>	-	<b>78 Ω</b>	<b>125mH</b>
<b>bus 36</b>	<b>11kv</b>	-	-
<b>bus 37</b>	-	<b>120Ω</b>	<b>150mH</b>
<b>bus 38</b>	-	<b>120Ω</b>	<b>168mH</b>
<b>bus 39</b>	-	<b>125Ω</b>	<b>130mH</b>
<b>bus 40</b>	<b>11kv</b>	-	-
<b>bus 41</b>	-	<b>110 Ω</b>	<b>138mH</b>
<b>bus 42</b>	-	<b>48Ω</b>	<b>100mH</b>
<b>bus 43</b>	-	<b>67 Ω</b>	<b>97mH</b>
<b>bus 44</b>	<b>11kv</b>	-	-
<b>bus 45</b>	-	<b>33Ω</b>	<b>65mH</b>
<b>bus 46</b>	-	<b>78 Ω</b>	<b>125mH</b>
<b>bus 47</b>	<b>11kv</b>	-	-
<b>bus 48</b>	-	<b>120Ω</b>	<b>150mH</b>
<b>bus 49</b>	-	<b>120Ω</b>	<b>168mH</b>
<b>bus 50</b>	-	<b>125Ω</b>	<b>130mH</b>

BUS	LINE IMPEDANCE	
	RESISTANCE	INDUCTANCE
bus 1-2	8 $\Omega$	30mH
bus 2-3	3 $\Omega$	38mH
bus 3-4	6 $\Omega$	40mH
bus 4-5	13 $\Omega$	37mH
bus 5-6	15 $\Omega$	30mH
bus 6-7	23 $\Omega$	26mH
bus 7-8	45 $\Omega$	56mH
bus 8-9	54 $\Omega$	63mH
bus 9-10	43 $\Omega$	100mH
bus 10-11	36 $\Omega$	113mH
bus 11-12	4 $\Omega$	55mH
bus 12-13	36 $\Omega$	85mH
bus 13-14	78 $\Omega$	125mH
bus 14-15	85 $\Omega$	79mH
bus 15-16	96 $\Omega$	150mH
bus 16-17	110 $\Omega$	138mH
bus 17-18	108 $\Omega$	124mH
bus 18-19	89 $\Omega$	119mH
bus 19-20	76 $\Omega$	106mH
bus 20-21	79 $\Omega$	98mH
bus 21-22	86 $\Omega$	110mH
bus 22-23	55 $\Omega$	103mH
bus 23-24	40 $\Omega$	75mH
bus 24-25	55 $\Omega$	69mH
bus 25-26	64 $\Omega$	78mH

<b>bus 26-27</b>	<b>81 <math>\Omega</math></b>	<b>93mH</b>
<b>bus 27-28</b>	<b>112 <math>\Omega</math></b>	<b>97mH</b>
<b>bus 28-29</b>	<b>106<math>\Omega</math></b>	<b>136mH</b>
<b>bus 29-30</b>	<b>93<math>\Omega</math></b>	<b>131mH</b>
<b>bus 30-31</b>	<b>89 <math>\Omega</math></b>	<b>124mH</b>
<b>bus 31-2</b>	<b>78 <math>\Omega</math></b>	<b>125mH</b>
<b>bus 32-33</b>	<b>85 <math>\Omega</math></b>	<b>79mH</b>
<b>bus 33-34</b>	<b>96 <math>\Omega</math></b>	<b>150mH</b>
<b>bus 34-35</b>	<b>110 <math>\Omega</math></b>	<b>138mH</b>
<b>bus 35-36</b>	<b>108<math>\Omega</math></b>	<b>124mH</b>
<b>bus 36-37</b>	<b>89 <math>\Omega</math></b>	<b>119mH</b>
<b>bus 37-38</b>	<b>76<math>\Omega</math></b>	<b>106mH</b>
<b>bus 38-39</b>	<b>79 <math>\Omega</math></b>	<b>98mH</b>
<b>bus 39-40</b>	<b>86 <math>\Omega</math></b>	<b>110mH</b>
<b>bus 40-41</b>	<b>55<math>\Omega</math></b>	<b>103mH</b>
<b>bus 41-42</b>	<b>40 <math>\Omega</math></b>	<b>75mH</b>
<b>bus 42-43</b>	<b>78 <math>\Omega</math></b>	<b>125mH</b>
<b>bus 43-44</b>	<b>85 <math>\Omega</math></b>	<b>79mH</b>
<b>bus 44-45</b>	<b>96 <math>\Omega</math></b>	<b>150mH</b>
<b>bus 45-46</b>	<b>110 <math>\Omega</math></b>	<b>138mH</b>
<b>bus 46-47</b>	<b>108<math>\Omega</math></b>	<b>124mH</b>
<b>bus 47-48</b>	<b>89 <math>\Omega</math></b>	<b>119mH</b>
<b>bus 48-49</b>	<b>76<math>\Omega</math></b>	<b>106mH</b>
<b>bus49 -50</b>	<b>79 <math>\Omega</math></b>	<b>98mH</b>
<b>bus 50-L</b>	<b>86 <math>\Omega</math></b>	<b>110mH</b>

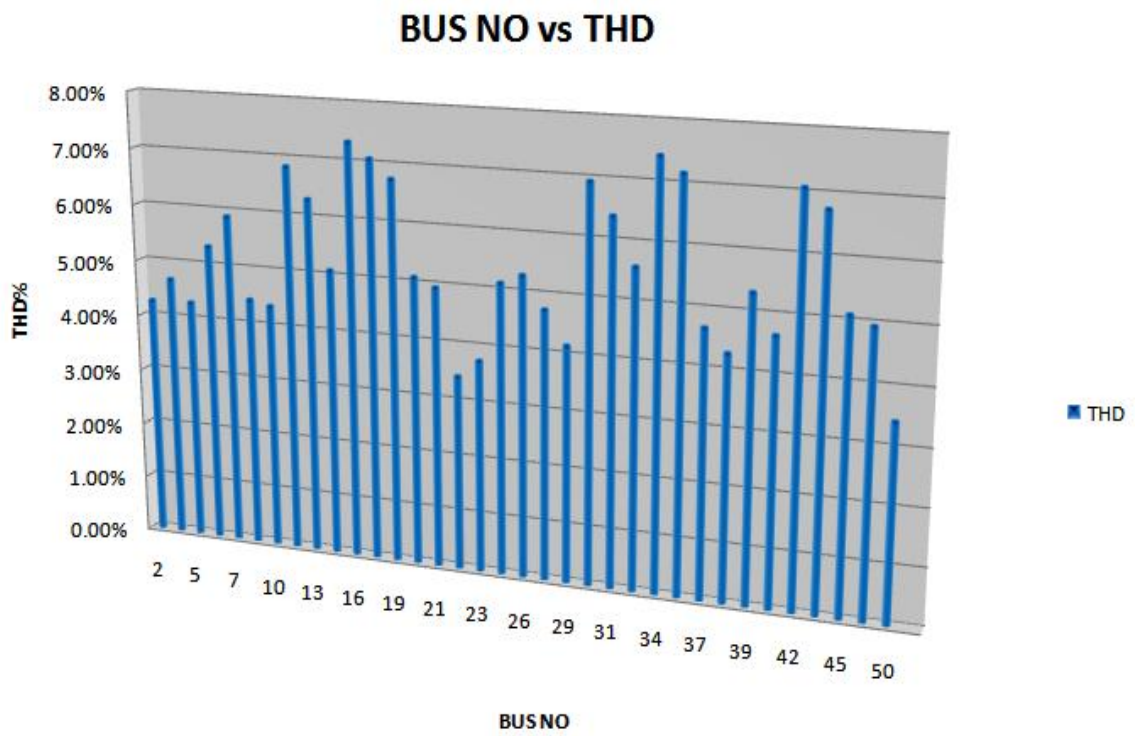
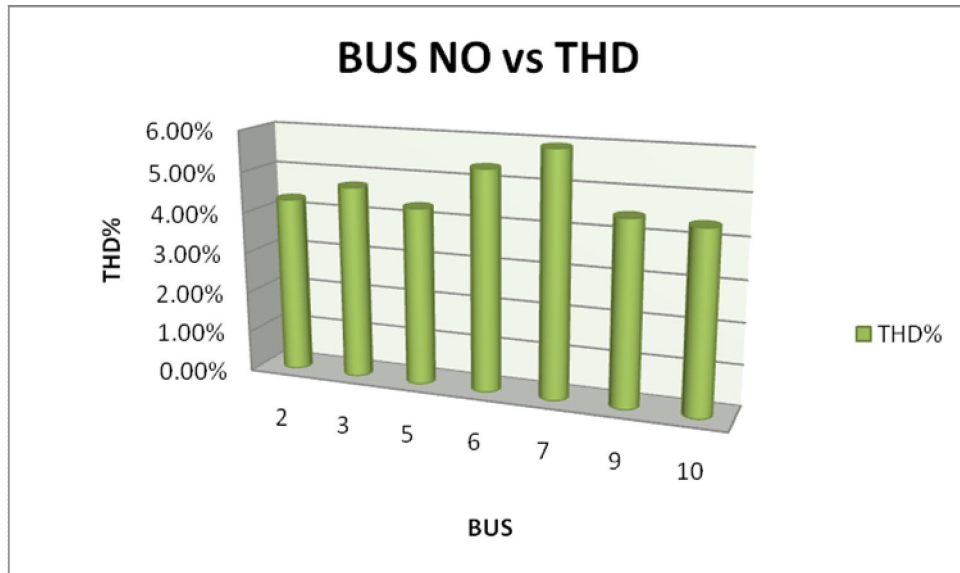
Bus	Voltage	load Impedance		line Impedance	
		Resistance	Inductance	Resistance	Inductance
BUS 1	11kv	-	-	8 Ω	30mH
BUS 2		10Ω	50mH	3Ω	38mH
BUS 3		25Ω	40mH	6 Ω	40mH
BUS 4	11kv	-	-	13 Ω	37mH
BUS 5	-	85Ω	110mH	15Ω	30mH
BUS 6	-	95Ω	125mH	23 Ω	26mH
BUS 7	-	125 Ω	180mH	45 Ω	56mH
BUS 8	11kv	-	-	54 Ω	63mH
BUS 9		135 Ω	167mH	43Ω	100mH
BUS 10	-	58 Ω	127mH	36Ω	113mH
BUS 11	-	100Ω	100mH	24 Ω	55mH
BUS 12	11kv	-	-	36 Ω	85mH
BUS 13	-	48Ω	100mH	78 Ω	125mH
BUS 14	-	67 Ω	97mH	85 Ω	79mH
BUS 15	11kv	-	-	96 Ω	150mH
BUS 16	-	33Ω	65mH	110 Ω	138mH
BUS 17	-	78 Ω	125mH	108Ω	124mH
BUS 18	11kv	-	-	89 Ω	119mH
BUS 19	-	120Ω	150mH	76Ω	106mH
BUS 20	-	120Ω	168mH	79 Ω	98mH
BUS 21	-	125Ω	130mH	86 Ω	110mH
BUS 22	-	25Ω	90mH	55Ω	103mH
BUS 23	-	110 Ω	138mH	40 Ω	75mH
BUS 24	11kv	-	-	55Ω	69mH
BUS 25	-	10Ω	100mH	64Ω	78mH



<b>BUS 26</b>	–	<b>10Ω</b>	<b>100mH</b>	<b>81 Ω</b>	<b>93mH</b>
<b>BUS 27</b>	<b>11kv</b>	<b>-</b>	<b>-</b>	<b>112 Ω</b>	<b>97mH</b>
<b>BUS 28</b>	–	<b>10Ω</b>	<b>100mH</b>	<b>106Ω</b>	<b>136mH</b>
<b>BUS 29</b>	–	<b>89Ω</b>	<b>189mH</b>	<b>93Ω</b>	<b>131mH</b>
<b>BUS 30</b>	–	<b>115Ω</b>	<b>198mH</b>	<b>89 Ω</b>	<b>124mH</b>
<b>BUS 31</b>	–	<b>48Ω</b>	<b>100mH</b>	<b>78 Ω</b>	<b>125mH</b>
<b>BUS 32</b>	–	<b>67 Ω</b>	<b>97mH</b>	<b>85 Ω</b>	<b>79mH</b>
<b>BUS 33</b>	<b>11kv</b>	–	–	<b>96 Ω</b>	<b>150mH</b>
<b>BUS 34</b>	–	<b>33Ω</b>	<b>65mH</b>	<b>110 Ω</b>	<b>138mH</b>
<b>BUS 35</b>	–	<b>78 Ω</b>	<b>125mH</b>	<b>108Ω</b>	<b>124mH</b>
<b>BUS 36</b>	<b>11kv</b>	–	–	<b>89 Ω</b>	<b>119mH</b>
<b>BUS 37</b>	–	<b>120Ω</b>	<b>150mH</b>	<b>76Ω</b>	<b>106mH</b>
<b>BUS 38</b>	–	<b>120Ω</b>	<b>168mH</b>	<b>79 Ω</b>	<b>98mH</b>
<b>BUS 39</b>	–	<b>125Ω</b>	<b>130mH</b>	<b>86 Ω</b>	<b>110mH</b>
<b>BUS 40</b>	<b>11kv</b>	–	–	<b>55Ω</b>	<b>103mH</b>
<b>BUS 41</b>	–	<b>110 Ω</b>	<b>138mH</b>	<b>40 Ω</b>	<b>75mH</b>
<b>BUS 42</b>	–	<b>48Ω</b>	<b>100mH</b>	<b>78 Ω</b>	<b>125mH</b>
<b>BUS 43</b>	–	<b>67 Ω</b>	<b>97mH</b>	<b>85 Ω</b>	<b>79mH</b>
<b>BUS 44</b>	<b>11kv</b>	–	–	<b>96 Ω</b>	<b>150mH</b>
<b>BUS 45</b>	–	<b>33Ω</b>	<b>65mH</b>	<b>110 Ω</b>	<b>138mH</b>
<b>BUS 46</b>	–	<b>78 Ω</b>	<b>125mH</b>	<b>108Ω</b>	<b>124mH</b>
<b>BUS 47</b>	<b>11kv</b>	–	–	<b>89 Ω</b>	<b>119mH</b>
<b>BUS 48</b>	–	<b>120Ω</b>	<b>150mH</b>	<b>76Ω</b>	<b>106mH</b>
<b>BUS 49</b>	–	<b>120Ω</b>	<b>168mH</b>	<b>79 Ω</b>	<b>98mH</b>
<b>BUS 50</b>	–	<b>125Ω</b>	<b>130mH</b>	<b>86 Ω</b>	<b>110mH</b>

<b>BUS NO</b>	<b>Load voltage</b>	<b>THD</b>
<b>BUS-2</b>	<b>9211</b>	<b>4.30%</b>
<b>BUS-3</b>	<b>8688</b>	<b>4.71%</b>
<b>BUS-5</b>	<b>9102</b>	<b>4.32%</b>
<b>BUS-6</b>	<b>8233</b>	<b>5.36%</b>
<b>BUS-7</b>	<b>8387</b>	<b>5.92%</b>
<b>BUS-9</b>	<b>8316</b>	<b>4.47%</b>
<b>BUS-10</b>	<b>7890</b>	<b>4.39%</b>
<b>BUS-11</b>	<b>9020</b>	<b>6.87%</b>
<b>BUS-13</b>	<b>8944</b>	<b>6.33%</b>
<b>BUS-14</b>	<b>8541</b>	<b>5.12%</b>
<b>BUS-16</b>	<b>7490</b>	<b>7.36%</b>
<b>BUS-17</b>	<b>9915</b>	<b>7.10%</b>
<b>BUS-19</b>	<b>9490</b>	<b>6.78%</b>
<b>BUS-20</b>	<b>8659</b>	<b>5.13%</b>
<b>BUS-21</b>	<b>8490</b>	<b>4.98%</b>
<b>BUS-22</b>	<b>8324</b>	<b>3.47%</b>
<b>BUS-23</b>	<b>7836</b>	<b>3.78%</b>
<b>BUS-25</b>	<b>7835</b>	<b>5.16%</b>
<b>BUS-26</b>	<b>8690</b>	<b>5.32%</b>
<b>BUS-28</b>	<b>8894</b>	<b>4.77%</b>
<b>BUS-29</b>	<b>9490</b>	<b>4.19%</b>

<b>BUS-30</b>	<b>8415</b>	<b>6.97%</b>
<b>BUS-31</b>	<b>8869</b>	<b>6.43%</b>
<b>BUS-32</b>	<b>7359</b>	<b>5.62%</b>
<b>BUS-34</b>	<b>8490</b>	<b>7.46%</b>
<b>BUS-35</b>	<b>9332</b>	<b>7.20%</b>
<b>BUS-37</b>	<b>7490</b>	<b>4.71%</b>
<b>BUS-38</b>	<b>9915</b>	<b>4.32%</b>
<b>BUS-39</b>	<b>9490</b>	<b>5.36%</b>
<b>BUS-41</b>	<b>8659</b>	<b>4.69%</b>
<b>BUS-42</b>	<b>8490</b>	<b>7.10%</b>
<b>BUS-43</b>	<b>8324</b>	<b>6.78%</b>
<b>BUS-45</b>	<b>8541</b>	<b>5.13%</b>
<b>BUS-46</b>	<b>7490</b>	<b>4.98%</b>
<b>BUS-49</b>	<b>9915</b>	<b>3.47%</b>
<b>BUS-50</b>	<b>8415</b>	<b>4.58%</b>



## REFERENCES

1. Akagi, H., and Fujita, H., "A new power line conditional for harmonic compensation in power systems", IEEE Trans. Power Del., Vol.10, no.3, pp.1570-1575, Jul 1995.
2. Akagi, H., Watanabe, E.H., and Aredes, M., "Instantaneous Power Theory and Applications to Power Conditioning", Wiley-IEEE Press, April 2007.
3. Aredes, M., "A combined series and shunt active power filter", in Proc. IEEE/KTH Stockholm Power Tech Conf., Stockholm, Sweden, pp.18-22, June 1995.
4. Akagi, H., and Fujita, H., "A new power line conditional for harmonic compensation in power systems", IEEE Trans power delivery, 10: 1570-1575, 1995.
5. Akagi, H.Y., Kanazawa and Nabae, A., "Instantaneous reactive power compensator comprising switching devices without energy storage components", IEEE Trans. India Appl.20: 625-630, 2007.
6. Aredes, M., and Watanabe, E.H., "New control algorithms for series and shunt three-phase four wire active power filters", IEEE Trans. Power delivery, 10: 1649-1656, 1995.
7. Aredes, M., Akagi, H., Watanabe, E.H., Salgado, E.V., Encarnacao, L.F., "Comparisons between the p-q and p-q-r Theories in Three Phase Four-Wire Systems," IEEE Transactions on Power Electronics, vol.24, no.4, pp.924-933, April 2009.
8. Alkas, I.H., and sharaf, A.M., "A Photovoltaic Array simulation model for Matlab – simulink GUI environment", clean Electrical power, ICCEP' 07 – International conference PP 341 – 345, 2007.
9. Ahed. Kazemi and Ali Azhdast, "Implementation of a Control Strategy for Dynamic Voltage Restorer (DVR) and Dynamic Voltage Compensator (DVC)", IEEE Power System Conference, pp.1-6, 2009.
10. Ahmed, A., Helal and Mohamed, H., Saied, "Dynamic Voltage Restorer Adopting 150% Conduction Angle VSI", IEEE Electrical Power and Energy Conference, pp. 1-6, 2008.

11. Ben-Brahim, L., and Tadakuma, S., "A novel multilevel carrier- based PWM- control method for GTO inverter in low index modulation region", IEEE Transactions on Industrial Applications, Vol 42 no.1 pp.121-127, 2006.
12. Banaei, M.R., Hosseini, S.H., and Gharehpetian, G.B., "Interline Dynamic Voltage Restorer Control using a Novel Optimum Energy Consumption Strategy", Simulation Modelling Practice and Theory 14, pp.989-999, 2006.
13. Bingsen Wang, G., Venkataraman, and Illindala, M., "Operation and Control of DVR using Transformer Coupled H-bridge Converter", IEEE Transactions on Power Electronics, Vol. 21, no.4, pp.1053-1061, 2006.
14. Basu, M., DAS, S.P., and Dubey, G.K., "Investigation on the performance of UPQC – Q for voltage sag", IET Generation, Transmission and Distribution-2, 414 – 423, 2008.
15. Barker, P.P., and De Mello, R.W., "Determining the impact of distributed generation on power systems. Part Radial distribution systems", Proc.IEEE power Eng.Sec.Summer Meeting 3, pp.1645-1656. 2000.
16. Basu, M.S.P., Das and Dubey, G.K., "Comparative evaluation of two models of UPQC for suitable interface to enhance power quality", Elec. power system Res, Vol.77, pp.821-830, 2007.
17. Blaabjerg F.Z Chen and Kjaer, S.B., "Power electronics as efficient interface in dispersed power generation systems", IEEE Trans. Power Elect, 19, pp.1184-1194, 2004.
18. Zhang, Y., and Milanoyic, J. V., "Techno-economic improvement of voltage sag performance with facts devices", Presented at the 9th Int. Conf. Electrical Power Quality and Utilization, Barcelona, Spain, 2006.
19. Chen Y., X.Zha, and Wang, J., "Unified Power Quality conditioner (UPQC): The theory, modeling and application," Proc. Power System Techlogy Powr Con Int. Conf., Vol.3, pp1329-1333, 2000.
20. Chi-Seng Lam, Man-Chung Wong and Ying-Duo Han, "Voltage Swell and Over Voltage Compensation with Unidirectional Power Flow Controlled Dynamic Voltage Restorer", IEEE Transactions on Power Delivery, Vol. 23, no.4 pp.2513-2521, 2008.

21. Chellai Benachiba and Brahim Ferdi, "Voltage Quality Improvement Using DVR, Electrical Power Quality and Utilization", Journal Vol.14, no.1, pp.39-45, 2008.
22. Chris Filtzer, Mike Barnes and Peter Green, "Voltage Sag Detection Technique for a Dynamic Voltage Restorer", IEEE Transactions on Industry Applications, Vol. 40, no.1 pp.203-212, 2004.
23. Davarai, M., Alc-Emran, S.M., Yazdanpanahi, H., Gharehpetian, G.B., "Modeling combination of UPQC and photovoltaic arrays with multi – input single out DC – DC converter", IEEE Trans. India, 2011.
24. Davati, S.M., Akemran, H., Nafisi, I., Salabeigi, G.B., and Gharehpetian, "Modelling the combination of UPQC and Photovoltaic arrays with multi-input single – output DC-DC converters in industrial technology", IEEE International conference 1-6, 2009.
25. Diez-Valencia, V., Annakage, U.D., and Jacobson, D., "Interline Power Flow Controller Steady State Operation", IEEE Canadian Conference on Electrical and Computer Engineering, pp.280-284, 2002.
26. Du, Z., Tolbert, L.M., and Chiasson, J. N., "Active harmonic elimination for multilevel converters", IEEE Transactions on Power Electronics, Vol.21, no. 2, pp. 459-469, 2006.
27. Esfandiari, A., Parniani, M., Emadi, A., Mokhtari, H., "Application of the Unified Power Quality Conditioner for Mitigating Electric Arc Furnace Disturbances", International Journal of Power and Energy Systems, Vol.28, no.4, pp.363-371, 2008.
28. Fabio Tosato, and Stefano Quaia, "Reducing Voltage Sag Through Fault Current Limitation", IEEE Transactions on Power Delivery, Vol. 16, no.1, 2001.
29. Fujita, H., and Akagi, H., "The unified power quality conditioner. The integration of series and shunt-active filters", IEEE Trans. Power Electron., Vol.13, no.2, pp.315-322, Mar 1998.
30. Fujita, H., and Akagi, H., "The unified power quality conditioner. The integration of series and shunt active filters", IEEE Trans. Power Elect, 13, 315-322, 1998.
31. Ghosh, A., and Ledwich, G., "A unified power quality conditioner (UPQC) for simultaneous voltage and current compensation", Electric Power. Syst.Res.59. 55-63, 2001.

32. Graovac, D., Katic, A., and Rufer, A., "Power Quality Problems Compensation with Universal Power Quality Conditioning System, IEEE Transaction on Power Delivery, Vol.22, no.2, 2007.
33. Gyugyi, L., Schauder, C.D., Williams, S.L., Reitman, T.R., Torgerson, D.R., and Edris, A., "The unified power flow controller: A new approach to power transmission control", IEEE Transaction Power Delivery, Vol.10, pp.1085-1097, 1995.
34. Han, B., Bae, B., Kim, H., and Back, S., "Combined Operation of Unified Power Quality Conditioner with Distributed Generation", IEEE Transaction on Power Delivery, Vol.21, no.1, pp.330-338, 2006.
35. Hingorani, N.G., and Gyugyi, L., "Understanding Facts, Concepts and Technology of Flexible AC Transmission Systems", IEEE Press, New York, 2000.
36. Hongfa Ding, Shu Shuangyan, Duan Xianzhong, and Gao Jun, "A Novel Dynamic Voltage Restorer and its Unbalanced Control Strategy based on Space Vector PWM", Electrical Power and Energy Systems, no.24, pp.693-699, 2002.
37. Hosseinpour, M., Mohamadrezapour, Y., "Combined operation of unified power quality conditioner and photovoltaic array", - journal of applied sciences 9(4). 680 – 688, 2009.
38. Hosseinpour, M., Yazdian, A., Mohamadian, M., and Kazempour, J., "Design simulation of UPQC to improve power quality and transfer wind energy to grid", Journal of applied sciences 8(21): 3770-3782, 2008.
39. Hossin Heydari and Amit Hassan Moghadasi Joly, "Optimization scheme in combinational UPQC and SFCL using normalized simulated Annealing", in IEEE Trans. On power delivery, vol 26, no.3, 2011.
40. Hyosung Kim and Seung-Ki Sul, "Compensation Voltage Control in Dynamic Voltage Restorers by use of Feed Forward and State Feedback Scheme", IEEE Transactions on Power Electronics Vol.20 no.5, pp.1169-1177, 2005.
41. Ismail Musirin, Nur Dianah Mohd. Radzi, Muhammad Murtadha Othman, Mohamad Khayat Idris, and Titik Khawa Abdul Rahman, "Voltage Profile Improvement Using Unified Power Flow Controller via Artificial Immune System", WSEAS Transaction on Power Systems Issue -4, Vol.3, pp.194-204, 2008.



42. Jason Yuryevich, and Kit Po Wong, "Evolutionary programming based optimal power flow algorithm", In IEEE Trans. Power System, Vol.14 no.4, pp.1245-1250, 1999.
43. Jowder, F.A.L., "Design and Analysis of Dynamic Voltage Restorer for Deep voltage Sag and Harmonic Compensation", IET Generation Transmission Distribution, Vol.3, Issue. 6, pp.547-560, 2009.
44. Jun Zhang, and Akihiko Yokoyama, "Optimal Power Flow Control for Congestion Management by .IPFC", Proceedings of international Conference on Power System Technology, pp.1-6, 2006.
45. Kaifei Wang, Fang Zhuo, Yandong Li, Xu Yang and Zhaoan Wang, "Three-phase Four-wire Dynamic Voltage Restorer Based on a new SVPWM Algorithm", Proceeding of the 35<sup>th</sup> Annual IEEE Power Electronics Specialists Conference, pp.3877-3882, 2004.
46. Kannan Sreenivasachar, Jayaram, S., and Salama, MM.A., "Dynamic stability improvement of multimachine power system with UPFC", Electric Power Systems Research, Vol.55, pp.27-37, 2000.
47. Karshenas, H.R., and Moradlou, M., "Design Strategy for Optimum Rating Selection in Interline DVR", Canadian Conference on Electrical and Computer Engineering, pp.1919-1924, 2008.
48. Khadkikar, V., Chandra, A., Barry, A.O., and Nguyen, T.D., "Steady State Power Flow Analysis of UPQC during Voltage Sag and Swell Condition for Selection of Device Ratings", IEEE Canadian Conference on Electrical and Computer Engineering, pp.289-293, 2006.
49. Khadkikar, V., Chandra, A., "A New Control Philosophy for a Unified Power Quality Conditioner (UPQC) to Coordinate Load – Reactive Power Demand between Shunt and Series Inverters", IEEE Trans. on Power Delivery, Vol.23, no.4, pp.2522-2534, 2008.
50. Kiskick, D.O., and Naurapescu, V., "Single phase unified power quality conditioner with optimum voltage angle injection for minimum VA requirement", in power Electronics specialists conference, IEEE, 574-579, 2007.
51. Lee, G.M., Lee, D.C., and Seok, J.K., "Control of series active power filter compensating for source voltage unbalance and current harmonics," IEEE Transaction on Industrial Electronics, vol.51, no.1, pp.132-139, Feb.2004.

52. Leon Vasquez-Arneza, R., and Luiz Cera Zenetta, "A Novel Approach for Modeling the Steady State VSC Based Multiline FACTS Controllers and their Operational Constraints", IEEE Transactions on Power Delivery, Vol.23, no.1, pp.457-464, 2007.
53. Li, B.H., Choi, S.S., and Vilathgamuwa, D.M., "Transformer-less Dynamic Voltage Restorer", IEE Proceedings-Generation Transmission Distribution, Vol. no.149, pp.263-273, 2002.
54. Liew Zhan Liu, Vigna Kumaran Ramachandaramurthy, K., Agileswari Ramasamy and Rengan Krishna Iyer, "Dynamic Voltage Restorer (DVR) using Three Dimensional Space Vector PWM Control Algorithm", Proceedings of the 9<sup>th</sup> International Conference, Electrical Power Quality and Utilization, pp.1-6, 2007.
55. Mahdi, M., EI-Arini, Youssefm, T., and Hamed H. Hendawy, "Voltage sag analysis and its reduction to improve power system performance", The Eleventh International Middle East Power Svstems Conference pp.87-92, 2006.
56. Mahinda Vilathgamuwa, D., Choi, S.S., and Wijekoon, H.M., "A Novel Technique to Compensate Voltage Sags in Multiline Distribution System - The Interline Dynamic Voltage Restorer", IEEE Transaction on Industrial Electronics, Vol.53, no.5, pp.1603-1611, 2006.
57. Mahinda Vilathgamuwa, D., Choi, S.S., and Wijekoon, H.M., "Interline Dynamic Voltage Restorer: A Novel and Economical Approach for Multiline Power Quality Compensation", IEEE Transactions on Industry Applications, Vol. 40. no.6, pp.1678-1685, 2004.
58. Mahinda Vilathgamuwa, D., Gannayake, C.J., RC Wl.i. Y. Loh, "Voltage sag compensation with Z source inerter based dynamic voltage restorer", IEEE Industrial Electronics Conference, pp.2242-2248, 2006.
59. Mariun, N., Alam, A., Mahmod, S., Haizam, H., "Review of Control Stategies for powe quality conditioners, power and energy conference proceedings", vol.2, pp.1515-1520, 2004
60. McGranaghan, M.F., D.R. Mueller, and Samotyj, "Voltage Sags in Industrial Systems", IEEE Transactions on Industry Applications, Vol. 29, no.2, 1993.
61. Menniti, A., Pinnarelli, and Sorrectino, N., "A Fuzzy Logic Controller for Interline Power Flow Controller Model Implemented by ATP-EMTP", IEEE Transactions on Power Systems, Vol. 17, no.4, pp.1140-1147,2002.

62. Menniti, D., and Pennarelli, A., "Modelling of Unified Power Flow Controller into Power Systems using P-Spice", IPST conference, Rio de Janero, Brazil, pp.24-28, 2001.
63. Mihilac, R., Zunko, P., and Povh, D., "Improvement of transient stability using unified power flow controller", IEEE Transaction Power Delivery, Vol. 11, pp.485-492, 1996.
64. Mishra, Dash, P.K., Hota, P.K., and Tripathy, M., "Genetically Optimized Neuro-Fuzzy IPFC for Damping Model Oscillations of Power System", IEEE Transaction on power, 2002.
65. Monteiro, L.F.C., Aredes, M., and Neto, L.A.M., "A control strategy for unified power quality conditioner", in Proc. IEEE Int. Symp. Ind. Electron., Vol.1, pp.391-396, Jun.2003.
66. Naidu, S.R., and Fernandes, D.A., "Dynamic voltage restorer based on a four-leg voltage source converter", IET Generation Transmission Distribution, Vol.3, Issue.5, pp.437-447, 2009.
67. Nashiren, F. Mailah and Senan M. Bashi, "Single Phase Unified Power Flow Controller (UPFC) Simulation and Construction", European Journal of Scientific Research Vol. 30 no.4 , pp.677-684, 2009.
68. Nguyen, P.T., and Tapan, K.S., "DVR against Balanced and Unbalanced Voltage Sags: Modeling and Simulation", Proceedings of the IEEE Industrial Electronics Conference, pp.1-6, 2004.
69. Oscar C.Montero- Hernandez, and Prased N. Enjeti, "A fast Detection Algorithm Suitable for Mitigation of Numrous Power Quality Disturbances", IEEE Transactions on Industry Applications, Vol.41 no.6, pp.1684-1690,2005.
70. Padiyar, K.R., and Kulkarni, A.M., "Control design and simulations of unified power flow controller", IEEE Transaction Power Delivery Vol.13, pp.1348-1354, 1998.
71. Padiyar, K.R., and Nagesh Prabhu, "Analysis of SSR with three-Level Twele Pulse VSC-Based Interline Power Flow controller", IEEE Transactions on Power Delivery, Vol.22, no.3, pp.1688-1694, 2007.
72. Paisan Boonchiam, T.S., and Nadarajah Mithulanathan, T., "Detailed Analysis of Load Voltage Compensation for Dynamic Voltage Restorer", Thammasat international journal of Science and Techonology, Vol. 11, no.3, pp.1-6, 2006.

73. Pedro Roncero, Jose Enrique, and Aurelio Garcia, "A Versatile Control Scheme for a Dynamic Voltage Restorer for power quality Improvement", IEEE Transaction on Power Delivery, Vol, 24, no.1, pp.277-284.
74. Peng, F.Z., McKeever, J.W., and Adams, D.J., "A power line conditioner using cascade multilevel inverters for distribution systems", IEEE Trans.Ind.Appl., vol.34, no.6, pp.1293-1298, Nov/Dec 1998.
75. Poh Chiang Loah, Mahinda Vilathgamuwa, D., Yue Sen Lai, Geok Tin Chua, and Yunwei Li, "Pulse Width Modulation of Z-source Inverters", Proceedings of the IAS Conference, pp.148-155, 2004.
76. Renz, B.A., Mehraben, A.S., Schauder, C., Stacey, E., Kovalsky, L., Gyugyi, L., and Edris, A., "AEP unified power flow controller performance", IEEE Transaction Power Delivery, Vol. 14 pp.1374-1381, 1999.
77. Rosli Omar and Nasrudin Muhammad Rahim "New Control Technique applied in Dynamic Voltage Restorer for Voltage Sag Mitigation", IEEE conference on Industrial Electronics, pp.848-852, 2009.
78. Rosli Omar, and Nasrudin Muhammad Rahim, "Modelling and Simulation for Voltage Sags/Swells Mitigation Using Dynamic Voltage Restorer (DVR)", Proceedings of the Australasian Universities Power Engineering conference, pp.1-5, 2008.
79. Round, S.D., Yu, Q., Norum, L.E., and Undeland, T.M., "Dynamic control of a unified power flow controller", proceedings of IEEE conference, pp.508-514, 1996.
80. Round, S.D., Yu, Q., Norum, L.E., and Undeland, T.M., "Performance of a Unified power flow controller using D-Q control system", IEE conference publication no.423 on AC and DC power transmission pp.357-362, 1996.
81. Ryszard Strzelecki, Zbigniew Fedyczak, and Grzegorz Benysek, "Interline Power Flow Controller- Probabilistic Approach", IEEE Power Electronics Conference, pp.1037-1044, 2007.
82. Sankaran, C., Power Quality, Boca Raton: CRC Press, pp.202, 2002.
83. Samina Elyas, R.K., Nema and Gayatri Agai, "Power Flow Control with UPFC in Power Transmission System", World Academy of Science, Engineering and Technology, Vol.47, pp.338-342, 2008.

84. Sasithran, S., and Mahesh Mishra, K., "Adaptive BandController for Dynamic Voltage Restorer", IEEE Applied Power Electronics Conference, pp.882-888, 2009.
85. Schauder, D., Gyugyi, L., Lund, M.R., Hamai, D.M., Rietman, T.R., Torgerson, D.R., and Edris, A., "Operation of the unified power flow controller (UPFC) under practical constraints", IEEE Transaction Power Delivery, Vol.13, pp.630-636, 1998.
86. Sen, K.K., and Stacey, E.J., "UPFC - Unified Power flow controller: Theory, modeling and applications", IEEE Transaction Power Delivery, Vol.13, pp.1453-1460, 1999.
87. Sharad W. Mohod, and Mohan V. Aware, "A STATCOM- Control Scheme for Grid Connected Wind Energy System for Power Quality Improvement", IEEE Systems Journal, Vol. 4., no.3 pp.346-352, 2010.
88. Srisungkram, W., Subsingha, W., & Boonctiam, P., "Voltage sag detection method in power Distribution systems for power quality issues", Power system Research center.
89. Toufan, M., and Annakkage, U.D., "Simulation of the unified power flow controller performance using PSCAD/EMTDC", Electric power systems research, Vol. 46, pp.67-75, 1998.
90. Walling, R.A., Saint, R., Dugan, R.C., Burke, J., and Kojovic, I.A., "Summery of Distributed Resources Impack on Power Delivery Systems", IEEE Trans, Power Delivery, Vol.23, no:3, pp.1636-1644, July 2008.
91. Wijekoon, H.M., Majhnda Vilathgamuw, D., and Choi, S.S., "Interline Dynamic Voltage Restorer An economical Way to Improve Interline Power Quality", IEEE Proceddings-Generation Transmission Distribution, Vol.150, no.5, pp513-520, 2003.
92. Xia Jing, Xingao Fang, Joe Chow, H., Abdel-Aty Edros, and Edvin Uzunovic, "Regulation and Damping Control Desgin for Interline Power Flow cotrollers", IEEE power Engineering Soceity metting, pp.1-8,2007.
93. Xuan Wei, Joe, H., Chow Fardanesh, B., and Abdel-Aty Edris, "A Dispatch Strategy for an Interline Power Flow Controller Operating at Rated Capacity", IEEE Power System Conference, pp.1-8, 2004.
94. Yan Zhang, and Jovica Milanovic, V., "Global Voltage Sag Mitigation with FACTS Based Devices", IEEE Transactions on Power Delivery, Vol. 25, no.4, pp2842-2850, 2010.

95. Yankui Zhang, Yan Zhang and Chen Chen, "A Novel Power Injection Model of IPFC for power Flow Analysis Inculsive of Practical Constraints", IEEE Transactions on Power Systems, Vol.21, no.4, pp.1550-1556, 2006.
96. Zhang, P., "Modelling of the Interline Power Flow controller and the Generalised Unified Power Flow Controllerin Newton Power Flows", IEE Proceddings-Generation Transmission Distribution. Vol.150, no.3, pp.268-274, 2003.

## PUBLICATIONS

1. Kannan, P. and Rajamani, V., “Design, Modelling and Simulation of UPQC in Fourteen Bus system,” *Journal of Theoretical and Applied Information Technology (JTAIT)*, Vol. 57, No 3, pp.540-548, 30<sup>th</sup> November 2013.
2. Kannan, P. and Rajamani, V., “Design, Modelling and simulation of UPQC in Thirty bus system,” *International Journal of Technology and Engineering Science (IJTES)*, Vol. 1(6), pp.1027-1038, September 2013.
3. Kannan, P. and Rajamani, V., “Design, modelling and simulation of UPQC in Eight bus system,” *Wulfenia*, Vol. 20 No 3, pp.51-59, March 2013.
4. Kannan, P. and Rajamani, V., “Reduction of Harmonics of UPQC system with PV array,” *European Journal of Scientific Research*, Vol. 85 No 3, pp.356-362, September 2012.
5. Kannan, P. and Rajamani, V., “Design, modelling and simulation of UPQC system with PV array”, *International Journal of Engineering Research & Technology (IJERT)* Vol. 7, pp.1-5, issue 6, August – 2012.